

| | | | | | | |
|---|-------------|-----------------------|---------------------------------------|------------------------------------|---|--|
| REPORT DOCUMENTATION PAGE | | | | | <i>Form Approved OMB No. 0704-0188</i> | |
| <small>The public reporting burden for this collection of information is estimated to average 1 hour per response, including the time for reviewing instructions, searching existing data sources, gathering and maintaining the data needed, and completing and reviewing the collection of information. Send comments regarding this burden estimate or any other aspect of this collection of information, including suggestions for reducing the burden, to Department of Defense, Washington Headquarters Services, Directorate for Information Operations and Reports (0704-0188), 1215 Jefferson Davis Highway, Suite 1204, Arlington, VA 22202-4302. Respondents should be aware that notwithstanding any other provision of law, no person shall be subject to any penalty for failing to comply with a collection of information if it does not display a currently valid OMB control number.</small> | | | | | | |
| PLEASE DO NOT RETURN YOUR FORM TO THE ABOVE ADDRESS. | | | | | | |
| 1. REPORT DATE (DD-MM-YYYY) | | 2. REPORT TYPE | | | 3. DATES COVERED (From - To) | |
| 4. TITLE AND SUBTITLE | | | | 5a. CONTRACT NUMBER | | |
| | | | | 5b. GRANT NUMBER | | |
| | | | | 5c. PROGRAM ELEMENT NUMBER | | |
| 6. AUTHOR(S) | | | | 5d. PROJECT NUMBER | | |
| | | | | 5e. TASK NUMBER | | |
| | | | | 5f. WORK UNIT NUMBER | | |
| 7. PERFORMING ORGANIZATION NAME(S) AND ADDRESS(ES) | | | | | 8. PERFORMING ORGANIZATION REPORT NUMBER | |
| 9. SPONSORING/MONITORING AGENCY NAME(S) AND ADDRESS(ES) | | | | | 10. SPONSOR/MONITOR'S ACRONYM(S) | |
| | | | | | 11. SPONSOR/MONITOR'S REPORT NUMBER(S) | |
| 12. DISTRIBUTION/AVAILABILITY STATEMENT | | | | | | |
| 13. SUPPLEMENTARY NOTES | | | | | | |
| 14. ABSTRACT | | | | | | |
| 15. SUBJECT TERMS | | | | | | |
| 16. SECURITY CLASSIFICATION OF: | | | 17. LIMITATION OF ABSTRACT | 18. NUMBER OF PAGES | 19a. NAME OF RESPONSIBLE PERSON | |
| a. REPORT | b. ABSTRACT | c. THIS PAGE | | | 19b. TELEPHONE NUMBER (Include area code) | |

Phase II SBIR Final Report
Report Period: 1 August 2000 – 30 March 2003

**Low Temperature Active Joining
of Structural and Electronic Composites**

Contract DASG60-00-C-0056

Term: 24 months

Award Amount: \$750,000

Funding Authorized: \$625,000
(12-31-02)

Submitted to:

Dr. Richard Rodgers
SMDC – TC - AP
US Army Space and Missile Defense Command
P.O.Box 1200
Huntsville, AL 35807-3801

Submitted by:

Materials Resources International

Dr. Ronald W. Smith
Travis M. Nelson
811 W. Fifth Street
Lansdale, PA 19446

Table of Contents

| | |
|---|-----------|
| LIST OF FIGURES | 3 |
| LIST OF TABLES | 8 |
| 1.0 SUMMARY | 9 |
| 2.0 PHASE II INTRODUCTION | 9 |
| 3.0 OBJECTIVE & WORK PLAN | 10 |
| 3.1 Project Objectives | 10 |
| 3.2 Work Tasks | 10 |
| 3.3 Technology Applications | 11 |
| 4.0 TASK SUMMARY & RESULTS..... | 13 |
| 4.1 Task 1.0 Lightweight Structures..... | 13 |
| 4.2 Task 2.0: Lightweight Armor | 29 |
| 4.3 Task 3.0 Electronic Components..... | 46 |
| 5.0 CONCLUSIONS / SUMMARY | 55 |
| 5.1 Structures | 55 |
| 5.2 Armor | 56 |
| 5.3 Electronics..... | 56 |
| 6.0 COMMERCIALIZATION | 57 |
| 6.1 S-Bond Technologies, LLC | 57 |
| 6.2 S-Bond Technologies, LLC, Business Mission..... | 59 |
| 6.3 S-Bond Market..... | 59 |
| 6.4 Commercialization / Summary | 61 |

LIST OF FIGURES

- Figure 1. A missile fin structure
- Figure 2. A thin wall, composite missile nosecone with S-Bond™'d trusses.
- Figure 3. Composite truss reinforced mirror concept, bonded with proposed S-Bond™ methods.
- Figure 4. Wear protection cladding on Al-MMC composite surfaces.
- Figure 5. S-Bond™ joining for electronic packaging or sensors.
- Figure 6. Coupon-Ring Push Test Configuration
- Figure 7. Single Lap Shear (SLS) Test Configuration
- Figure 8. Tube-Tube Shear Test Configuration
- Figure 9. Rod-Rod Butt Joint Test Configuration
- Figure 10. Coupon-Ring Tensile-Push Tests Results
- Figure 11. Rod/Rod tensile test results with Alloy 220
- Figure 12. Joints shear strength for single lap shear
- Figure 13. Effect of doubling the joint width on the shear strength.
- Figure 14. Effect of adding fillets on the joint strength for tube/flange configuration
- Figure 15. Shear strength of Tube/Flange joints for two different solder alloys
- Figure 12. Effect of tube diameter on the shear strength of Tube/flange joints
- Figure 17. SEMicrograph of u/s prewetted, S-Bond 220 joined Al-Al cross section.
- Figure 18. SEMicrograph of U/S prewetted, S-Bond 400 joined Al-Al cross section.
- Figure 19. Micrograph of Al-Al cross section with S-Bond 220 foil inserted only.
- Figure 20. Al-Al cross section with S-Bond 400 foil inserted only. Note the extensive reaction.
- Figure 21. Micrograph of Al-Al cross section with manually wiped S-Bond 220.
- Figure 22. Al-Al cross section with manually wiped S-Bond 400. Note the extensive reaction.
- Figure 23. SS/SS joint cross section with U/S prewetted S-Bond 220.
- Figure 24. SS/SS joint cross section with U/S prewetted S-Bond 400.

Figure 25. SS/SS joint cross section with non-prewetted (foil insert) S-Bond 220.

Figure 26. SS/SS joint cross section with non-prewetted (foil insert) S-Bond 400.

Figure 27. SS/SS joint cross section with manually prewetted S-Bond 220.

Figure 28. SS/SS joint cross section, manually prewetted with S-Bond 400.

Figure 24. Ti/Ti joint cross section with U/S prewetted S-Bond 220. Manual prewetting produced a very similar looking joint structure.

Figure 31. Ti/Ti joint cross section with U/S prewetted S-Bond 400. Note more extensive interaction than the S-Bond 220 joint.

Figure 30. Ti/Ti joint cross section with foil inserted (non-prewetted) S-Bond 220.

Figure 32. Ti/Ti joint cross section with foil-inserted (non-prewetted) S-Bond 400. The manually prewetted S-Bond 400 joint looked very similar.

Figure 33. Anodized Al/Al joint made with S-Bond 220. The S-Bond wetted the anodized surface and the base metal below.

Figure 34. Anodized Al/Al joint made with S-Bond 400. Note areas where S-Bond got through cracks in the anodized layer and diffused into the Al.

Figure 35. Chromated Al/Al joint made with S-Bond 220.

Figure 36. Chromated Al/Al joint made with S-Bond 400.

Figure 37. Stainless steel/Aluminum joint made with S-Bond 220.

Figure 38. Stainless steel/Titanium joint made with S-Bond 220.

Figure 39. Aluminum/Titanium joint made with S-Bond 220.

Figure 40. Stainless steel joined to Aluminum with S-Bond 400 foil.

Figure 41. Stainless steel joined to Al with S-Bond 400 using ultrasonic wipe prewetting.

Figure 43. Stainless Steel/Stainless steel joint made with S-Bond 220 after grit blasting.

Figure 42. Stainless Steel/Ti joint made with S-Bond 400 using ultrasonic wipe prewetting.

Figure 44. Stainless Steel/Stainless steel joint made with S-Bond 400 after grit blasting.

Figure 45. Ti/Ti joint made with S-Bond 220 after grit blasting.

Figure 46. Ti/Ti joint made with S-Bond 400 after grit blasting.

Figure 47. Ti side of a Ti/Al joint made with S-Bond 220 paste and vacuum premetallization.

Figure 48. Stainless steel/Al joint made with S-Bond 220 paste and vacuum premetallization

Figure 49. Proposed lightweight armor concept using aluminum foam backing.

Figure 50. Al_2O_3 /Al-Foam joint using S-Bond 400 with ultrasonic wipe prewetting.

Figure 51. Alumina bonded to Al-Foam with vacuum pretreated S-Bond 220.

Figure 52. SiC bonded to Al-Foam with vacuum pretreated S-Bond 220.

Figure 53. SiC/Al-Foam joint using S-Bond 400 with ultrasonic wipe prewetting.

Figure 54(49). SiC/Al-Foam joint using S-Bond 400 foil only (no prewetting).

Figure 55. Vacuum pretreated Si:SiC ultra-sonically joined to Al-Foam using S-Bond 220.

Figure 56. Si:SiC and Al-Foam ultrasonically joined using S-Bond 400.

Figure 57. Si:SiC interface with S-Bond 220 after vacuum pre-treatment.

Figure 58. SiC interface with S-Bond 400 after ultrasonic prewetting.

Figure 59. Si:SiC interface with S-Bond 400 after ultrasonic prewetting.

Figure 60. Si:SiC interface with S-Bond 220 after vacuum/paste pretreatment.

Figure 61. Si:SiC interface with S-Bond 220 after ultrasonic prewetting.

Figure 62. Si:SiC/Al-Sponge joint using S-Bond 400 foil only (no prewetting).

Figure 63. Si:SiC/Al-Foam joint using S-Bond 220 with nickel particles.

Figure 64. Si:SiC/Al-Foam joint using S-Bond 220 with SiC particles.

Figure 65. Si:SiC/Al-Foam joint using a 40vol% Al:SiC transition layer and S-Bond 220.

Figure 66. Double lap shear (DLS) specimen before and after joining

Figure 67 and 68. Pictures of failed composite armor test samples.

Figure 69. Shear test results on Al-foam: ceramic double lap shear samples

Figure 65. Effect of surface treatment on the shear strength of armor joints.

Figure 71. 4 x 4 inch ballistic test sample showing Al-Foam joined to SiC faceplate.

Figure 72. 4x4 inch ballistic test sample shown in Figure 2, after CTE mismatch led to bond failure (2 days elapsed time).

Figure 73. Illustration of a particulate composite S-Bond™ joint for composite armor.

Figure 74. Illustration of an Al:SiC transition piece joint for composite armor.

Figure 75. Macro view of Al:SiC transition piece / S-Bond™ joined composite armor plates

Figure 76. SiC plate S-Bond™ 220 joined

Figure 77. Si:SiC composite plate S-Bond™ 220 joined directly to 3/4" aluminum plate

Figure 78. SiC plate S-Bond™ 220 joined directly to 3/4" aluminum plate.

Figure 79. SiC plate corner fillet detail, bonded with S-Bond™ Alloy 220.

Figure 80. S:SiC plate S-Bond™ 400 joined directly to 3/4" aluminum plate.

Figure 81. Si:SiC plate S-Bond™ 400 joined directly to 3/4" aluminum plate partially on bonded side.

Figure 82. SiC plate S-Bond™ 400 joined directly to 3/4" aluminum plate, showing the fractured S-Bond™

Figure 83 – Epoxy joined SiC to 0.75" Al armor plate, with laser sight centered on target, prior to firing.

Figure 84 – Plate 1E (SiC tile w/ mechanical activation only) – The strike velocity was nearest the 2160 fps constructed V50.

Figure 85 – Plate 2D – (SiC tile w/ mechanical activation and an Al:SiC intermediate layer) – The strike velocity was nearest the 2171 fps constructed V50.

Figure 86 – Plate 7D – (SiC tile vacuum treated w/ S-Bond 220) – The strike velocity was nearest the 2221 fps constructed V50.

Figure 87 – Plate 8D – (SiC tile w/ mechanical activation and an Al:SiC intermediate layer) – The strike velocity was nearest the 2062 fps constructed V50.

Figure 88– Plate 9C – (SiC tile joined with 3M 7100 epoxy bonding film) The strike velocity was nearest the 2290 fps constructed V50.

Figure 89 – Plate 16D (Si:SiC composite tile vacuum pretreated with S-Bond 220 paste) – The strike velocity was nearest the 2243 fps constructed V50

Figure 90. Photographs of SiC / Ti 6-4 plates joined by MRi for the US Army Research Lab, using S-Bond™ Alloy 220.

Figure 91. Schematic cross section of an electronic package with thermal management components.

Figure 92. Illustration of hermetic electronic enclosure.

Figure 93. Power electronic device bonded to AL-MMC heat spreader.

Figure 94. Die attachment on leadframe.

Figure 95. Illustration of double notch shear specimen designed and used to test the shear strengths of varying ceramic/composite joint combinations.

Figure 96. Al:Gr joined to Al:Gr with S-Bond 220 using brush / U-S press method.

Figure 97. Al:Gr joined to Al:Gr with S-Bond 400 using brush / U-S press method.

Figure 98. Al:Gr joined to Kovar with S-Bond 220.

Figure 99. Al:Gr joined to Kovar with S-Bond 400.

Figure 100. Al:SiC joined to Kovar with S-Bond 220 foil.

Figure 101. Al:SiC joined to Kovar with S-Bond 400 foil.

Figure 102. AlSiC bonded to Al:SiC with S-Bond 400 using manual wipe prewetting.

Figure 103. Al:SiC joined to Kovar with S-Bond 400.

Figure 104. Illustration of the hermetic package test sample.

Figure 105. Al:SiC composite electronic packages assembled using S-Bond™ / showing area of leaking

Figure 106. High magnification view of Al:SiC/Kovar® joint in an electronic package assembled using S-Bond™ 220.

Figure 107. Al:SiC/Kovar® joint in an electronic package assembled using S-Bond™ 220.

Figure 108. New composite electronic package design for S-Bond™ sealing trials.

Figure 109. A power hybrid IC package used in satellite devices where an Al:SiC box and a Kovar® lid are attached. Note that these parts are gold coated, but S-Bond™ would not require such coatings to facilitate bonding.

Figure 110. Automated S-Bonder™ Carousel System

Figure 111. View of Carousel System with Infrared Heater Lamp Stations

Figure 112. View of Ultrasonic S-Bonder™ Press Station

LIST OF TABLES

Table 1 – Composite Armor Ballistics Testing Matrix

Table 2. Ballistics Testing Results

Table 3. Shear Strengths of Ti-SiC Joints Made for ARL

Table 4. Candidate Materials for Electronic Components

Tables 5 and 6. Summary of DNS Testing on Electronic Materials

Table 7. Hermeticity Testing Results for Kovar Lid/Sides and Al:SiC Base Samples

Table 8. Commercial Prospects for S-Bond™ Joining/Lightweight Structures & Electronics

Table 9. Summary 5-Year SBT Financial Projections

Table 10. Projected Licensed Technology Users

Table 11. Market Areas for S-Bond Joining Technology

Table 12. Commercial Prospects for S-Bond™ Joining/Lightweight Structures & Electronics

1.0 SUMMARY

MRi has completed is Phase II SBIR focused on understanding the active solder (S-Bond®) bonding and is potential for application joining aluminum metal matrix composites (Al-MMC) in structures and electronics. The studies aimed at developing active solder (S-Bond®) joining process, evaluating joint microstructures, characterizing joint properties and assessing S-Bond® joining in several potential components with application in missile defense applications.

The studies have shown the S-Bond® joining using active solders based in either Sn-Ag-Ti (S-Bond® Alloy 220) or Zn-Al-Ce-Ga (S-Bond® 400) can produce exceptional joints with a wide range of Al-MMC's. The processes investigated showed robustness and ability to translate to production joining. As presented in other publications, S-Bond® joining requires mechanical agitation to break the oxide scales that form on the molten S-Bond® filler metals during joining in air. Although as described in sections of this report additional means such as vacuum metallization of ceramics and certain metals (high temperature, ~ 850°C, wetting with S-Bond® filler metals in vacuum atmospheres) have been developed that enhance S-Bond® adherence. Bond strengths have been found to range from ~ 30 – 112 MPa, depending on base materials and processes. The project investigated Al-SiC of varying SiC content, Al-Graphite, Kovar®, titanium, stainless steel, aluminum, Al₂O₃ and AlN with the objective to investigate the range of applications that S-Bond® joining was able to join. The structures of joints showed S-Bond® Alloy 220 and 400 to have excellent interaction with many materials, and depending on S-Bond® joining process, developed excellent joint characteristics, such as strength, thermal conductivity, thermal cycling capacity, and/or leak tightness.

Overall, the project has shown S-Bond®, active solder joining, to be versatile and capable of joining structures and electronic packages, within the limitation of the materials' strengths and temperatures range. Joints have been successfully made in a wide range of configurations and under varying conditions. Investigations have concluded that S-Bond® joining of Al-MMC's in structures and electronic components were successful and depending on specific component design criteria, could be used in fabrication of many components that are considering Al-MMC's. Investigations evaluated structural joining (generic joints), armor plate (ceramic to aluminum, titanium, and Al-MMC's), and electronic packages including a hermetic enclosure. These investigations, with the exception of ceramic armor plate concluded that S-Bond® joining had application.

MRi is commercializing its S-Bond® joining technology through a combination of direct OEM (original equipment manufacturer) licenses and authorized service providers. As this investigation has shown, S-Bond® joining, although capable and versatile, is a process not just a unique filler metal. As such, a significant degree of technology transfer is required as MRi sells it product. MRi currently sells S-Bond® materials, joining services, equipment and is now selling "licenses" to OEM's and service providers. This approach is more rapidly growing the capacity for S-Bond® to be used in DoD and commercial applications. MRi has several licenses pending in the joining of Al-MMC for use in electronic assembly equipment. The value of these licenses and sales of product will exceed ~\$0.5M over the next three years. As these applications mature, it is expected that many other Al-MMC joining applications will emerge. MRi is in several "qualification" studies for S-Bond® joining of AL-MMC's in electronic packages. It is expected that these applications will lead to additional licenses with a market value of over \$1M.

2.0 PHASE II INTRODUCTION

S-Bond™ Sn- and Zn-based active solder joining processes were shown in Phase I work to be unique and enabling technology that could speed the use of Al-MMC and other MMC's into fabricated components for missile, rocket engine, and/or space-based platform component fabrications. MRi, in its Phase I investigation, demonstrated the technical feasibility and versatility of its low temperature active joining

process, S-Bond™, on aluminum matrix-ceramic composite materials reinforced with Al-SiC, Al-Al₂O₃, and/or B₄C. Phase II development was used to implement this joining technology into component fabrications.

The proposed Phase II project focused on joining of Al:SiC MMC's for application in tubing and fittings for rocket engine and structural satellite components, in electronic packaging, and for composites used in lightweight armor. For evaluating structural S-Bond® joining, MRi teamed with the US Army to study the suitability of S-Bond™ joining in lightweight armor bonding. The work focused on understanding how S-Bond™ joining works under various conditions and geometries (e.g., flat sheets, tubes, fittings, and spars), aiming to develop design parameters that fit typical S-Bond™ joint characteristics and properties. During Phase II, MRi developed S-Bond™ joining alloys and systems to advance the commercialization of this unique joining technology for use in missiles and space platforms as well as in other applications, including thermal management devices.

3.0 OBJECTIVE & WORK PLAN

The object of the Phase II project was to demonstrate S-Bond joining and develop the necessary designs and process controls for implementing S-Bond for joining Al-MMC's and MMC's in actual applications in missile and space platform components.

3.1 Project Objectives

- i. Develop and improve S-Bond® joining procedures
- ii. Characterize S-Bond® joints with a range of missile candidate materials
- iii. Measure joint performance

The specific applications identified were:

- i) fittings and trusses for instrument attachments on satellites
- ii) tubing and flanges for cryogenic fuel handling and
- iii) lightweight composite armor for the protection of critical missile and satellite components
- iv) electronic packaging.

The goal of the work was to integrate S-Bond joining into these designs and plan for its use in Al-MMC fabrications. Educating users about S-Bond's capabilities, testing the joints in actual configurations, developing design data, and more fully characterizing the materials and processes for joining the various materials and configurations were all necessary to accomplish this. The four (4) major tasks were:

3.2 Work Tasks

Task 1.0 Structures

This task aimed at developing the S-Bond joining processes to produce structural joints for service between 180 and 350°C. Joints were made between Al:MMC materials, aluminum, stainless steel and titanium. Joint geometries included flat overlap for joining sheet, tube-flange, tube-tube, and rod-rod joints. Joint strengths as joined and after thermal cycling (-55 to 150°C) were measured and reported.

Task 2.0 Armor

This task aimed to develop a composite lightweight armor tile based on aluminum foam backing joined to various candidate faceplate armor tiles, including CMCs (Si:SiC), Al:MMCs and ceramic such as SiC and Alumina. Development centered on developing viable manufacturing procedures, measuring joint strengths and selecting the most promising candidates for ballistic testing. In this task, MRi collaborated with Fraunhofer Institute USA and Simula, aiming at US Army lightweight vehicle initiatives as well as Navy and AirForce initiatives in lightweight armor. Later, aluminum foam backing was replaced by solid aluminum backing, and the ceramics submitted for ballistics testing were SiC and Si:SiC composite. H.P. White Inc. (Street, MD) was contracted to perform the ballistics testing.

Task 3.0 Electronic Components/Packaging

Initially, a collaborative demonstration with partners such as Lockheed Martin Astronautics, dMC² and MMCC, this task aimed to show that S-Bond joining can be used to make electronic packages and obtain hermetically sealed units with Al:MMC materials. In this task S-Bond joining was developed for the combinations of materials, test packages were made and testing was completed to validate the joining processes. Additionally, MRI planned to conduct evaluations of AlN, Al₂O₃ and Si joining to each other and to the Al:MMCs to support a growing commercial opportunity in power electronic modules.

Task 4.0 Reporting

This task reports the quarterly progress on the Phase II work and the results.

3.3 Technology Applications

The project proposals had cited such applications as missile structures, avionics enclosures, actuators, optical mirrors, antenna supports and booms, and electronic packaging. Other fabrications considered included missile structures, such as fins/stabilizers, aerodynamic surface actuators, laser mirrors, antenna/nosecones and electronic substrates or electronic thermal management devices. These applications are again presented here to review some of the possibilities for S-Bond joining, though not all of these applications were directly pursued as part of this contract. Figures 1-5 illustrate several of the cited applications that were targeted as candidates for S-BondTM joining technology.

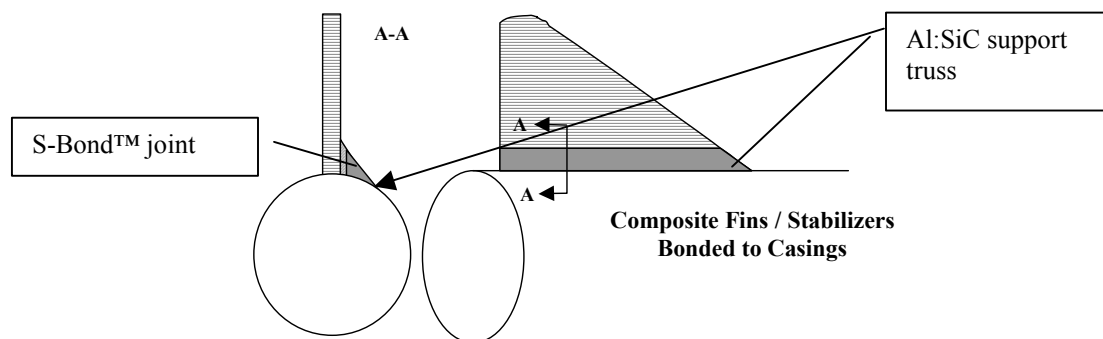


Figure 1. A missile fin structure

In the missile stabilizer fin, above, Al matrix composite frame pieces could be bonded to the casing and the fin (typically aluminum alloys) without the use of mechanical fasteners, thus significantly lowering weight. In Figure 2, below, the nose cone wall could be made thinner if structural Al composites were used to stiffen and support the avionics and antenna mounts. The extra stiffness in the nose cone will enable faster maneuverability. Note such assemblies could be joined via S-BondTM, eliminating the extra weight and stress concentration of fasteners.

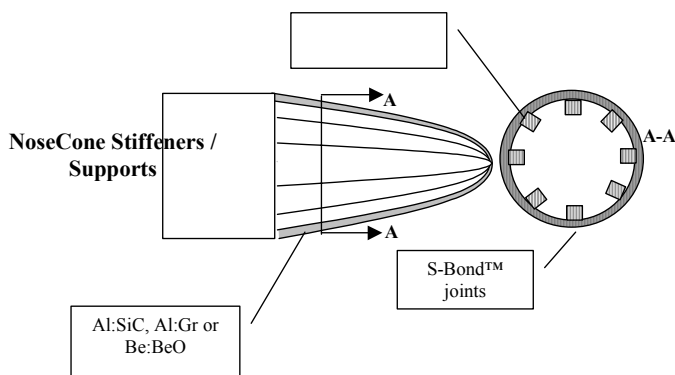


Figure 2. A thin wall, composite missile nosecone with S-BondTMd trusses.

Figure 3 illustrates how thinner, lighter and/or stiffer laser mirror assemblies could be made with optical surface materials combined with Al:SiC or other metallic composites being used as reinforcing trusses backing up the mirror surfaces. Currently some mirrors are cast, however, castings of these mirror materials with the stiffening ribs requires thicker sections for production ease. If the cast parts could be made as a fabrication, the mirror could be made from thinner requisite optical surfaces that could be stiffened with trusses made from the low CTE composites such as Al:SiC. S-Bond™ technology would then have the potential to join the trusses, seen in Figure C, below. Such designs would enable much lighter weight and stiffer mirror systems for space and aircraft based laser mirror platforms, increasing their accuracy and durability.

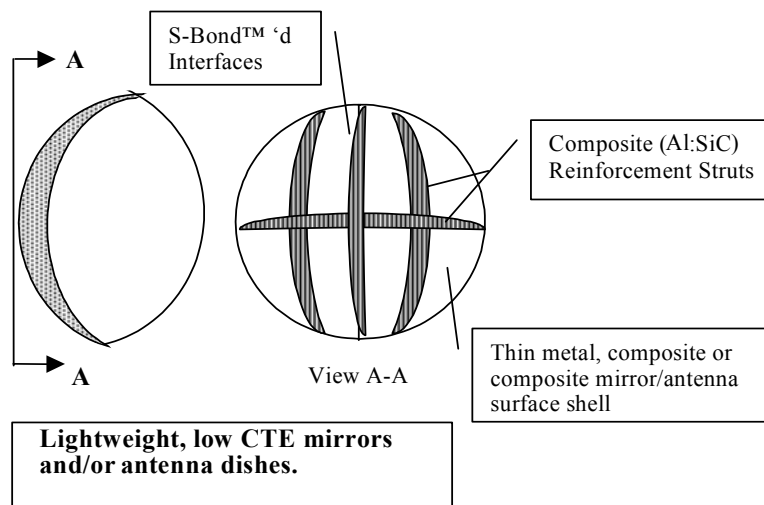


Figure 3. Composite truss reinforced mirror concept, bonded with proposed S-Bond™ methods.

Figure 4 illustrates how S-Bond™ could be used to bond thin, wear resistant tool steel or ceramic (oxide or carbide) locally on the surfaces of composite materials. This type of component could be used in actuators or at intersections of aerodynamic control surfaces.

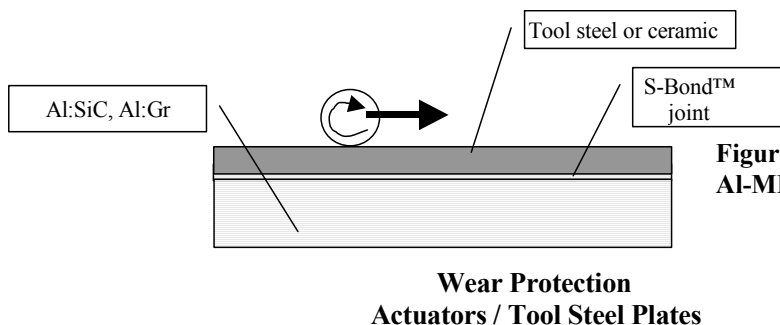


Figure 4. Wear protection cladding on Al-MMC composite surfaces.

In the electronic packaging and or sensor application, S-Bond™ permits the direct bonding of silicon/silicon devices to any of the indicated base materials. Figure 5 illustrates a Si-device on a composite substrate. Low CTEs, low weight, high stiffness and high thermal conductivity make this combination for electronic packaging very promising. Low cost, reliable, low temperature joining of Si to composites also opens the possibility for Si-based sensors to be directly bonded to critical missile structures to measure force, accelerations, or temperatures making the integration of “smart” materials into such composite structures possible.

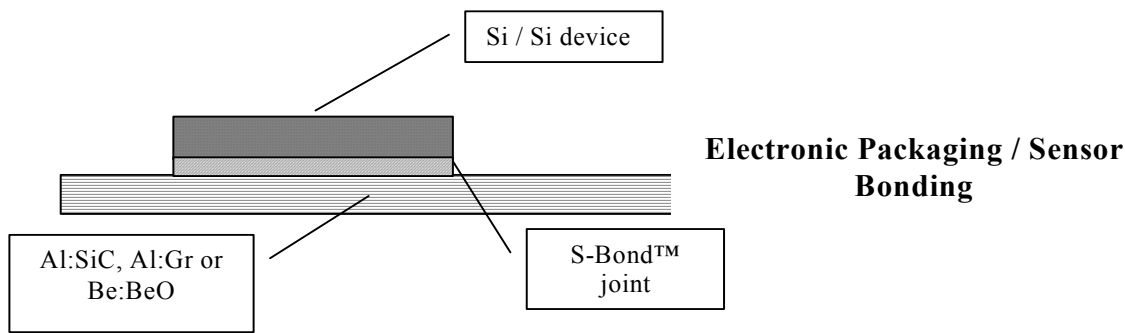


Figure 5. S-Bond™ joining for electronic packaging or sensors.

The applications cited in Figures 1-5 illustrated the potential for Al-MMC's and S-Bond® joining. These applications would use the properties and characteristics of the joints in different ways. In order to understand if AL-MMC's and S-Bond® joints would have the capacity to meet the needs of such a diverse set of applications, the development project focused on application areas then developed joining processes and characterized the joints to assess general suitability of the S-Bond® technology. The development project broke these evaluations into the following tasks:

- Lightweight Structures
- Lightweight Armor
- Electronic Components

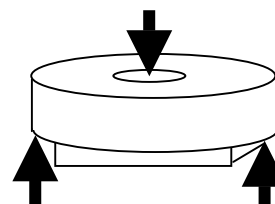
4.0 TASK SUMMARY & RESULTS

4.1 Task 1.0 Lightweight Structures

Lightweight structures that may be used in missile defense were illustrated in the previous section. The project conducted scouting studies of materials and geometries that might apply in some of these or other missile or satellite applications. For example, titanium is used in many fittings that attach devices to the structures of space platforms, though some designers would like to substitute Al-MMCs for these to save weight. Their applications would include the bonding of tube-flange type fittings, to be joined to bulkheads with Al-SiC composite flanges. Depending on the size and the expected load, S-Bond™ joining may be applicable, especially if higher thermal conductivity and/or occasional disassembly were necessary.

This task assessed the capability of S-Bond® to produce joints on selected materials combinations. For each of the joint configurations and materials combinations, both lap shear and separate button tensile test specimens were produced and tested. MRI originally investigated three bonded configurations, but later modified one of these as available data suggested that other joint geometries would yield more accurate results.

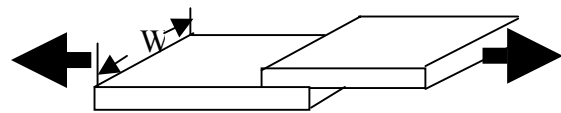
1. Full overlap flat joint (Coupon-Ring Push-Test). See Figure 6. These joints were designed to represent the bond typical of a rod/flange or tube/flange connection that might be used for structural components. It was found that the flat aluminum coupons bowed during testing and created a stress concentration that prevented the test from accurately determining the tensile strength of the joints, so this configuration was replaced by a rod-rod butt joint.



**Figure 6.
Coupon-Ring
Push Test
Configuration**

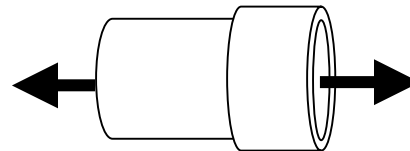
2. Partial overlap (Single-Lap Shear, SLS). See Figure 7. This style of test joint was intended to represent the types of flat, overlapping joints and seams that may be necessary for joining larger panels and small, flat cross sections. The design was modified in order to achieve a representative test of the shear strength of a typical, flat S-Bond joint.

Figure 7. Single Lap Shear (SLS) Test Configuration



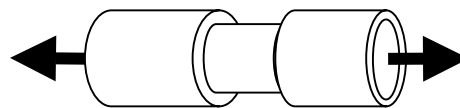
3. Tube-to-tube joint (tube shear tests). See Figure 8. In some applications, it may be necessary to join tubes directly to each other, and so tube-tube joints were designed to test the shear strength of a circumferential S-Bond joint in shear.

Figure 8. Tube-Tube Shear Test Configuration



4. Rod-rod butt joint (replaced coupon-ring). See Figure 9. These tests were conducted to replace the non-representative coupon-ring push test. The rod configuration eliminated potential stress concentrations due to the corners formed by bonding a flat coupon to a ring, allowing the true shear strength of the joint to be assessed.

Figure 9. Rod-Rod Butt Joint Test Configuration



The SLS samples had two different widths, $\frac{1}{2}$ " and 1", to study the effect of joint dimensions on the strengths of the materials. For the tube-tube joints, three different diameters were tested: $\frac{1}{2}$ ", 1" and 2" for the same reason. Iterative experiments were run to develop optimum bonding processes for untreated aluminum, anodized aluminum, chromated aluminum, titanium, stainless steel and Al:SiC.

As was described in earlier work and proposals, MRI's S-Bond® joining is based on using its patented active solder alloys, Alloy 220 which is Sn-4Ag-4Ti-0.1Ga-0.1Ce, and Alloy 400, which is Zn-4Ag-2Al-0.1Ga-0.1Ce. These alloys are unique in that they bond to metals, ceramics and composites without the use of chemical fluxes and under air atmospheres. However, the characteristics of joining with S-Bond® alloys is that the filler metals do not wick and fill joints and when melted the oxide films that form on the filler metal must be disrupted, either mechanically or thermally. As such, the following joining processes apply and were evaluated:

1. Pre-wetting / Preplacement techniques:

- Ultrasonic wiping (pewetting) of molten solder. This involved applying the solder while the part was at the joining temperature on a hotplate and using a modified ultrasonic polishing tool to mechanically disrupt the solder surface. The high frequency, low amplitude agitation helped to disrupt the S-Bond surface oxides and base metal surfaces so that the S-Bond could thoroughly adhere to the base materials. This method is effective, but the tool must have a spatula tool that is appropriate in size and shape for the surface to be pre-wetted.
- Manual wiping of molten solder. This method involved heating the base metals to the joining temperature on a hotplate and them manually scrubbing, brushing, Vibra-peening or scraping the surface with a spatula tool to accomplish the needed mechanical activation of the S-Bond and base metal surfaces.

- Foil insert without wiping. This method involved applying S-Bond alloy foil to a base material at the joining temperature, or to a cold joint, which can then be heated under pressure, but with no further mechanical activation. This method was the easiest, but also offered the least metallurgical interaction between the S-Bond materials and the base materials, as there is very little mechanical activation to break up surface oxides. This placement method also has to be done in conjunction with the U/S press, described below, when the filler foil performs after melting is mechanically disrupted in position by ultrasonic cavitation.

- Paste pre-coating and vacuum treatment at 850°C (S-Bond 220 only). This method required the application of S-Bond 220 paste to a cold base material, drying the paste at ~100°F until the solvent in the binder evaporated, and vacuum heat-treating the coated part at temperatures in excess of 860°C. This allowed for metallurgical interaction with materials such as ceramics, titanium alloys and stainless steels, which would normally only achieve an “atomic attraction” type of bond without this treatment. It cannot be used with aluminum, which melts at least 200°C below the normal vacuum heat treatment temperature, and it is not recommended for copper or its alloys, as the Sn-Cu intermetallics that form may tend to embrittle the joint. Because S-Bond 400 is largely composed of zinc, which has a very low vapor pressure, this method could only be used with S-Bond 220.

2. S-Bond® (active solder) alloys:

- S-Bond™ 220 (for service to 190°C). This is a modified Sn-3.5%Ag eutectic solder with titanium and other active elements. Its melting range is 221 to 238°C, it has a room temperature tensile strength of 53 MPa, and it has been found to wet to most metals, ceramics and glasses.

- S-Bond™ 400 (for service to 375°C). This is a Zn-4Ag-2Al solder with other active elements that has a melting range between 400 and 420°C, which has a room temperature tensile strength of 69 MPa, and also wets most metals, ceramics and glasses.

3. Joining procedures:

- Ultrasonic press joining involves assembling the prewetted parts to be joined, typically with excess S-Bond solder in the joint, at the joining temperature on the base of the press. The press is then activated, with pre-set levels of ultrasonic frequency and amplitude, to apply both pressure and ultrasonic pulses for mechanical activation during loading. The load then remains applied to the joined part until it has cooled to approximately 50°C below the solidus temperature of the S-Bond alloy.

- Slide / Oscillate / Rotate: This is an alternative to the ultrasonic press method, when the geometry not conducive to mating to an ultrasonic horn. This mechanical joining process involves the placement of two S-Bond® prewetted surfaces together while the filler metal is molten, then sliding the surfaces sufficiently that the surfaced oxides on the prewetted, molten S-Bond® is disrupted to expose fresh filler metal. After sliding a dead weight is normally applied to complete the joint.

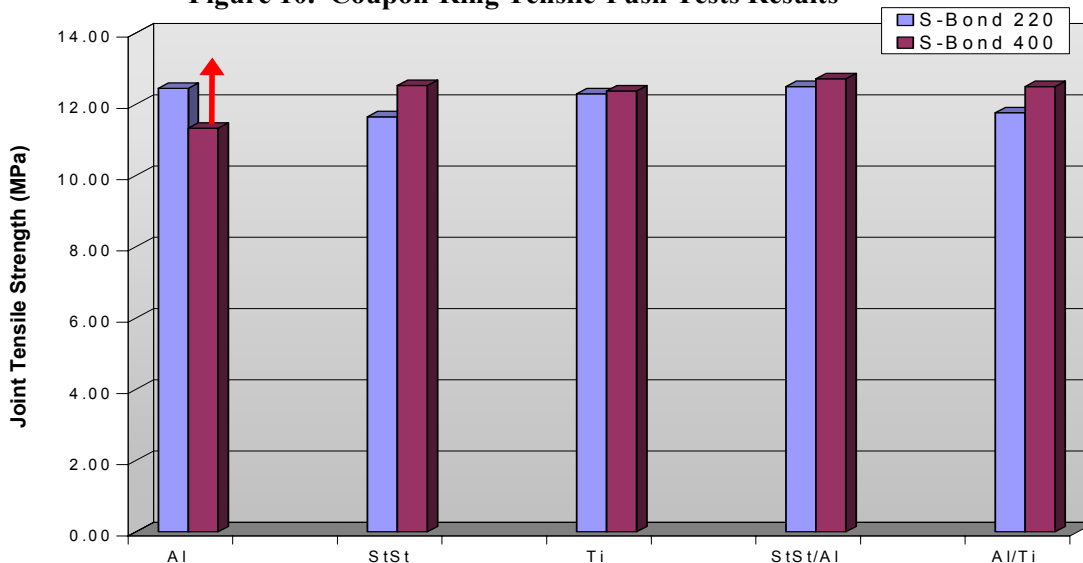
4.1.1 Structures: Mechanical Testing Results

The *Coupon/Ring Push* test showed average tensile strengths of 12 MPa for joints of Al, Ti, SS and their combination. Figure 10 shows that there was not much scatter of the data for all the materials tested for both S-Bond 220 and S-Bond 400 alloys.

All these samples were ultrasonically pre-wetted and joined under the ultrasonic press. The unexpectedly and consistently low tensile strengths cast some suspicion on the test results and/or configuration. It was

suspected that the deflection of the thinner plates created a stress concentration at the edge of the hole, lowering the apparent strength. To eliminate this, a rod/rod butt-tensile test specimen design was used. The results of initial tensile tests for samples joined with S-Bond 220 are shown in Figure 11.

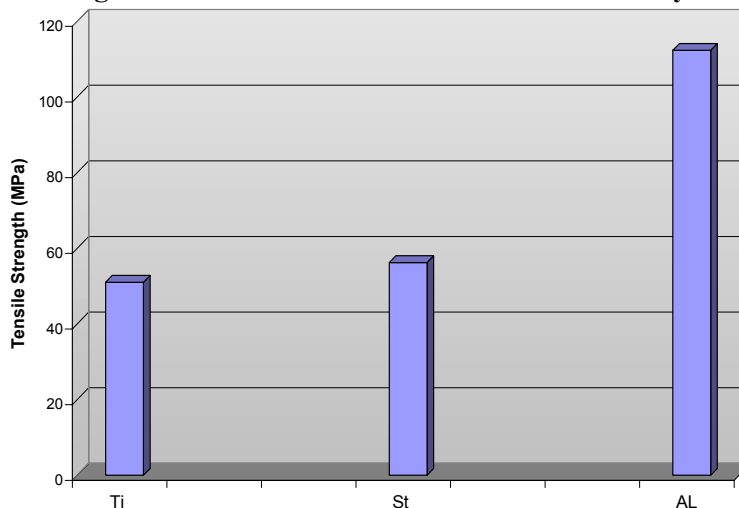
Figure 10. Coupon-Ring Tensile-Push Tests Results



For all tested samples, failure occurred at the joint-base metal interface. Except for Al samples joined with S-Bond 400, failure occurred in the aluminum button itself, rather than the joint. The repeatability of the failure indicated that the joint strength was more than that of the 1/8" aluminum coupon, and that the stress concentration created by deforming the aluminum coupon made the test non-representative of the S-Bond joint strength. Therefore, the flat coupon / ring push test (Figure 6) was abandoned in favor of the rod-rod butt (Figure 9) joint configuration.

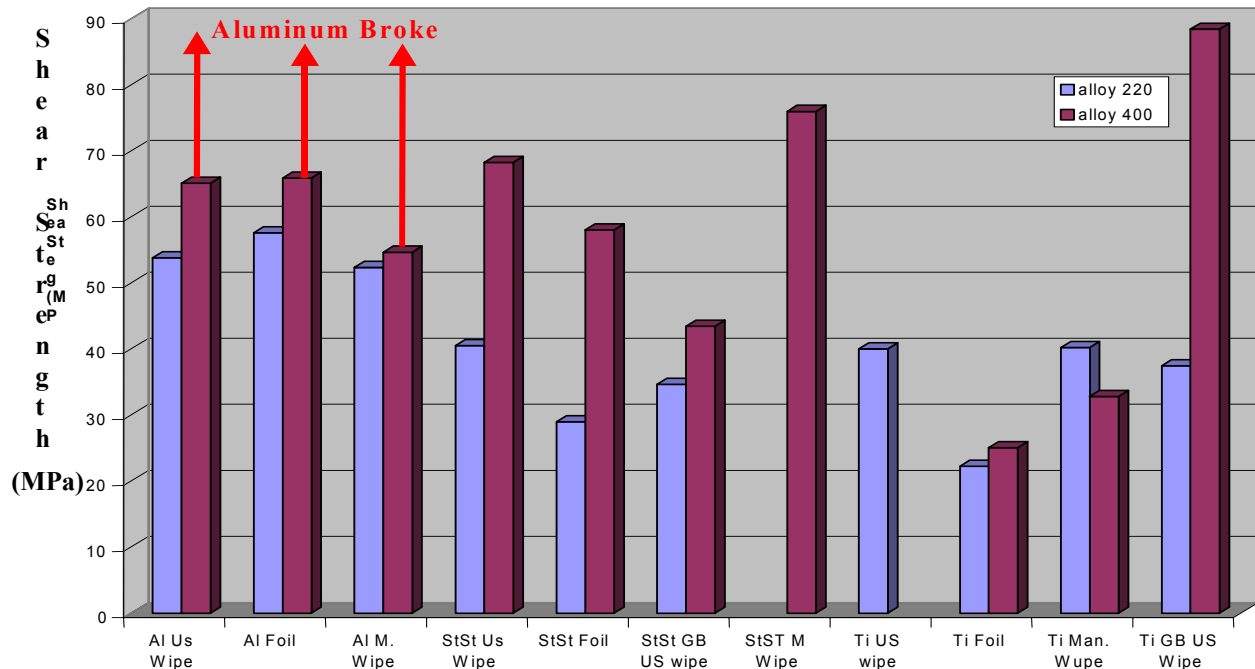
Rod-rod butt joint tensile tests were conducted and yielded high joint strengths, up to 112 MPa for Al/Al. For Ti and stainless steel the tensile strengths were 51 and 56 MPa, respectively. This demonstrated that high joint tensile strengths can be achieved with this test configuration, and therefore this test was used as the tensile strength test for all future work.

Figure 11. Rod/Rod tensile test results with Alloy 220



Single Lap Shear tests showed shear strengths as high as 88 MPa for ultrasonically pre-wetted S-Bond 400 joints on grit-blasted Ti. The lowest strength was 22 MPa for Ti joined by S-Bond 220 foil insert without pre-wetting, as shown in Figure 12. Though the same base metal, the rough surface, pre-wetting step and S-Bond 400 all contributed to higher strength, suggesting strong interaction between Ti and S-Bond 400.

Figure 12. Joints shear strength for single lap shear

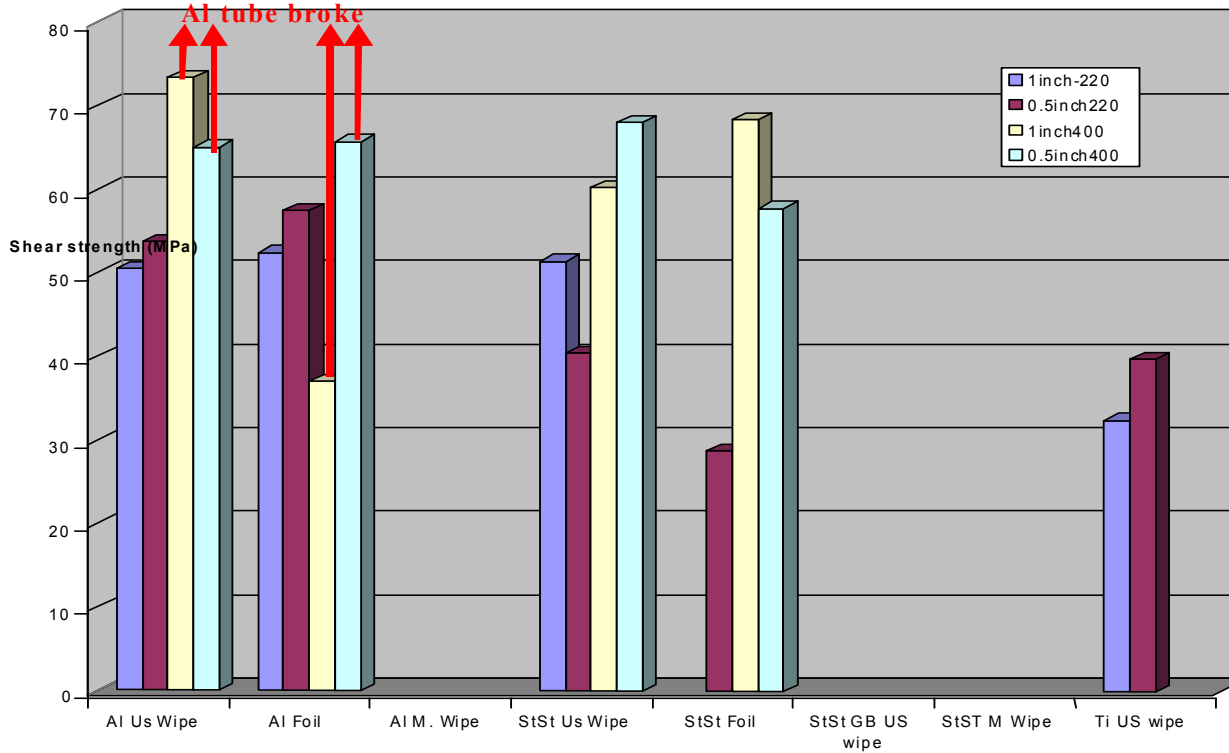


For *aluminum*, the highest strengths were 65 MPa for S-Bond 400 and 57 MPa for S-Bond 220. The samples joined with S-Bond 400 failed in the aluminum sheet, not the joint. The fact that the Al reached its ultimate tensile strength before the S-Bond joints failed indicated that properly assembled aluminum S-Bond joints can be stronger than the aluminum itself. Comparing all pre-wetting techniques, only small changes in the shear strengths (52-57 MPa) for S-Bond 220 were observed. However, for S-Bond 400, the strength was notably higher for the ultrasonic pre-wetting and the foil insert than for the manual wiping technique.

For *stainless steel*, S-Bond 400 joints showed almost double the strength of S-Bond 220 under the same conditions. The highest strengths were 85 MPa for S-Bond 400 and 40 MPa for S-Bond 220. The lowest were 43 MPa for S-Bond 400 and 23 MPa for S-Bond 220. Grit blasted stainless joints showed lower strengths than expected, perhaps due to porosity on the interface, discovered during metallography tests. The ultrasonic and manual wiping techniques yielded higher strength than the foil insert non-wiping technique. Failure occurred in the joints for all stainless steel samples.

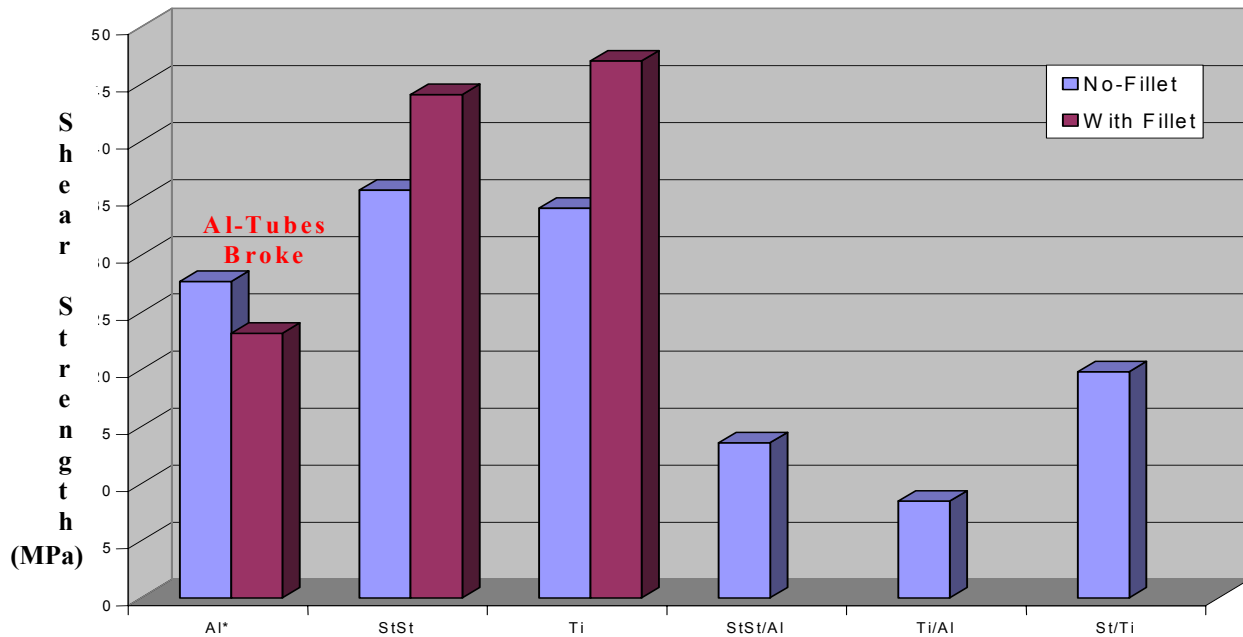
For *titanium*, S-Bond 400 joints made by ultrasonically pre-wetting grit blasted titanium showed the highest strength (88 MPa), which was double the strength for S-Bond 220 under the same conditions. Joints made with an S-Bond 220 foil insert, no pre-wetting, and manual wiping did not differ much from S-Bond 400 joints with the same conditions. Both manual and ultrasonic wiping of Ti gave the same strength for S-Bond 220. The foil insert joints showed lower strength in Ti than stainless steel and Al. Failure for all Ti samples occurred at the interface of the solder and the Ti surface. Doubling the widths of the joint did not significantly change the joint shear strengths for the various materials. However, some smaller joints showed slightly higher strengths than larger joints for Al and Ti, as shown in Figure 13.

Figure 13. Effect of doubling the joint width on the shear strength.



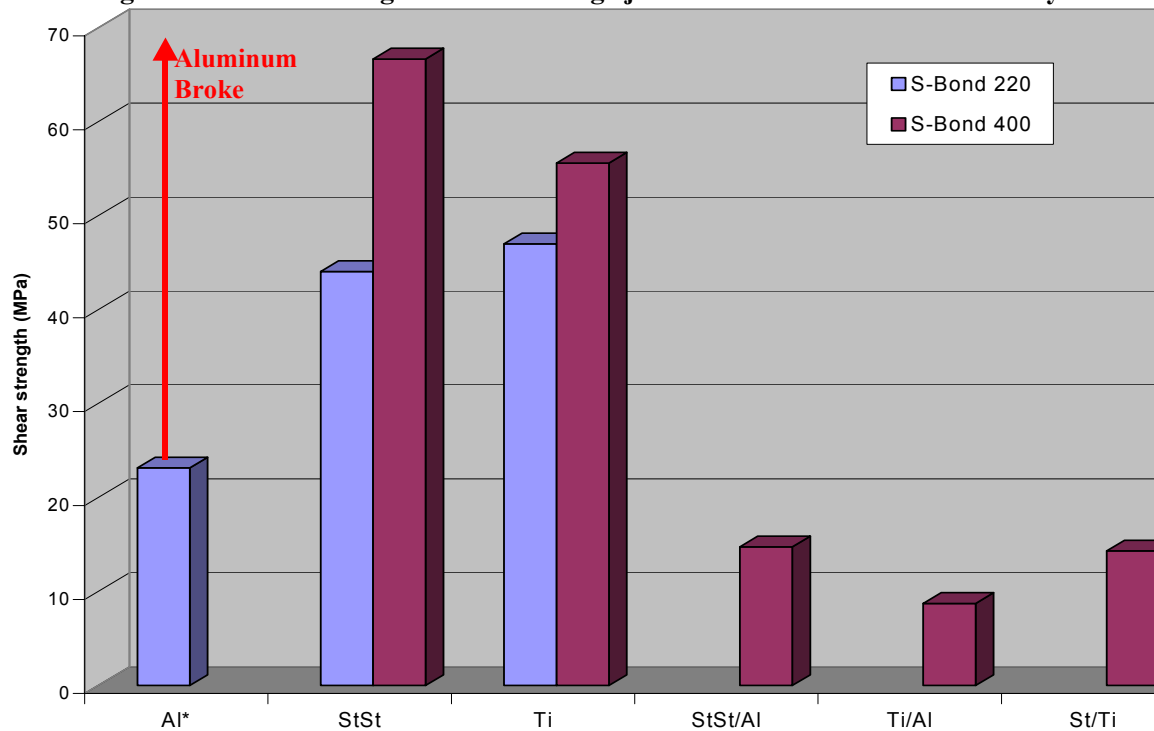
For the *tube-rod joints*, the shear strengths of joints with fillets and joints without fillets were evaluated. All aluminum samples failed in the tubes rather than in the joints, so the samples were redesigned and tested. Joints with fillets exhibited higher strengths than joints without fillets for ½” tubes joined with S-Bond™ 220, as shown in Figure 14.

Figure 14. Effect of adding fillets on the joint strength for tube/flange configuration



The highest strength for S-Bond 220 was 47 MPa for Ti/Ti tubes with fillets. The shear strengths of dissimilar metal tube joints were lower than those for tubes joined from similar material. Tubes with larger differences in the coefficient of thermal expansion (CTE) exhibit lower shear strengths, such as Ti/Al, with CTEs of 8.5 and $23.4 \times 10^{-6}/^{\circ}\text{C}$, respectively. The smallest CTE difference was between Ti and SS, 8.5 and $15.8 \times 10^{-6}/^{\circ}\text{C}$ respectively. Joints made from these material combinations showed more than double the shear strength of the joints made from Ti/Al.

Figure 15. Shear strength of Tube/Flange joints for two different solder alloys

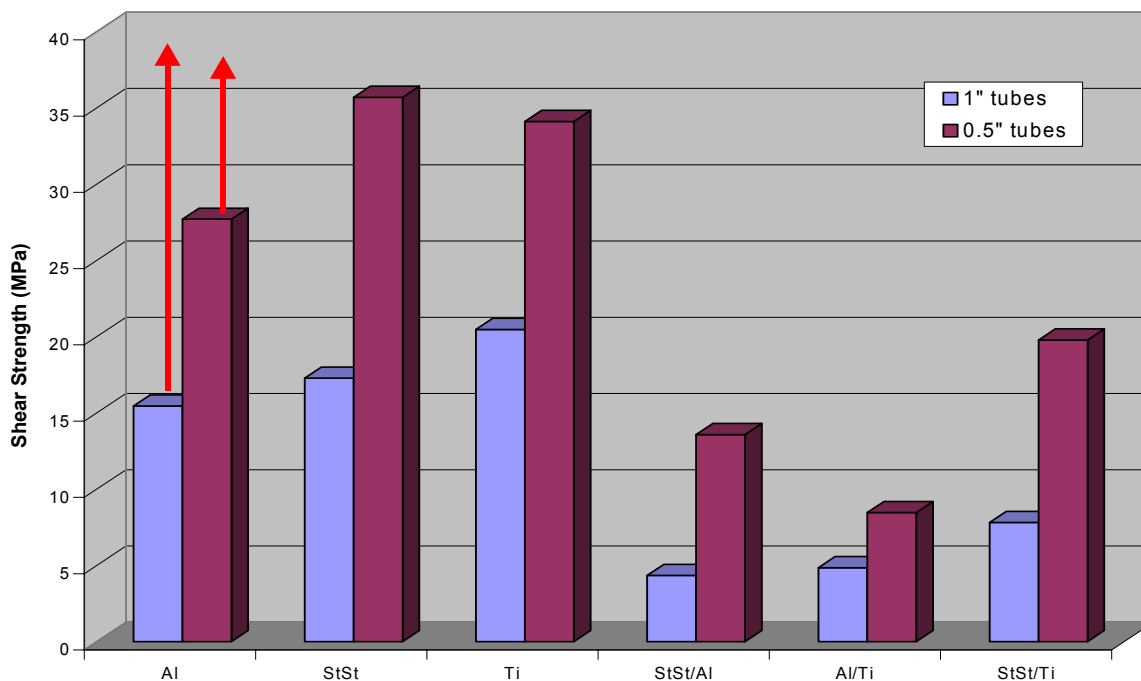


S-Bond 400 showed higher strength than S-Bond 220 for all materials combination as shown in Figure 15. Stainless steel ½” tubes experienced 50% increase in the shear strength by changing the solder from S-Bond 220 to S-Bond 400.

Large tubes showed lower shear strength than small tubes joined under the same conditions. Although doubling the tube diameter doubles the joint area, 1” tubes showed almost half the strength of ½” tubes, as shown by Figure 16. The CTE difference effect became clear from the comparison of the shear strength for dissimilar tubes. Smaller CTE differences increase the shear strength for the smaller tube diameter samples. Residual tensile stresses occur in the joint after solidification because the low CTE materials compose the tubes and the higher CTE materials compose the rods inside the tubes. Decreasing the CTE difference lowers this residual tensile stress and thereby increases the shear strength of the joint.

The shear strength for stainless steel joined to either Ti or Al with the small tube configuration was 3 times the strength found for the large tubes of similar composition. The small tube Al/Ti joint, with the largest CTE difference, exhibited shear strength twice that of the large samples. The sample design was intentionally kept so that the tubes had a smaller CTE and the rods had the higher CTE, in order to test the joint strength under the worst possible circumstances, i.e. the highest residual tensile stresses. As shown in Figure 11, even under these circumstances, the Ti (tube)/Al (rod) joints held shear strength up to 8.5 MPa before failure.

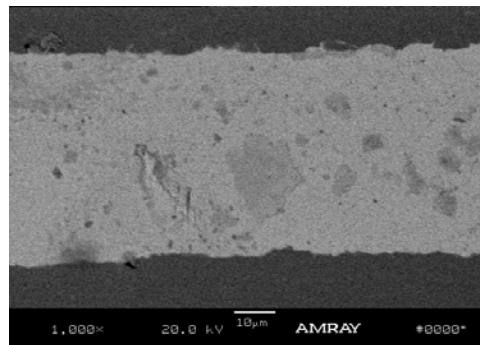
Figure 12. Effect of tube diameter on the shear strength of Tube/flange joints



4.1.2 Metallography Results / Summary

Light optical microscopy and scanning electron microscopy were used to characterize numerous S-Bond joints. The follow section describes some of the more important observations.

Figure 17. SEMicrograph of u/s prewetted, S-Bond 220 joined Al-Al cross section.



Aluminum

Ultrasonic pre-wetting:

Optical and SEM micrographs of Al/Al joints made with S-Bond 220 and S-Bond 400 and ultrasonic wiping showed sound joints, including a noticeable reaction at the interface between the Alloy 220 and Al. S-Bond 400 had a sufficiently strong reaction with Al to make it hard to distinguish between the alloy and the joined surfaces after bonding, as shown in Figures 17 and 18. This strong metallurgical interaction explains the high joint strengths seen in mechanical testing results, where the aluminum alloy was failing first.

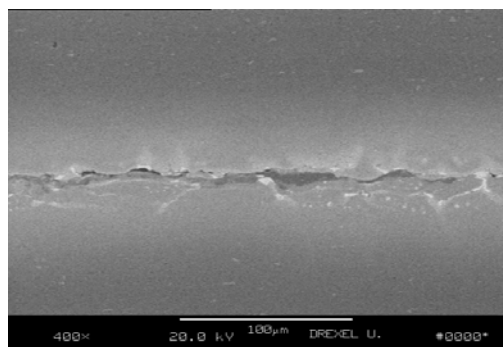


Figure 18. SEMicrograph of U/S prewetted, S-Bond 400 joined Al-Al cross section.

Foil insert:

Metallography of Al joined with S-Bond 220 foils, without initially pre-wetting, showed sound joints with slight interaction at the interface, as shown in Figure 19. S-Bond 400 also exhibited strong metallurgical interactions with the aluminum base metals, despite being applied in foil form without pre-wetting, as shown in Figure 20. Metallographic cross sections of joint interfaces were no longer flat and it was apparent that the alloy diffused through the Al.

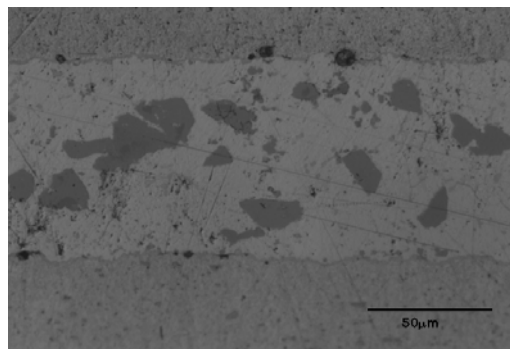


Figure 19. Micrograph of Al-Al cross section with S-Bond 220 foil inserted only.

Manual wiping pre-wetting:

As before, S-Bond 220 joints showed some reaction at the interface with the Al surface and the metallography showed sound joints, as shown in Figure 21. S-Bond 400, not only reacted with Al but dissolved significantly, as was seen in high magnification SEM photomicrographs, as shown in Figure 22.

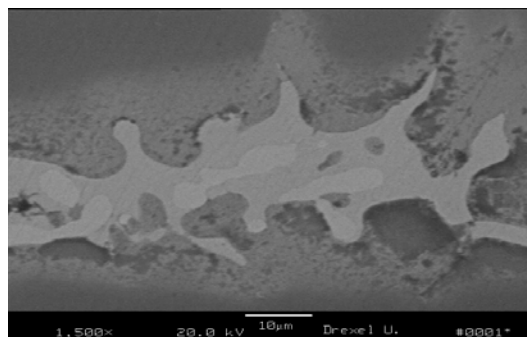


Figure 20. Al-Al cross section with S-Bond 400 foil inserted only. Note the extensive reaction.

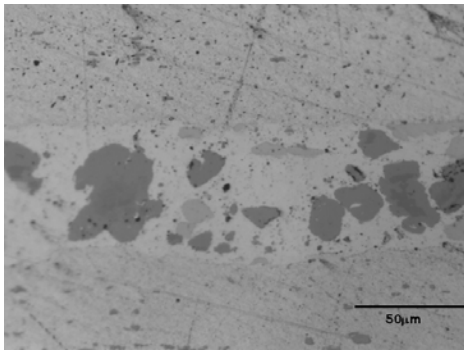


Figure 21. Micrograph of Al-Al cross section with manually wiped S-Bond 220.

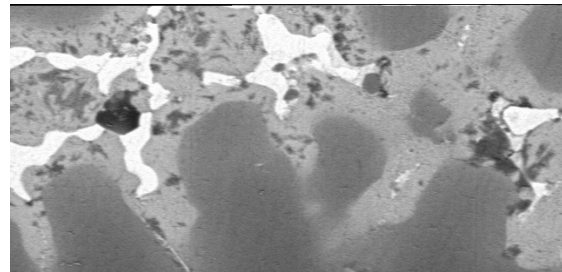


Figure 22. Al-Al cross section with manually wiped S-Bond 400. Note the extensive reaction.

Stainless steel

Ultrasonic pre-wetting:

Stainless steel S-Bond™ joining proved to be more of a challenge than joining Al. Some metallography of the joints showed voids, which may explain the lower joint strengths. The voids disappeared when samples were re-tested, without changing any of the joining conditions, which suggests that human variance has a strong influence on stainless steel joining. Figure 23 shows a quality joint made with this method. Figure 24 shows a successfully joined S-Bond 400/stainless steel joint made with ultrasonic pre-wetting, without any noticeable voids.

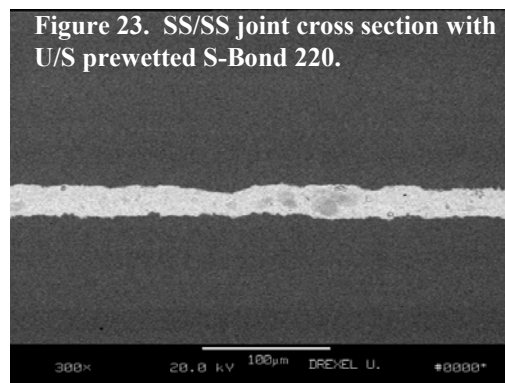


Figure 23. SS/SS joint cross section with U/S prewetted S-Bond 220.

Foil insert:

Both S-Bond 220 and 400 in the foil form produced good joints without separation on the interface, as shown in Figures 25 and 26.

Manual wipe pre-wetting:

Manual wipe pre-wetting with S-Bond 220 produced joints free of defects (Figure 22), though some voids were observed after manually pre-wetting with S-Bond 400, as shown in Figure 23, though these are believed to be due to application error.

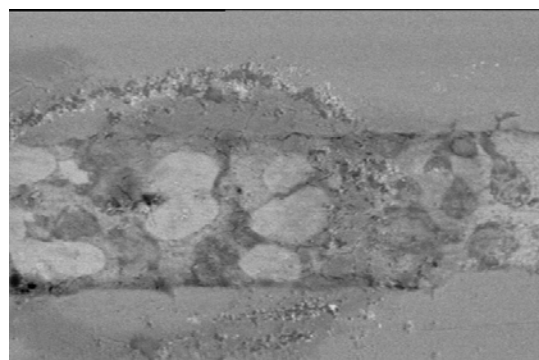


Figure 24. SS/SS joint cross section with U/S prewetted S-Bond 400.

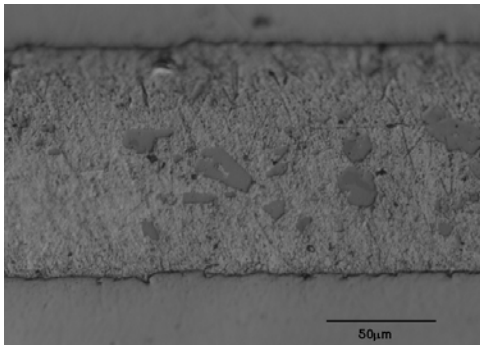


Figure 25. SS/SS joint cross section with non-pretreated (foil insert) S-Bond 220.

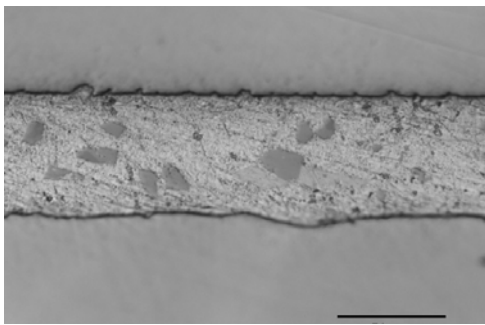


Figure 27. SS/SS joint cross section with manually pretreated S-Bond 220.

Titanium

Ultrasonic pre-wetting:

Ultrasonic pre-wetting with S-Bond 400 produced good interface, with visible reaction/diffusion beyond the original Ti surface, as shown in Figure 31. Some micro-porosity was seen distributed in the S-Bond™ 220 joint, as shown in Figure 29.

Manual wipe pre-wetting:

Manual wipe pre-wetting produced good Ti joints with both S-Bond 220 and 400, with some porosity at the S-Bond 400 interface. These joints appeared very similar to the ultrasonically pretreated samples shown in Figures 30 and 32.

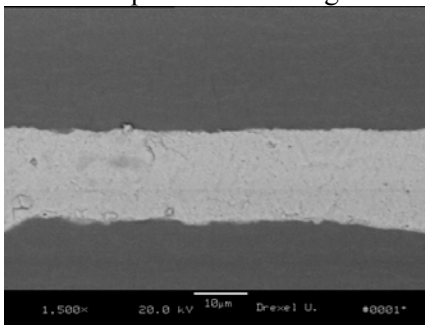


Figure 30. Ti/Ti joint cross section with foil inserted (non-pretreated) S-Bond 220.

Materials Resources International

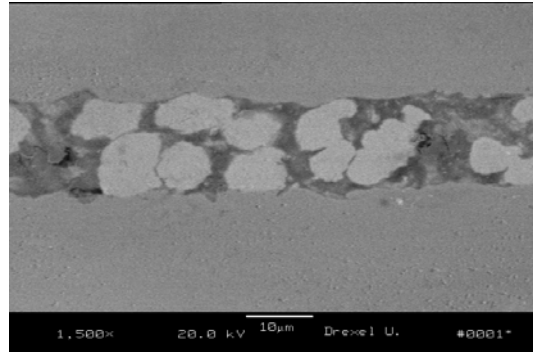


Figure 26. SS/SS joint cross section with non-pretreated (foil insert) S-Bond 400.

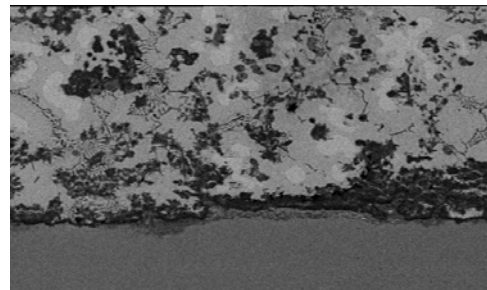


Figure 28. SS/SS joint cross section, manually pretreated with S-Bond 400.

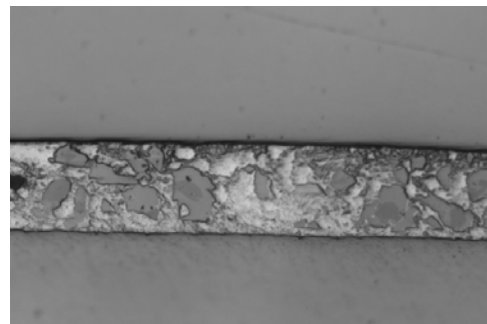


Figure 24. Ti/Ti joint cross section with U/S pretreated S-Bond 220. Manual pretreatment produced a very similar looking joint structure.

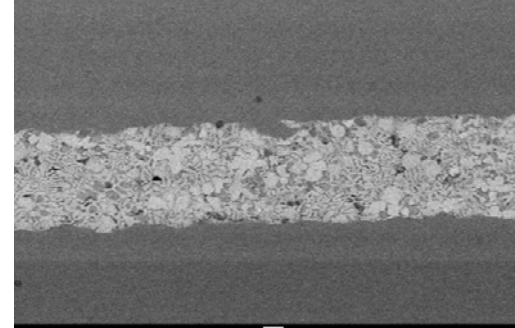
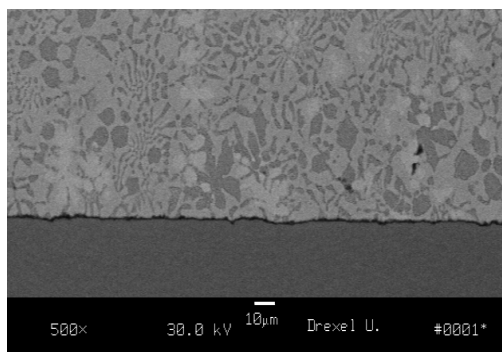


Figure 31. Ti/Ti joint cross section with U/S pretreated S-Bond 400. Note more extensive interaction than the S-Bond 220 joint.

Foil insert:

Bonding Ti with S-Bond 220 foil showed good wetting without separation at the interface, as shown in Figure 30, though the joint made by S-Bond 400 foil did not show as strong interaction at the interface (Figure 27).

Figure 32. Ti/Ti joint cross section with foil-inserted (non-pretreated) S-Bond 400. The manually pretreated S-Bond 400 joint looked very similar.



Coated Aluminum:

Coatings for wear or corrosion-resistance are often used on aluminum and/or aluminum matrix composites, so it was decided to test samples the effect of anodizing or chromating (iruditing) on S-Bond joining. To evaluate this, bonded aluminum samples were coated with two different techniques.

Anodized Aluminum

S-Bond 220 was able to join anodized Al and seemed to bond to both the coating and the base Al by flowing into the CTE mismatch-induced cracks in the anodized layer. See Figure 33. Figure 34 shows that S-Bond 400 bonded the anodized Al specimen by adhering to the coating and by reacting with the aluminum. More extensive cracking was observed in the anodized layer with S-Bond 400 joining than had been seen with S-Bond 220. This was most likely due to the higher bonding temperatures (~420°C) and therefore higher CTE mismatch between the aluminum and the anodized layer.

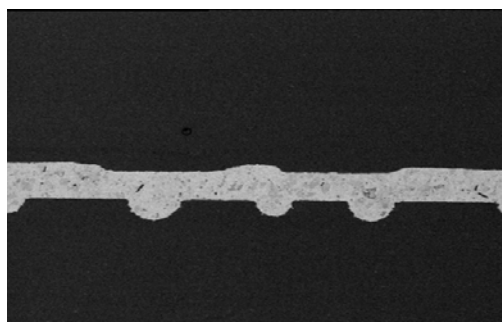


Figure 33. Anodized Al/Al joint made with S-Bond 220. The S-Bond wetted the anodized surface and the base metal below.

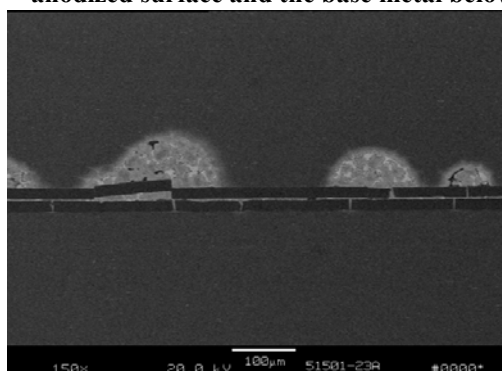


Figure 34. Anodized Al/Al joint made with S-Bond 400. Note areas where S-Bond got through cracks in the anodized layer and diffused into the Al.

Chromated (Irudited) Aluminum

Figures 35 and 36 illustrate the joint structures of the chromated aluminum. The chromated layer was not distinguishable under the microscope. S-Bond 220 bonded to the coating without porosity or separation. Despite the chromated layer on the surface of the aluminum, S-Bond 400 showed a strong interaction with the base material.

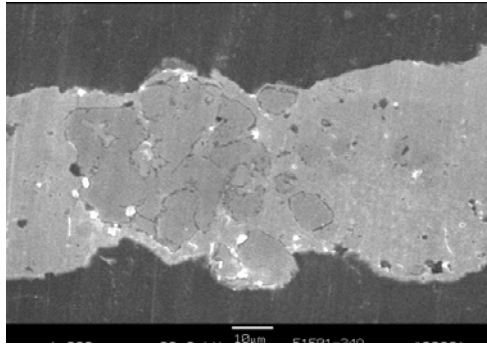


Figure 35. Chromated Al/Al joint made with S-Bond 220.

Dissimilar Material Joints:

S-Bond is capable of joining dissimilar materials despite CTE differences and wetting characteristics. S-Bond 220 showed joints free of defects for all Al, stainless steel and Ti combinations, as shown in Figures 37-39. S-Bond 400 also showed promising results in joining dissimilar materials, as shown in Figures 40-42. Good joints were observed between Al and Ti even when the alloy was used in the foil form, without pre-wetting. For stainless steel and Al, S-Bond 400 using ultrasonic pre-wetting showed good adherence to the surfaces without any separation. Some porosity was observed, which was attributed to joint thickness, as thicker joints have a higher probability of shrinkage porosity during solidification. Thinner joints were made to avoid such shrinkage, with better results. Stainless steel joined to titanium with S-Bond 400 using ultrasonic wipe pre-wetting showed high shear strength but metallography revealed some voids on the interface.

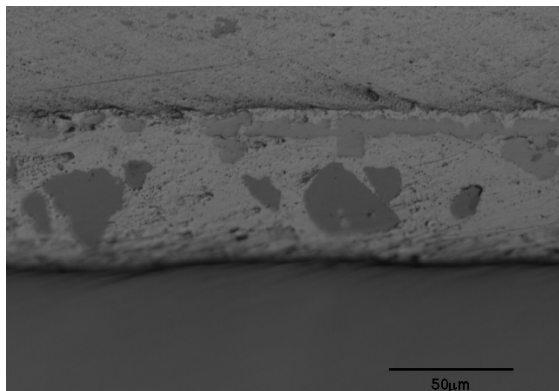


Figure 39. Aluminum/Titanium joint made with S-Bond 220.

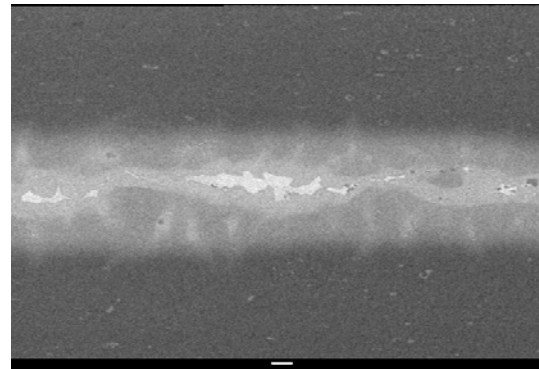


Figure 36. Chromated Al/Al joint made with S-Bond 400.

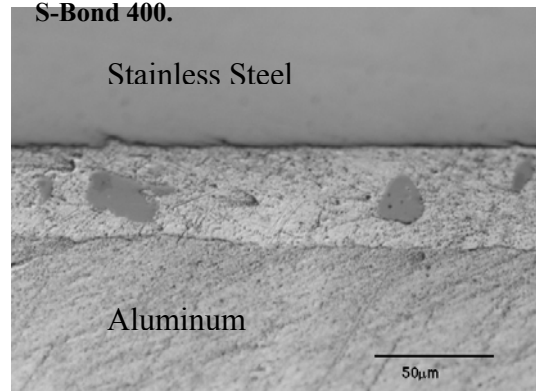


Figure 37. Stainless steel/Aluminum joint made with S-Bond 220.

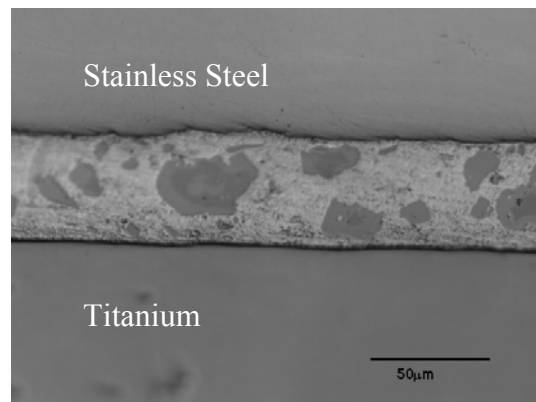


Figure 38. Stainless steel/Titanium joint made with S-Bond 220.

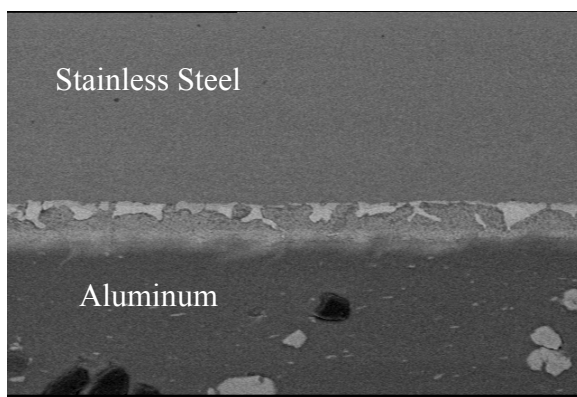


Figure 40. Stainless steel joined to Aluminum with S-Bond 400 foil.

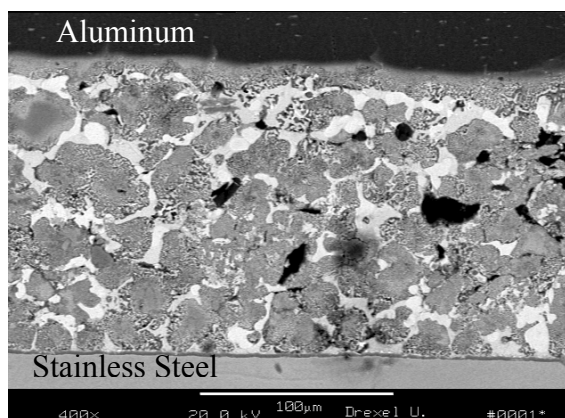


Figure 41. Stainless steel joined to Al with S-Bond 400 using ultrasonic wipe pretreatment.

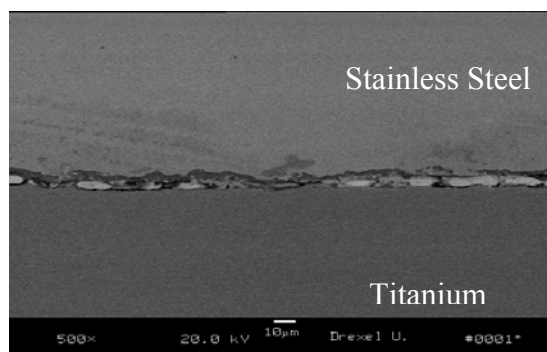


Figure 42. Stainless Steel/Ti joint made with S-Bond 400 using ultrasonic wipe pretreatment.

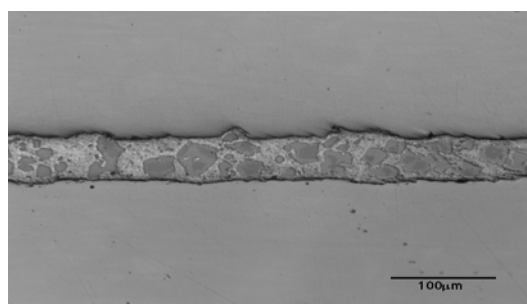


Figure 43. Stainless Steel/Stainless steel joint made with S-Bond 220 after grit blasting.

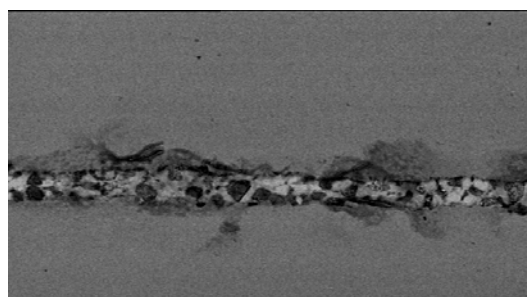


Figure 44. Stainless Steel/Stainless steel joint made with S-Bond 400 after grit blasting.

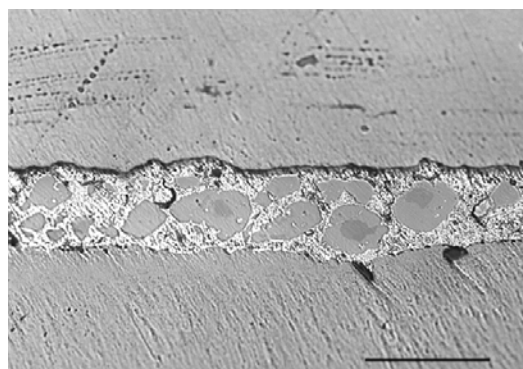


Figure 45. Ti/Ti joint made with S-Bond 220 after grit blasting.

Surface treatment before joining:

For S-Bond™ 220 joining, two surface preparation methods were evaluated as a way to enhance bond strengths. The first was roughening the surface by grit blasting. The second was premetallizing the joining surface with S-Bond 220 by coating the surfaces to be reacted with S-Bond 220 paste followed by vacuum heat-treatment at 850°C, in a vacuum of at least 1×10^{-4} torr. Both techniques improved joint strengths on ceramic and on metallic surfaces.

Grit blasting:

Stainless steel bonded by S-Bond 220 showed some embedded grit in the surface, though this varied among three different samples. Surfaces were ultrasonically degreased after each grit-blasting to help eliminate this factor. Figure 43 demonstrates that it is possible to achieve a joint with no embedded grit after the blasting process. Joining grit blasted stainless steel with S-Bond

400 showed some grit embedded in the surface of the joint, as shown in Figure 44. Figure 45 shows that grit blasted titanium bonded with S-Bond 220 exhibited good joint structure despite some grit embedded in the surface. S-Bond 400 showed joints free of defects except a little grit on the surface of the Ti, as shown in Figure 46.

Vacuum Treated Paste

Titanium to aluminum joints were made using vacuum pre-treatment with S-Bond 220 paste and subsequently joining with S-Bond 220 using ultrasonic wipe pre-wetting. These joints exhibited good adherence between the S-Bond and the reacted layer on the Ti, as shown in Figure 47. Dendrites were apparent at the interface between the coating and the S-Bond alloy, which were expected to grow during the high temperature heat treatment. The coating should be Ti-rich intermetallic due to the diffusion of titanium into the molten S-Bond during the heat treatment.

Stainless steel bonded to aluminum using the S-Bond 220 vacuum paste treatment showed good adherence at the interface and a noticeable reaction between S-Bond 220 and the stainless steel, as shown in Figure 48. Some interdiffusion of Fe, Ni and Cr from the stainless steel and Sn from the melted S-Bond 220 paste during heat treatment was expected and may have resulted in an intermetallic layer at the surface of the stainless steel.

Figure 48. Stainless steel/Al joint made with S-Bond 220 paste and vacuum premetallization.

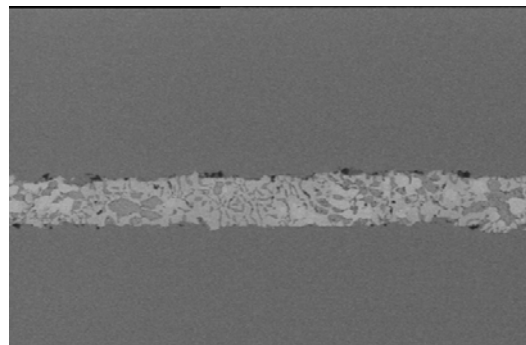


Figure 46. Ti/Ti joint made with S-Bond 400 after grit blasting.

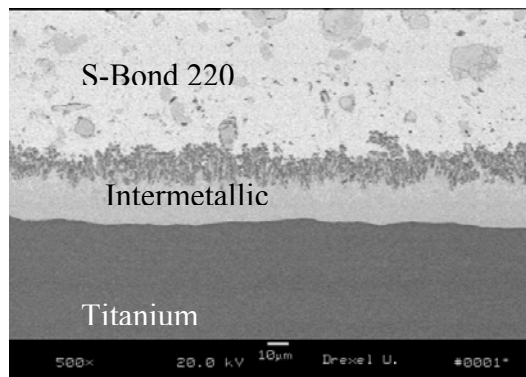
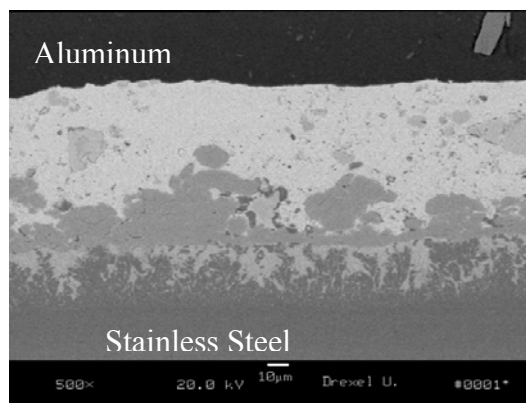


Figure 47. Ti side of a Ti/Al joint made with S-Bond 220 paste and vacuum premetallization.



4.1.3 Task 1.0: Structures – Conclusions

Summary of Conclusions for Lightweight Structures

These investigations have shown that S-Bond® joining has the capabilities to join Al-MMC's to a range of other structural materials that may be used in missiles and satellites. Although not a comprehensive data base, this body of information has identified processing methods and the effects of various parameters and geometries on the structure and strengths of S-Bond® Alloy 220 and Alloy 400 joints.

Aluminum alloys and MMC's, which are very common for such applications, wet very easily with both S-Bond 220 and 400. Titanium and stainless steel were also shown to produce strong joints under certain joining circumstances, for applications where higher strength is required. Surface treatments such as grit blasting or vacuum pre-treating of stainless steel and titanium were found to enhance bonding, but were not

necessary. Even coated aluminum materials, such as with yellow chromate finish or anodized layer, did not prevent S-Bond from effectively joining the base metals.

Overall the conclusion is that S-Bond® joining does have application in joining Al-MMC's in a range of structures applications, limited by the tensile capability and temperatures that are in the range of the alloys capabilities, for S-Bond® 220 that is up to 190°C while for Alloy 400 that is up to 350°C.

A summary of significant and specific results of these structural tests follow:

S-Bond™ Alloy 220

- U/S pre-wetting or more aggressive mechanical agitation of S-Bond 220 onto joint surfaces is recommended for ceramics, Al:SiC and metals other than aluminum or copper. This assures the maximum adherence of the S-Bond 220 layers and prepares the surfaces for subsequent joining.
- For ceramics and metals such as titanium or stainless steel, vacuum pre-treating at temperatures above 850°C with S-Bond 220 paste provided an excellent means of accomplishing a metallurgically reacted layer on the faying (surfaces to be bonded) surfaces.
- Agitation of the S-Bond alloys during joining was mostly accomplished using ultrasonic vibration, though oscillation or rotation produced nearly the same results. For flat joints, “sliding” components relative to each other while the S-Bond is still molten accomplishes similar results.
- Placement of foil in a joint and subsequent use of ultrasonic agitation to activate the S-Bond™ 220 alloy was deemed inconsistent for joining the range of investigated light metals and Al-MMCs.
- CTE mismatch can stress certain joint geometries and cause joints to either fail or exhibit lower bond strength. Tests on dissimilar metal tube joints over ½” in diameter exhibited this effect.
- The optimum process involved grit blasting the joining surfaces to roughen them (not needed for Cu, Al or Al-MMC), and ultrasonically spreading/brushing the S-Bond onto the joining surfaces.
- In some geometries, ultrasonic agitation during joining was not easily accomplished, such as in tube joining. For these, simple oscillation or counter rotation of joining surfaces yielded acceptable results.

S-Bond™ Alloy 400

- Increased the joints' usable temperature to 350°C, whereas S-Bond 220 was strong only to 190°C.
- Joined the same metals and composites as S-Bond 220, with stronger joints, especially titanium joints.
- Interaction with Al and Al-MMCs was strong due to rapid diffusion of the zinc from the S-Bond 400 into the Al. Pre-wetting procedures were necessarily more rapid and the contact time of the S-Bond 400 onto aluminum materials had to be short.
- Ultrasonic agitation of pre-placed foils, without first wetting the surfaces to be joined with molten S-Bond™ 400 alloy, did not work well.
- Manual or ultrasonic pre-wetting provided higher strength and better interaction with base materials and is therefore the recommended procedure.

Comparison of S-Bond 220 and S-Bond 400

- S-Bond 400 showed stronger interaction with certain base materials than S-Bond 220, as supported by higher strengths for some S-Bond 400 joints, especially aluminum joints. S-Bond 400 interacts with aluminum to form joints that are stronger than the aluminum base material, making S-Bond 400 an excellent high-temperature joining alloy for this base material.
- Manual or ultrasonic pre-wetting showed higher strength and better interaction with the base materials than the foil insert without pre-wetting.
- Titanium and stainless steel could be joined by either S-Bond 220 or 400, with some variation in joint strengths depending upon pre-wetting technique.

Surface treatment / Coatings:

- Grit blasting enhanced joint strengths on Ti and stainless steel, though it should be noted that embedded grit could lower joint strength. Thorough ultrasonic cleaning is recommended.
- Pre-wetting stainless steel and Ti samples by vacuum heat treatment with S-Bond 220 paste showed stronger interaction and resulted in higher joint strengths than other Alloy 220 pre-wetting techniques. This was also found to be an excellent method for use with ceramics, but is not recommended for use with S-Bond 400, because of the high zinc content.
- Flat lap joints showed fewer interface voids than cylindrical joints, especially between dissimilar materials with large CTE differences. For cylindrical joints, small gaps and fillets are recommended. It was found that increasing the diameter of the cylindrical dissimilar metal joints weakened the joints because the CTE mismatch was more pronounced.
- Push button tensile tests showed lower strength than rod/rod tensile tests, so the rod/rod tensile test was focused on and additional testing was conducted using this technique.
- 1/8" joint overlap for Al joints yielded failure of the Al base metal, not the S-Bond joints. 0.07" joint overlap allowed for failure in the joint area, enabling measurement of the strength of the joints.
- Anodizing S-Bond 220 or 400 joined specimens resulted in dissolution of the solder in the anodizing bath. However, chromating (iruditing) was successful with the same samples.
- Pre-anodized or pre-chromated samples could be joined with both S-Bond 220 and S-Bond 400. Chromated samples exhibited stronger interaction than anodized samples.

4.2 Task 2.0: Lightweight Armor

4.2.1 Introduction / Objectives

An outgrowth of the structural investigations was the assessment of using S-Bond® to join Al-MMC, Al-foams and other lightmetal backing to ceramic and/or composite strike plates. As such, MRi proposed to conduct investigations into the application, as shown in Figure 49. In this work, over the term of the contract MRi teamed with Fraunhofer USA for their application of aluminum foams, HPMG for application of their ceramic and Al-MMC composites and with the US Army Research Lab, for their interest in SiC strike plates joined to titanium backing plates. This diagram illustrates a composite armor concept that consists of the MMC layer bonded to lightweight aluminum foam, finally backed by Kevlar®. The idea was that a strong and ductile bond at the MMC/foam interface would transfer and absorb the kinetic energies of the impacting projectile, a charge for which S-Bond alloys are well suited. Their bonds were ductile and the alloys have been shown to wet and join both the Al-MMC's and the aluminum foams.

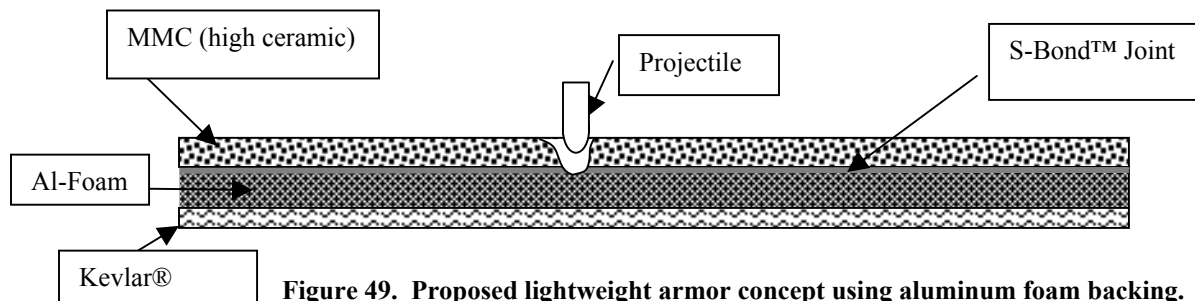


Figure 49. Proposed lightweight armor concept using aluminum foam backing.

The project selected this as one of the demonstrators, since certain space platforms could benefit from such armor to deflect projectiles and/or space debris. Such lightweight armor may also be suitable to “harden” certain missiles. The advancement of such armor concepts would yield an enabling technology for producing lightweight armor that would impact other US Army programs. Aluminum foams from

Fraunhofer, Al:SiC from HPMG, dMC², and SiC from CoorsTek were all used at various phases of the contract. Objectives were:

1. Develop S-Bond® procedures for various armor concepts
2. Demonstrate bonded armor 4" x 4" test panels.
3. S-Bond join selected ballistic test components.
4. Conduct ballistic testing of actual joined components.
5. Provide data to on ballistic tests.

In this work, MRi investigated several configurations of armor that had been suggested by partners or potential users. These configurations included:

1. SiC Ceramic Strike Plate on Al-Foam (Figure 49)
2. Si:SiC composite, SiC and/or Al-SiC on solid aluminum backing plate.
3. SiC ceramic strike plate on titanium backing plate (per US Army Research Lab)

MRi conducted S-Bond® joining evaluations on all of these configurations, separately looking at the issues and developing processing methods to counteract the coefficient of thermal expansion (CTE) mismatch problems that were encountered in each configuration.

4.2.2 Aluminum Foam / SiC Armor Evaluation

Bonded configuration:

Sets of standard joints were made and characterized to document the strength and the structure of the joints under different loading conditions. The following test samples were selected for investigation:

1. Double lap shear (DLS) specimens made from 1" x 1" x 1/8" faceplates joined to 1" cubes of Al foam from both sides with partial overlap of 0.25".
2. Metallography samples made from 1" x 1" x 0.125" faceplates joined to 1" cubes of Al-foam on one side with full over lap.
3. Ballistic test samples made from 4" x 4" x 0.125" faceplates joined to 4" x 4" x 1" Al-foam.

Double Lap Shear (DLS) samples, 1" square metallographic samples and 4" square ballistic test samples were produced for various material combinations and joining conditions. DLS samples were mechanically tested to measure the shear strengths of the joints. Metallographic samples were characterized by both optical microscopy and scanning electron microscopy. Ballistic test samples were sent to Fraunhofer for nondestructive and destructive tests.

4.2.2.1 - Al-Foam / Ceramic & Composite Metallography

1. Al-foam by PM-Hydride [Fraunhofer USA] Alumina

S-Bond 220 and S-Bond 400 are capable of bonding to ceramic faceplates and to any oxide skins on the aluminum foams. Both S-Bond alloys bonded to alumina without noticeable separation at the interfaces. See Figures 50 and 51.

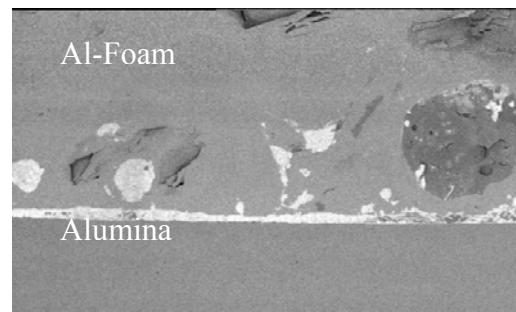


Figure 50. Al₂O₃/Al-Foam joint using S-Bond 400 with ultrasonic wipe prewetting.

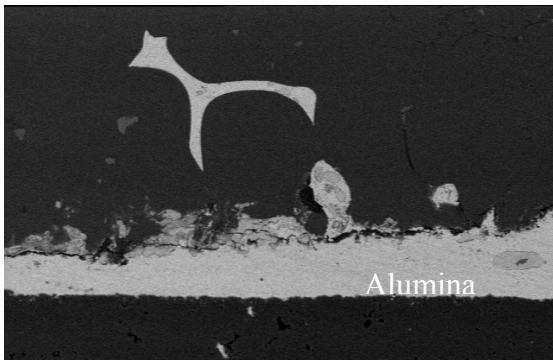


Figure 51. Alumina bonded to Al-Foam with vacuum pretreated S-Bond 220.

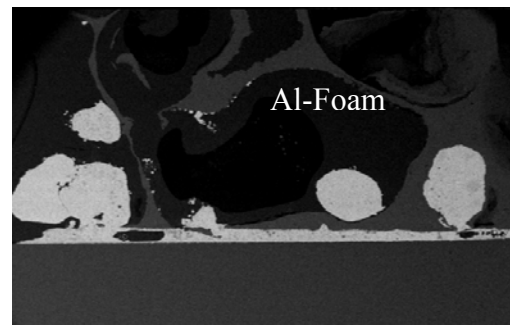
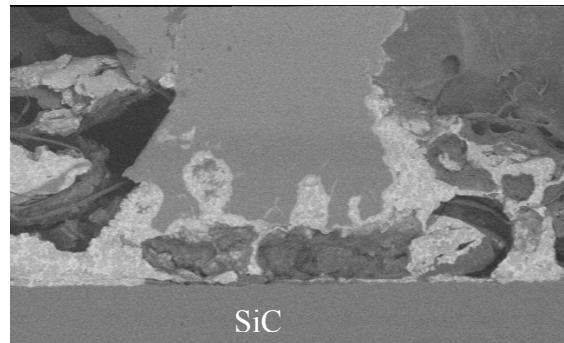


Figure 52. SiC bonded to Al-Foam with vacuum pretreated S-Bond 220.

Silicon carbide

Both S-Bond 220 and 400, using ultrasonic wipe pre-wetting, bonded SiC to Al-foam without separation at the interface, as shown in Figure 53. Some small voids were apparent, but these varied from one joint to another and disappeared when thinner joints and careful wiping were used. SiC that had been vacuum pre-metallized with S-Bond 220 paste bonded to Al-foam without any voids or separation at the interface, as shown in Figure 52. S-Bond 220 filled the holes in the Al-foam and bonded to the Al webs, yielding strong joints. Using S-Bond 400 in foil form (no prewetting) produced a sound joint that reacted strongly with the aluminum foam by filling the cavities in the surface of the foam as well as reacting with the Al itself, as shown in Figure 54.



Silicon-Silicon Carbide Composite (Si:SiC)

S-Bond 220 and 400 bonded to Si:SiC without separation in the interface or noticeable voids in the joint. The interaction between the solder and Si:SiC was stronger than with SiC, due to the irregularities in the interface surfaces, as can be seen in Figures 55 and 56. The S-Bond 220 paste exhibited strong metallurgical interaction with Si:SiC during vacuum heat treatment, as shown in Figure 57. The silicon matrix dissolves, leaving SiC particles in a Si-rich Sn phase. Also, at the interface between the S-Bond 220 and the reacted paste, a possible continuous Ti (Si) rich phase separates the Si-rich S-Bond from the added S-Bond 220 alloy. These results indicate that the S-Bond 220 paste with vacuum treatment produced stronger bonds with Si:SiC.

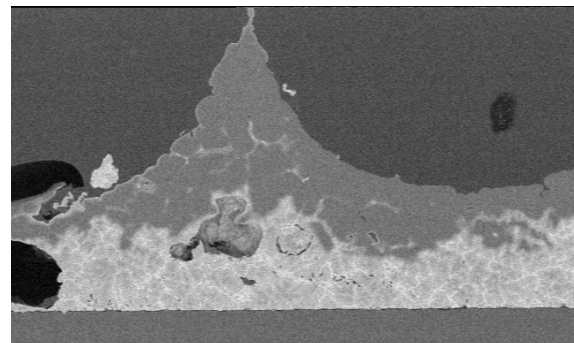


Figure 54(49). SiC/Al-Foam joint using S-Bond 400 foil only (no prewetting).

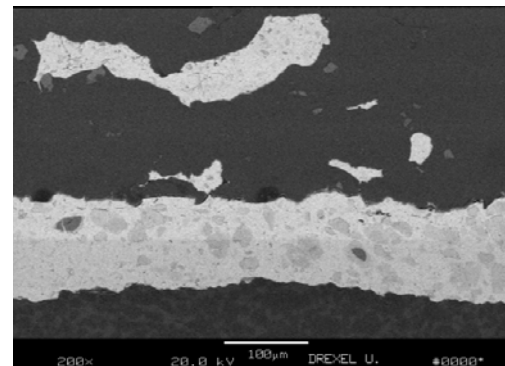


Figure 55. Vacuum pretreated Si:SiC ultra-sonically joined to Al-Foam using S-Bond 220.

were similar to the photomicrograph shown in Figure 56.

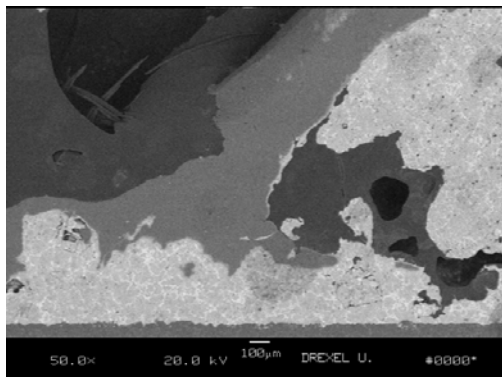


Figure 56. Si:SiC and Al-Foam ultrasonically joined using S-Bond 400.

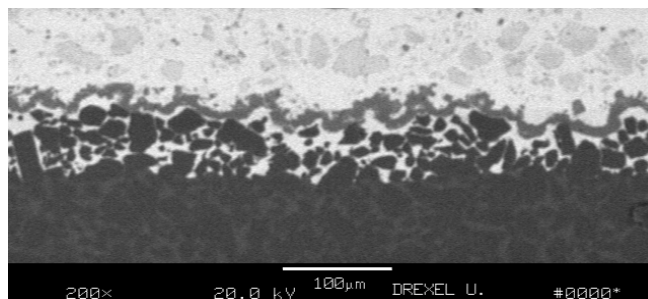


Figure 57. Si:SiC interface with S-Bond 220 after vacuum pre-treatment.

2. Gas Injected Al-Sponge [Cymat]

MRi had been contacted by another manufacturer of aluminum foams, Cymat, whom made their foams by adding small amounts of SiC with melted aluminum scrap and then by blowing inert gas through the melt prior to solidification. The structure produced by this process was much more open cell and larger pores than the Fraunhofer (P/M metal hydride) aluminum foams. This investigation looked at these foams to determine S-Bond joining to these Cymat foam types.

S-Bond 400 bonded alumina, SiC and Si:SiC to Al-sponge with sound joints free of voids, using ultrasonic wipe pre-wetting. A representative photomicrograph of such a ceramic joint is shown in Figure 58, while the Si:SiC composite joint is shown in Figure 59.

Two different pre-wetting techniques were evaluated for joining Si:SiC to Al-sponge. Si:SiC that had been vacuum pre-metallized with S-Bond 220 paste (Figure 60) showed more interaction with Si:SiC than pre-wetting by ultrasonic wiping (Figure 61).

S-Bond 400 foil produced as sound a joint as that made by ultrasonic pre-wetting, as shown in Figure 62. A reaction layer was observed at the interface between S-Bond and Si:SiC, which is

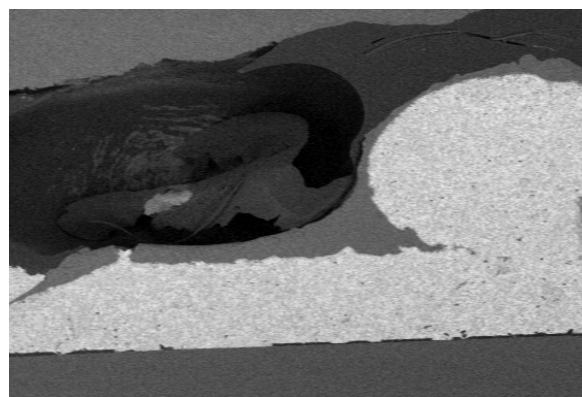


Figure 58. SiC interface with S-Bond 400 after ultrasonic prewetting. Alumina looked very similar.

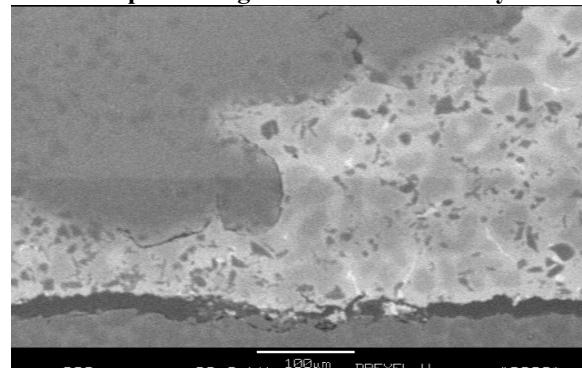


Figure 59. Si:SiC interface with S-Bond 400 after ultrasonic prewetting.

presumably from the diffusion of Si into the solder.

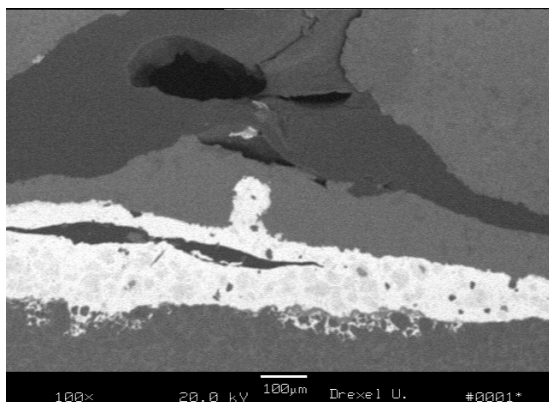


Figure 60. Si:SiC interface with S-Bond 220 after vacuum/paste pretreatment.

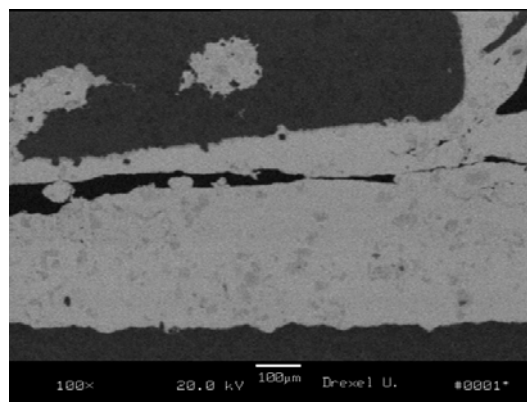


Figure 61. Si:SiC interface with S-Bond 220 after ultrasonic pretreatment.

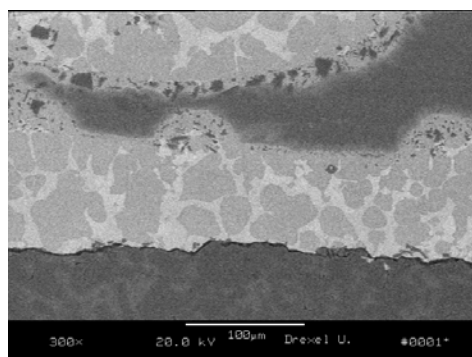


Figure 62. Si:SiC/Al-Sponge joint using S-Bond 400 foil only (no pretreatment).

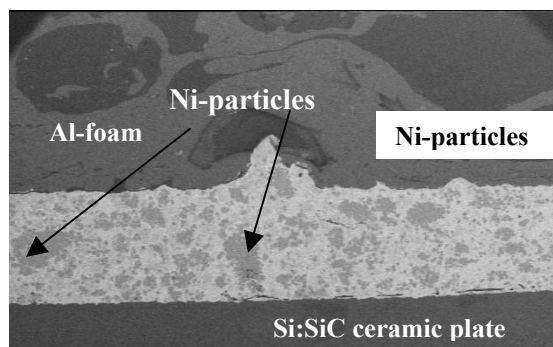


Figure 63. Si:SiC/Al-Foam joint using S-Bond 220 with nickel particles.

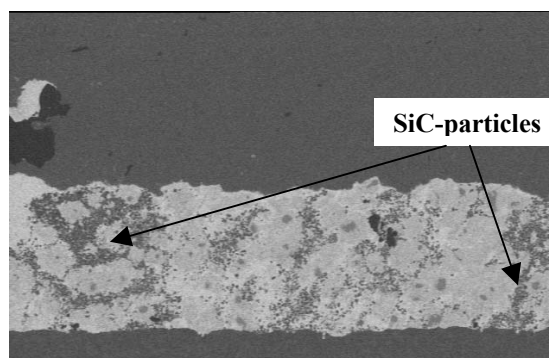


Figure 64. Si:SiC/Al-Foam joint using S-Bond 220 with SiC particles.

S-Bond Transitional Composite Joints:

Due to CTE-mismatch induced cracking observed in some of the earliest produced 4" square test samples, experiments were done with transitional layers in the S-Bond joints. These composite transitional layers consisted variously of S-Bond with nickel or SiC particles, or S-Bond with a transitional layer of solid Si:SiC composite between the Al foam and the SiC, to help compensate for the significantly different thermal expansion coefficients.

Metallographic tests of S-Bond 220/nickel particle composite joints revealed that there was good metallurgical interaction between the composite S-Bond joint and both the Al base plate and the Si:SiC face-plate, as shown in Figure 63. Nickel particles were well adhered to the S-Bond alloy and were well interspersed, though with some small agglomerates of the nickel particles and some local cracking at the interface of the composite S-Bond and the aluminum foams, where the thermal strains are highest. These localized cracks were not continuous, so the overall joint was successful.

Metallographic tests of the SiC powder particles/S-Bond composite joints showed excellent interaction between the S-Bond composite and both the aluminum and ceramic plates, as shown in Figure 64. The SiC particles were not as well dispersed as the Ni-particles had been, but at higher magnification it was apparent that the SiC agglomerates were well wetted by the S-Bond 220 matrix. The Al foam/S-Bond interface was continuous, well adhered and exhibited no signs of cracking. This initial evaluation indicated, at least for the particulate S-Bond composite joints, that SiC was a better choice for this application than Ni-particles.

The other approach used a continuous thin (~0.050") Al:SiC composite layer (provided by HPMG) between the Al foam and the Si:SiC plate. These joints were successfully adhered with no macroscopically apparent de-bond of the S-Bond composite joint, using both 20 volume % and 40 volume % SiC. Metallography results, Figure 65, indicated that the Al:SiC layer, Al base plate and Si:SiC plate were all wetted well by the S-Bond 220 alloy. Naturally, this configuration provided a much more consistent cross section than the particulate composite joints had. Metallographic results showed that the 40 volume % Al:SiC exhibited less micro-cracking, presumably due to the better-matched CTE, so it was decided to focus on this material for further transitional layer experiments.

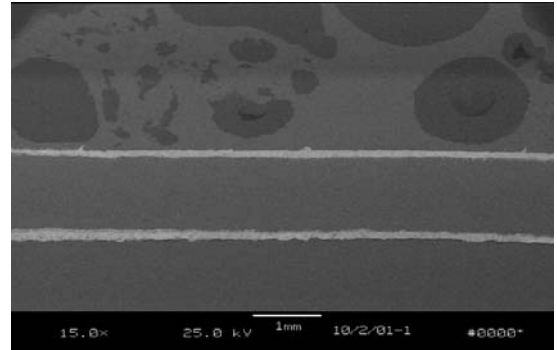


Figure 65. Si:SiC/Al-Foam joint using a 40vol% Al:SiC transition layer and S-Bond 220.

4.2.2.2 - Al Foam/SiC Shear Testing

Double lap shear (DLS) samples were compression tested to measure the shear strengths of S-Bond joints between various ceramic face-plates and aluminum foam backing. Figure 66 shows the style of joints studied. This off-set style permitted compression testing to load the ceramic face-plates in shear until failure. Figure 69 presents a summary of the maximum joint shear strength for each style joint. Figures 67 and 68 illustrate the types of failures that were mainly experienced, where the aluminum foams failed or fracture in the ceramic occurred, indicating strong S-Bond joints.



Figure 66. Double lap shear (DLS) specimen before and after joining

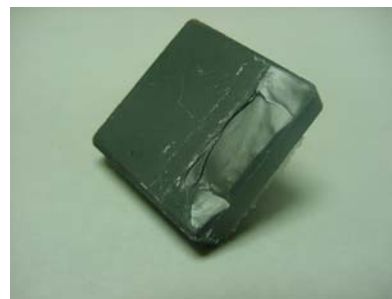
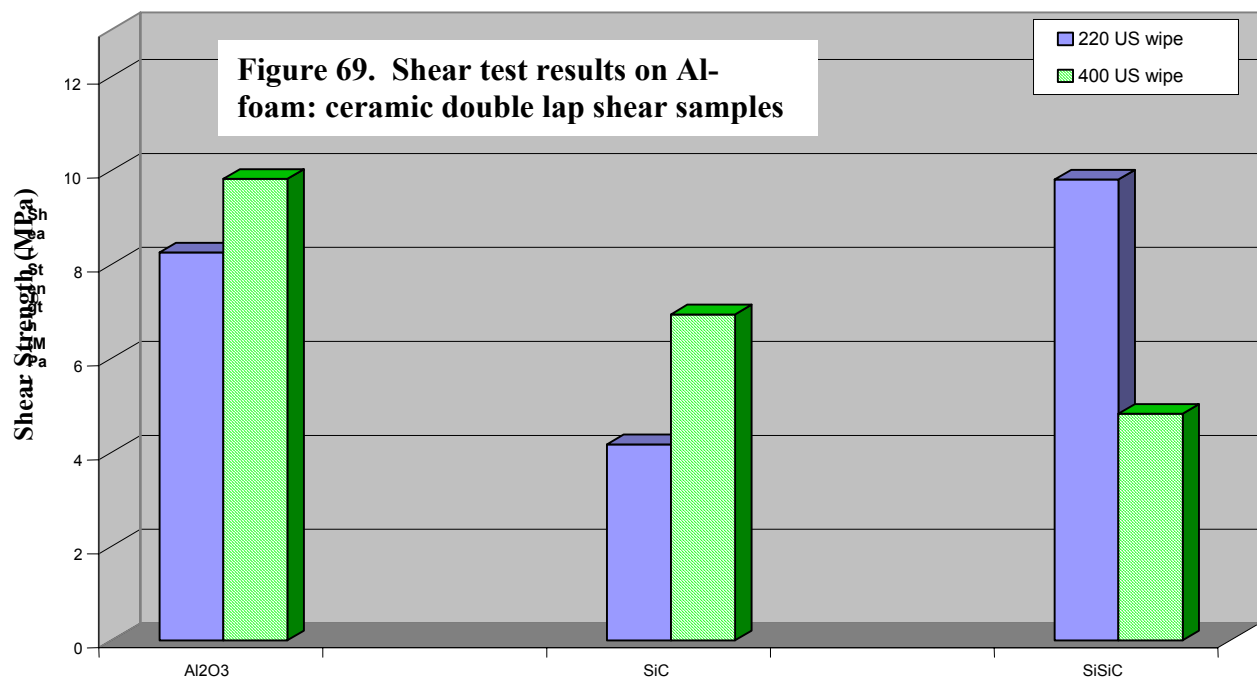


Figure 67 and 68. Pictures of failed composite armor test samples.

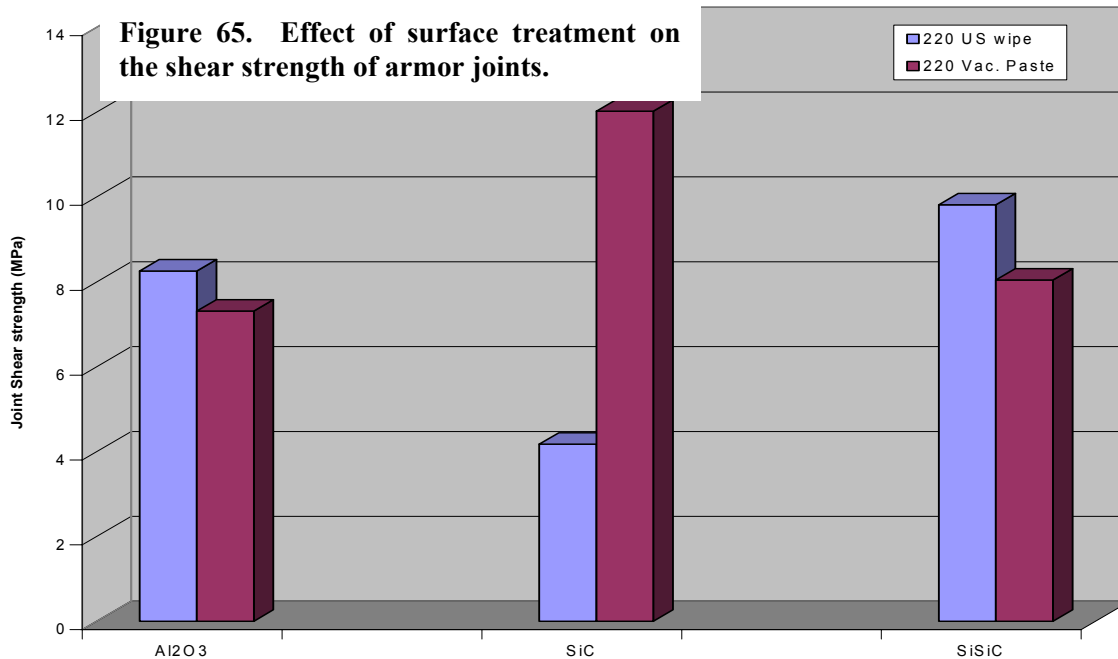


These faceplate materials were bonded to closed cell aluminum foams made by Fraunhofer [using powder metallurgy-hydride procedures], to evaluate joint structures and strengths. Candidate faceplates were also bonded to Al-foams made by Cymat Aluminum Corp. [using gas injection in melt] to evaluate the change in the joint structure with the foam manufacturing technique. Small scale test specimens were used to identify the process parameters best suited for testing the bonds on larger samples.

Shear Testing Results:

The maximum shear strength of the tested samples was found to be 12 MPa for SiC joined by vacuum pre-treating SiC with S-Bond 220 paste at 850°C. All failures were in the foam. The lowest shear strength was 4 MPa for SiC joined by S-Bond 220 with ultrasonic pre-wetting. For SiC the vacuum paste pretreatment produced shear strength three times the shear strength of the samples joined with S-Bond 220 without any pretreatment. For Al₂O₃ and Si:SiC the difference between pre-wetting with S-Bond 220 with and without vacuum treatment was about 1 MPa, as shown in Figure 65.

S-Bond 400 showed the highest strength, 9.8 MPa, for Al₂O₃ joined to Al-foam and the lowest strength, 4.8 MPa, for Si:SiC faceplates. Studying the fractured specimens revealed that failures always occurred either in the foam or in the faceplate. None of the 24 samples failed in the S-Bond joint, indicating that the joints were stronger than both base materials. All pre-wetting techniques and S-Bond alloys used produced strong sound joints, which did not break before the base material.



These studies led to the following recommended processing conditions, using various armor candidate faceplates including ceramic and CMC's.

1. Heat the base materials (aluminum foam and ceramic plate) to either 250 or 415°C, depending upon the joining medium, S-Bond 220 or S-Bond 400, respectively.
2. Melt S-Bond alloy onto both surfaces to be coated.
3. Mechanically spread the alloy using a pneumatically driven ultrasonic spatula.
4. Place the two surfaces together at the joining temperature after melting and applying a uniform, thin (~ 0.003") layer of S-Bond.
5. Press the hot surfaces together, and while the S-Bond alloy is molten, use an ultrasonic horn in contact with the top ceramic layer (NOTE: Al-foam was too acoustically absorbing) to agitate the molten S-Bond and break up surface oxides.
6. Remove heat source and cool, maintaining ~ 10 psi pressure on the ceramic faceplate until the S-Bond alloy is solid, roughly 50°C below the liquidus.

4.2.2.3 - Al-Foam / SiC 4" x 4" / Armor Plate Testing

MRi, in this sub-task, developed S-Bond procedures and tooling to bond larger sample armor panels in order to test bonds under realistic ballistic impact testing. These specimens were to be 4 x 4" panels joined for ballistic tests and for non-destructive testing, including x-ray, ultrasonic and/or thermal wave imaging methods. These panels were to be tested in high-energy impact tests to determine if S-Bond joining between the MMC and the aluminum foams could yield improved ballistic impact resistance compared to other bonding methods.

Penetrator strike plates 4" x 4" x 1/4" ceramic (Al₂O₃, SiC and Si:SiC) plates were to be bonded to 4" x 4" x 1" molded Al-foam backing plates. Figure 71 illustrates one of the first assembled and joined Si:SiC ceramic plates bonded. However, after successful S-Bond 220 bonding and during cooling (from 250°C), cracking sounds emanated from the joined part. After about two days, the Si:SiC parts were completely separated, as can be seen in Figure 72. This joint fracture was determined to be CTE driven where these larger 4" x 4" plates, having little expansion, developed large joint stresses as the Al-foam tried to shrink

more than the ceramic face-plate. It was apparent from the cracked faceplate and the fractured bond that the CTE mismatch between the ceramic and the aluminum backing plate had to be better managed.

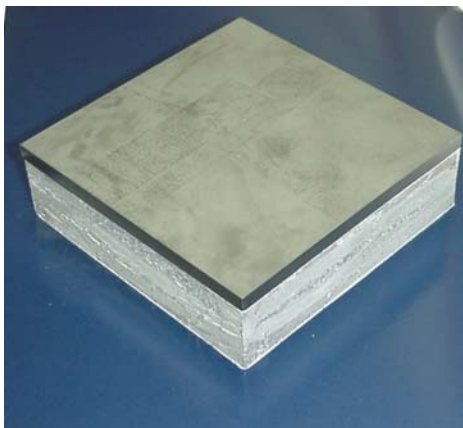


Figure 71. 4 x 4 inch ballistic test sample showing Al-Foam joined to SiC faceplate.



Figure 72. 4x4 inch ballistic test sample shown in Figure 2, after CTE mismatch led to bond failure (2 days elapsed time).

To lower thermal expansion mismatch-induced strains and to better accommodate the localized interface stresses, thicker, composite joints were developed, consisting of either a particulate composite joint (S-Bond infiltrated with Nickel or SiC particles, for example) or a layered composite joint (a layer of Si:SiC composite between the Al foam and the SiC armor plate). Figures 73 and 74 illustrate the two solutions, that were to be tested.

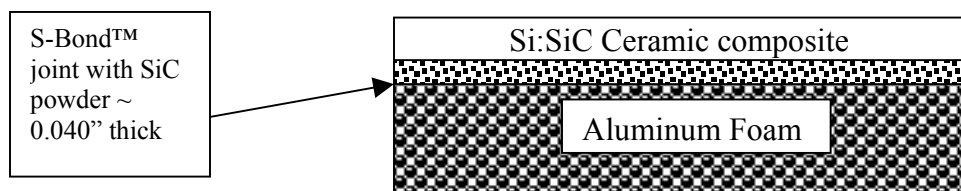


Figure 73. Illustration of a particulate composite S-Bond™ joint for composite armor.

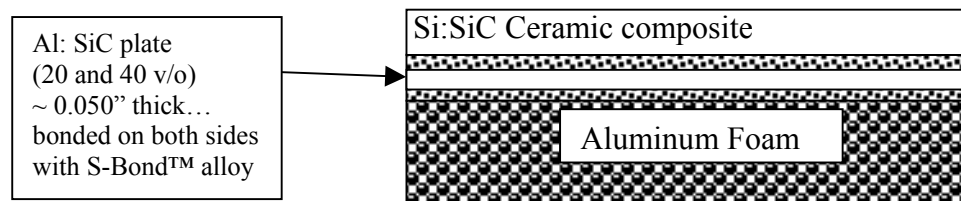


Figure 74. Illustration of an Al:SiC transition piece joint for composite armor.

Small, metallographic samples of the particulate composite bond, after cooling and after a few days, exhibited only slight cracking near the edge of the ceramic plate. Compared to the S-Bond only joint, these particulate composite joints significantly improved the joining of the composite armor. S-Bond 220 wetted and joined Al:SiC transition plates, both 20 volume % and 40 volume % SiC, as well as the Al-foam and the ceramic strike plates, as discussed in the Metallography results, above. Despite the occasional, small cracks, it was clear that good joints could be made with some optimization and process development. The transition layers provided a solution to the CTE mismatch issue for larger armor components.

MRi developed procedures for joining 4" square SiC and Si:SiC armor plate coupons to Al foam using composite interlayers, as shown in Figures 73 and 74. Initial conclusions regarding the improvements were that both composite joint approaches improved the bonding and enabled a joint to be made without cracking the ceramic strike plate or fracturing the entire S-Bond interface. However, in the S-Bond matrix/Ni or SiC particulate composite, there were some interface failures due to the lack of uniformity of the particulate distribution in the S-Bond matrix. Though there may be ways to improve the S-Bond particulate joint approach, it was decided that the potential of the bonded Al:SiC plate interlayer would be more controllable and offer the advantage of added ballistic protection. Therefore, MRi emphasized designs and methods, such as that illustrated in Figure 74, that utilize an intermediate Al:SiC transition plate. These intermediate layers would help to compensate for the differences in the CTEs of Si:SiC or SiC strike plates and those of backing materials such as Al plate or Al foam.

Figure 75 shows the joined 4" square composite armor plates that used a 20 vol% SiC and 40 vol% SiC Al:MMC plate (0.050" thick). [Note: The higher volume % of SiC lowers the CTE.] The joints made with these were successful, and are well adhered with no macroscopically apparent de-bond of the S-Bond joined composite armor plates.



Figure 75. Macro view of Al:SiC transition piece / S-Bond™ joined composite armor plates

4.2.2.4 Al Foam / Ceramic Armor Conclusions

Results of these tests and evaluations indicated that the Aluminum foam or sponge backing, as well as the Al-MMC materials used in transitional layers, could be bonded well by either S-Bond 220 or S-Bond 400. Several methods could be used to do this, including ultrasonic and manual wiping as well as foil pre-placement. Ceramics such as SiC and Al_2O_3 , and composites such as Si:SiC were also wetted by both vacuum paste pretreatment (for S-Bond 220) and ultrasonic wiping (for S-Bond 220 or 400).

With these successes, MRi planned to produce arrays of 4" square aluminum foam/ceramic or composite armor plates with transitional Al:MMC layers to help compensate for thermal expansion mismatch. The closure of dMC² and the availability of Al:SiC composite armor strike plate materials led to the inclusion of High Performance Materials Group. HPMG, (a holding company for Lanxide products) into the project this added a new partner with interest in solid aluminum backing plates instead of aluminum foams, and because of the cost of ballistics testing it was decided to not to pursue the Al-foam backed plates into ballistics testing, despite the fact that techniques to bond larger, 4" x 4" SiC or Si:SiC strike plates to Al-foam was successfully developed.

4.2.3 Solid Aluminum Plate-Backed Composite Armor

4.2.3.1 Four-Inch Square SiC and Si:SiC Armor Plate Trials

After discussions with Army Research personnel and with the addition of HPMG the aluminum foam ballistic testing was deferred with experiments to use solid aluminum plate-backed armor panels. Initially, 0.325" thick plate was utilized, but even with the proposed CTE-mismatch remedies described previously, tiles bonded with either S-Bond 220 or S-Bond 400 continued to fail. After several trials of S-Bond 220 bonds with ~0.197" SiC tiles bonded directly to 0.325" Al (with or without interlayers of Al:SiC), it was

apparent that failures of the SiC and Si:SiC ceramic composite were still occurring. Detailed measurements of the bonded components before the SiC cracked revealed that the Al base was deflecting or bowing. It was proposed that the *bending, not the shear stress* accumulation, had led to the SiC armor faceplate cracking.

After this observation, 0.75" thick plates were ordered and S-Bond 220 was used to join to these thicker aluminum plates (0.75") to SiC directly, without the intermediate SiC plate. Figures 76-79 illustrate the ceramic strike plate (4" x 4") bonded to an 8" x 8" x 0.75" aluminum alloy plate. The method of S-Bond joining entailed precoating the aluminum and the SiC or Si:SiC ceramic plate with S-Bond 220, applying extra S-Bond alloy, and then sliding the pretreated ceramic plate onto the Al plate. The sliding method has been found to be a good way of reducing the entrapped air that occurs if the ceramic plate is placed directly on the S-Bond alloy layer.

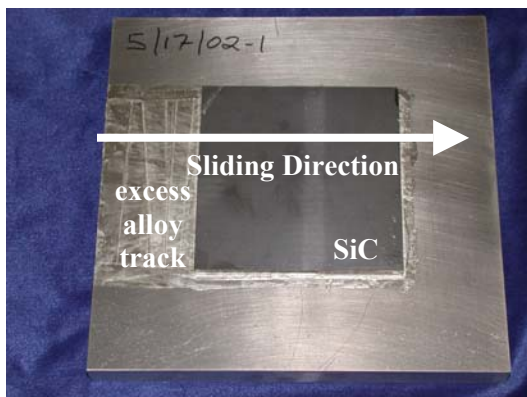


Figure 76. SiC plate S-Bond™ 220 joined



Figure 77. Si:SiC composite plate S-Bond™ 220 joined directly to 3/4" aluminum plate

It was apparent that even without the Al:SiC interlayer, the 4" x 4" x 0.197" SiC strike plates were successfully joined without the ceramic plate cracking. The increased thickness of the aluminum plate, without otherwise changing any of the S-Bond alloys or joining procedures, reduced the induced bending moment and eliminated the cracking in the SiC ceramic. This supports the theory that the CTE-induced bending of the aluminum plate had been the cause of the observed cracking in the ceramic plates. Figure 77 illustrates that the method also worked well for the Si:SiC ceramic composite plate. Figures 78 and 79 show closer details of the SiC bonded to the thickened aluminum plates. Note that the corner fillet section in Figure 74 shows an integral joint, something that had not been achieved before.

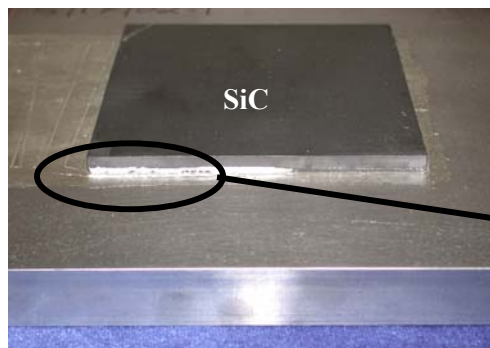


Figure 78. SiC plate S-Bond™ 220 joined directly to 3/4" aluminum plate.

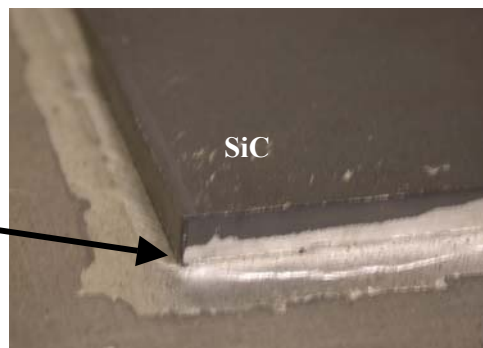


Figure 79. SiC plate corner fillet detail, bonded with S-Bond™ Alloy 220.

There was also interest in trying Zn-based S-Bond 400 for it higher strength. S-Bond 400 requires that the ceramic and the aluminum plate be heated to 410 to 420°C. The alloy bonded well, however on cooling the



Figure 80. Si:SiC plate S-Bond™ 400 joined directly to 3/4" aluminum plate.



Figure 81. Si:SiC plate S-Bond™ 400 joined directly to 3/4" aluminum plate partially on bonded side.

CTE strain mismatch caused the ceramic and/or the S-Bond 400 interface to fail. Figures 80 – 82 illustrate the failed S-Bond 400 interfaces/ceramics. Due to this failure it was decided to drop S-Bond 400 from further consideration for this application.

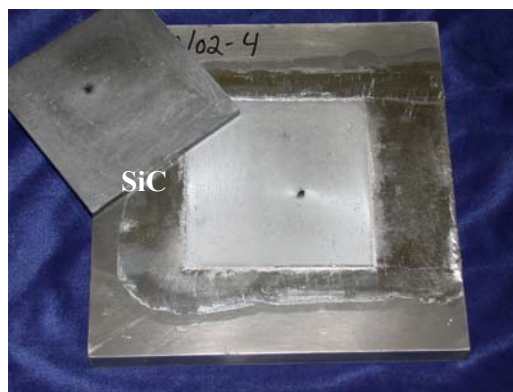


Figure 82. SiC plate S-Bond™ 400 joined directly to 3/4" aluminum plate, showing the fractured S-Bond™

In order to determine the quality of the S-Bond joined ceramic and composite, lightweight armor test panels, they were submitted for ballistics testing to determine a constructed V-50 value. The V-50 for a particular type of armor and a certain caliber threat is nominally defined as the projectile velocity at which the target has a 50% chance of penetration. "Penetration" indicates that a thin, aluminum sheet (hung loosely behind the target) has been punctured or otherwise broken by the projectile, shrapnel, or any portion of the target. This is done by choosing a caliber and type of threat (projectile), estimating a starting velocity from MIL-DTL-46027 or another appropriate specification for armor plate, and then narrowing down the velocity around this number based on the results of each subsequent test firing. Such testing typically requires approximately six to eight shots at different areas of a given target plate of assumed uniform mechanical properties. Our testing included six shots at individually joined test plates assumed to have approximately similar mechanical properties to each other. This produces a "constructed" V-50 for each set of bonding conditions, which can then be compared to data on file for similarly sized armor plates.

Table 1 – Composite Armor Ballistics Testing Matrix

| ID # | Base Plate | Ceramic Type | | Joint Type | | | |
|------|------------|--------------|--------|--------------------------|-----------------------|-------|-----------------|
| | | SiC | Si-SiC | Wipe/Layer S-Bond 220 | Paste 220 Ther-Vac | Epoxy | Al-SiC Layer |
| 1 | X | X | | X | | | |
| 2 | X | X | | X | | | X |
| 7 | X | X | | | X | | |
| 8 | X | X | | | X | | X |
| 9 | X | X | | | | X | |
| 16 | X | | X | | X | | |

It was initially decided to use .30 caliber AP (armor piercing) rounds. However, when it was found that even at velocities in excess of 2750 feet per second (higher than normal muzzle velocity) the projectile did not penetrate the test panel, it was decided to use .50 caliber AP rounds instead.

Five different sets of S-Bond joined plates were tested, along with one set of epoxy joined armor plates, as shown in Table 1. The epoxy used was 3M 7100 thermosetting film adhesive, which was developed specifically for bonding metals. The results of the tests are shown in Table 2. Wording on the HP White certifications for each set of samples was as follows:

Testing was conducted in accordance with the provisions of MIL-STD662F, dated 18 December 1997, using caliber .50AP, M2, 708-grain projectiles. The test samples were rigidly mounted on an indoor range 45.0 feet from the muzzle of the test barrels to produce zero degree obliquity impacts. Redundant pairs of photoelectric lumiline screens were positioned at 15.0 feet and 35.0 feet. In conjunction with electronic chronographs, they provided projectile velocities 25.0 feet from the muzzle. Standard drag coefficient tables were used to calculate striking velocities. Penetrations were determined by visual examination of a 0.020" thick sheet of 2024T3 aluminum positioned 6.0 inches behind and parallel to the test sample.

The only exceptions to this were the first two tested panels from sample set #9, which were tested with caliber .30AP, M2, 166-grain projectiles.

Table 2. Ballistics Testing Results

| Sample # | Ballistic Threat | | Ballistic Limit (feet/second) | | |
|-----------|------------------|-----------------|-------------------------------|--------------|--------------|
| | Caliber | Shots Total/V50 | V50 BL[P] | High partial | Low Complete |
| 1 | .50 AP, M2 | 6/4 | 2160 | 2160 | 2202 |
| 2 | .50 AP, M2 | 6/4 | 2171 | 2163 | 2181 |
| 7 | .50 AP, M2 | 6/4 | 2221 | 2213 | 2209 |
| 8 | .50 AP, M2 | 6/4 | 2062 | 2055 | 2066 |
| 9 (Epoxy) | .50 AP, M2 | 4/2 | 2290 | 2274 | 2307 |
| 16 | .50 AP, M2 | 6/4 | 2243 | 2265 | 2206 |

The epoxy joints offered the highest V50, but only by a small margin. The closest results to the epoxy-joined plates were #16 (vacuum-treated Si:SiC composite with no intermediate layer) and #7 (vacuum-treated Si ceramic with no intermediate layer). Sets #1 and #2 represented the foil wipe layer (mechanical activation only) joining method, where set #2 had an intermediate Al:SiC layer and set #1 did not. These two were very close to each other, and were the next closest to the best results. The lowest results came

from the thermally treated SiC with the intermediate composite layer, #8. Even so, these results are all fairly close to each other. Figure 83 shows the setup of one of the epoxy joined armor plates. Figures 84 through 89 show the condition of the test plates after the firing of a shot approximately at the V50 speed. In some cases, the some of the projectile and/or copper jacket can be seen in the hole. One can also see the “dull grey” pattern that is believed to be the “fractured” S-Bond® layer, although one can also see remnants of the SiC strike plate that was fractured by the penetrator impact.

The S-Bond® interfaces did not fair any better the epoxy joints with the joint being the major failure point. There were two theories of lack of increase in V-50 over epoxy. One was that the cooling from the S-Bond® joining temperatures ($\sim 250^{\circ}\text{C}$) put the ceramic strike plates in pre-tensile state, thus propagating cracks with less energy. The other was that the S-Bond® layers either weakened from adiabatic heating or from overload rupture. These test plates did no lend themselves to differentiate between the failure reasons. The only conclusion for sure was that the S-Bond® joints performed on par with epoxy bonding.

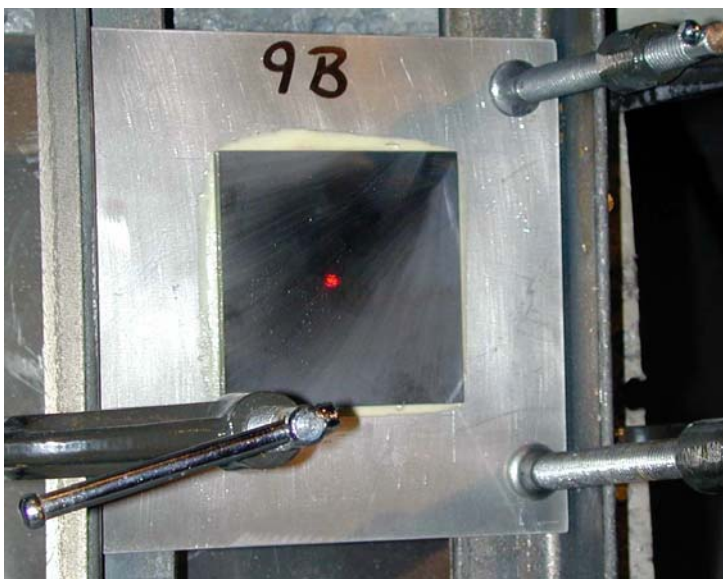


Figure 83 – Epoxy joined SiC to 0.75” Al armor plate, with laser sight centered on target, prior to firing.



Figure 84 – Plate 1E (SiC tile w/ mechanical activation only) – The strike velocity was nearest the 2160 fps constructed V50.



Figure 85 – Plate 2D – (SiC tile w/ mechanical activation and an Al:SiC intermediate layer) – The strike velocity was nearest the 2171 fps constructed V50.

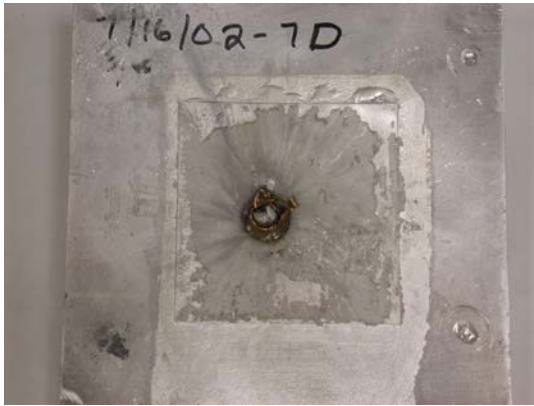


Figure 86 – Plate 7D – (SiC tile vacuum treated w/ S-Bond 220) – The strike velocity was nearest the 2221 fps constructed V50.

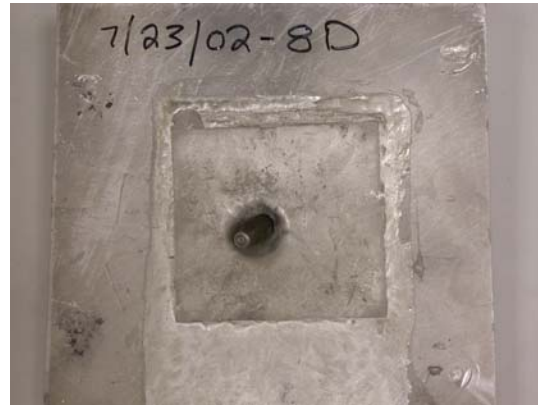


Figure 87 – Plate 8D – (SiC tile w/ mechanical activation and an Al:SiC intermediate layer) – The strike velocity was nearest the 2062 fps constructed V50.

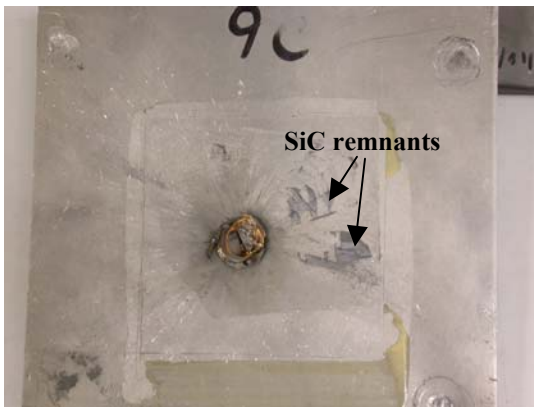


Figure 88– Plate 9C – (SiC tile joined with 3M 7100 epoxy bonding film) The strike velocity was nearest the 2290 fps constructed V50.



Figure 89 – Plate 16D (Si:SiC composite tile vacuum pretreated with S-Bond 220 paste) – The strike velocity was nearest the 2243 fps constructed V50

4.2.3.3 Solid Aluminum-Backed Armor Conclusions

Results of ballistics tests with solid aluminum-backed armor revealed that S-Bond 220 could be used to effectively join both SiC and Si:SiC composite to aluminum plates, provided that the Al plate is sufficiently thick to resist the stresses associated with thermal expansion mismatch between the armor tile and the aluminum that lead to ceramic plate bending and tensile loading. Tests also indicated that Al:SiC composite interlayers could be used to help compensate for some of this thermal expansion mismatch stress for S-Bond 220 joints. S-Bond 400 was shown to have too high a melting temperature to effectively join armor plates without short-term failure of the joint, even with the Al:MMC interlayers. These interlayers did not seem to add to the ballistic impact resistance of these plates, as had been postulated prior to testing. Comparison of S-Bond 220 joined ballistic test plates to epoxy-joined plates revealed that a constructed V50 could be achieved similar to, but not in excess of, that of the epoxy-joined samples, for these tested samples. However, the relatively easy repair and reassembly offered by S-Bond 220 represents an advantage over epoxy joining without appreciably losing ballistic impact resistance.

4.2.4 Solid Titanium-Backed Armor Plates

US Army Research Lab (ARL), Aberdeen, MD

After the Phase II effort had been initiated, ARL approached MRi to conduct evaluations of the S-Bond joining for certain lightweight armor concepts. As lightweight composite armor is a subject of this Phase II SBIR, MRi included this work for ARL in this MDA report to demonstrate the need for and application of S-Bond joining in this area. Unlike the MRi/Fraunhofer USA concept, the ARL concept uses a SiC ceramic strike-plate bonded to a Ti-6Al-4V alloy backing plate. Figure 90 shows S-Bond joined SiC plates joined to 4" x 4" Ti alloy plates. (NOTE: SiC and Ti have similar CTE values, so a composite joining layer was not necessary.) The evaluated joining procedures included as-bonded conditions where molten S-Bond 220 was mechanically spread onto grit blasted Ti and SiC plates and then pressed and ultrasonically vibrated to complete the joint. The other major joining method used the thermal vacuum premetallization of S-Bond 220 onto the Ti and/or the SiC surfaces, which were later joined in air at 250°C using the ultrasonic press. Testing of these bonded armor plates in an actual firing range was completed by ARL and the results were encouraging. However, results suggested that the Zn-bases S-Bond 400 might perform better since observation of the failed composite armor showed that the high velocity penetrator impact might impart enough adiabatic heating into the composite armor to cause localized remelting of the S-Bond 220, which begins to melt at 221°C. ARL delivered new armor Ti and SiC plates for MRi to bond with S-Bond 400, which MRi joined with S-Bond 400, although the SiC were initially vacuum metallized with S-Bond® 220 (Sn0Ag-Ti), for ballistic testing. The large caliber ballistic penetration test results were not as good as the plates joined with S-Bond 220, possibly because the higher CTE strain from higher temperature joining (420°C) consummate with the S-Bond 400 alloy likely led to higher residual tensile/bending stresses in the SiC plates, thereby lowering their ballistic impact resistance.

In addition to ballistic testing, ARL also had MRi bond shear test samples using S-Bond 220 and 400 for comparison to two types of epoxy joined methods. The results of shear testing are shown in Table 3. Although good strengths were produced by S-Bond alloys, with S-Bond 220 being more consistent, the joint shear strengths offer no strength increase over epoxy bonding.

Table 3. Shear Strengths of Ti-SiC Joints Made for ARL

| Samples | Joining Method | Material Condition | Avg. Strength (MPa) | Individual Test Results (MPa) |
|----------------|-----------------------|---------------------------|----------------------------|--|
| 2 | S-Bond 220 | Grit Blasted | 26.9 | 30.2 Mpa, 23.6 |
| 2 | S-Bond 220 | Vacuum Treated | 34.05 | 32.2, 35.9 |
| 2 | S-Bond 400 | Grit Blasted | n/a | samples did not survive preparation |
| 2 | S-Bond 400 | Vacuum Treated | 26.4 | 26.4 |
| 7 | 2-Part Epoxy | none | 27.3 | 27.4, 19.7, 28.5, 28.8, 31.6, 29.6, 25.7 |
| 3 | Film Epoxy | Grit Blast & Silane | 34.33 | 30.3, 39.6, 33.1 |

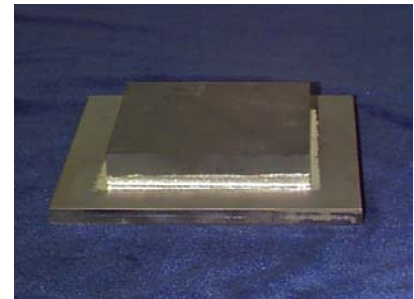
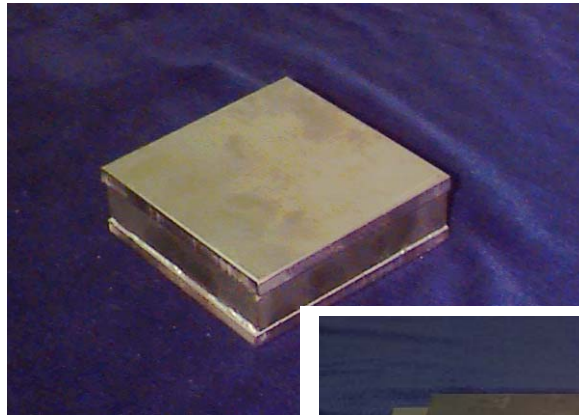
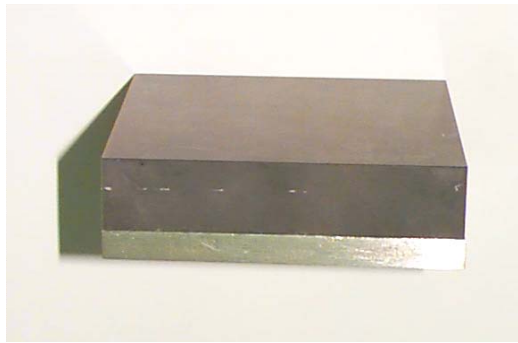


Figure 90. Photographs of SiC / Ti 6-4 plates joined by MRI for the US Army Research Lab, using S-Bond™ Alloy 220.

The 2-part epoxy consisted of Epon resin 815 and Versamid 125, while the film epoxy was FM73 from Cytec. The second set of epoxied samples was grit blasted followed by a silane treatment, which is typical for epoxies but is not necessary for S-Bond materials. For the S-Bond 220, where vacuum treating is denoted, both the titanium alloy and the SiC were coated with S-Bond and heat treated in high vacuum at temperatures in excess of 850°C. Similarly, where grit blasting was used for surface preparation, but the Ti and the SiC were grit blasted.

4.2.5 Composite Armor Conclusions

Both S-Bond 220 and S-Bond 400, applied by either ultrasonic pre-wetting or by vacuum pre-treatment of the faceplates with S-Bond 220 paste, produced strong joints able to withstand shear strengths higher than the ultimate shear strength of either the Al-foam or the faceplates. S-Bond 400 foil yielded the lowest (2.5 MPa) shear strengths, but it did provide a good joint, the strength of which could potentially be improved with further study. Moreover, vacuum paste pre-treating showed a strong reaction with most of the material used. So vacuum metallization using S-Bond® 220 alloy on the SiC / ceramic strike plates is recommended to enhance the strength of the ceramic strike plate to backing joints.

For the Al-foam- and thinner solid aluminum-backed ceramic or composite strike plates, a composite S-Bond method was required. If Ti alloy or thicker solid aluminum backing plates are used, normal S-Bond-only joining methods can be used. The exact procedures for joining can vary, though it was found that thermal vacuum pre-treatments, grit-blasting and/or ultrasonic mechanical activation of the S-Bond alloy were all helpful means of increasing metallurgical interaction between the base material and the S-Bond, thereby increasing the joint strengths. For the aluminum foam backing, the intermediate Al:SiC layer method appears most promising and controllable and may offer additional ballistic protection in some circumstances, though this was not observed in the limited ballistics testing performed for this contract. Both the particulate composite S-Bond joint and the Al:SiC composite interlayer are viable options, though only the solid Al:SiC interlayer was ballistically tested.

S-Bond joining has also made notice with the US Army Research Lab and was evaluated as a method to fabricate their SiC/Ti-6Al-4V armor plate designs. The potential advantages of S-Bond joining included increased joint toughness (over epoxy-joined plates), easy repair of S-Bond joints as the S-Bond alloy

would merely need to be re-heated and joined, rather than ground off or otherwise removed like epoxy, and that S-Bond® joining methods are easily scaled to field applications and/or to larger armor plates.

Task 2.0 on Ceramic / Composite Armor concluded that S-Bond® joining, with either S-Bond® 220 or S-Bond® 400 alloys, could produce joints with nearly the same performance as epoxy joined armor plates. The added advantage being the S-Bond® joined armor plates could be disassembled and rejoined, where epoxy could not. Despite this advantage, the US Army Research Laboratory discontinued their work on S-Bond® joining since their interest was to find joining methods that were a ballistic improvement over epoxy joined parts. Although ARL discontinued their interest, the SBIR project work demonstrated the S-Bond® joining could be used to make lightweight ceramic / composite armor plate that were at least equivalent to epoxy joining. This positive result has led to new investigations that are continuing with another company that has developed a way to heat only the interfaces being joined, eliminating the need to heat the ceramic and the backing plate to over 250°C. This technology, if successful, would nearly eliminate residual tensile and bending stresses on the ceramic strike plate, thus possible increasing its ballistic performance. If this approach yields improved ballistic improvement over epoxy joining, S-Bond® joining will still have a role in producing ceramic composite armor.

4.3 Task 3.0 Electronic Components

4.3.1 Introduction/Objectives

This task was aimed at investigating the potential for S-Bond® joining to be utilized in the fabrication of electronic packages that may be used in missile defense systems, missiles or space borne platforms. Figure 91 illustrates an electronic package with a thermal management element added. S-Bond® could be utilized at the die attach, interconnects or as Figure 92 illustrates in sealing hermetic enclosures.

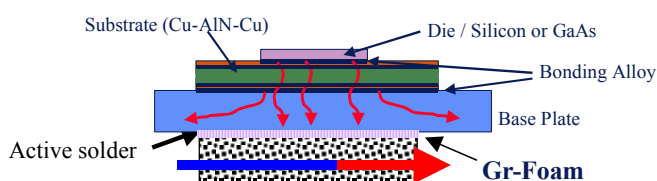


Figure 91. Schematic cross section of an electronic package with thermal management components.

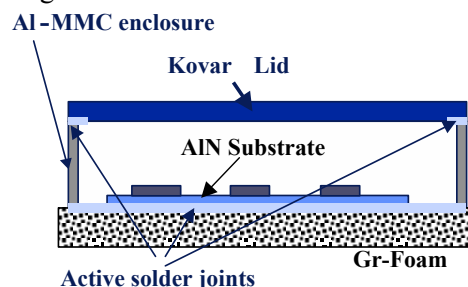


Figure 92. Illustration of hermetic electronic enclosure.

Figure 93 illustrates the S-Bond® joining of a power electronic chip to an Al-MMC heat spreader. This projects work was focused on this application as well as the hermetic enclosure shown in Figure 92. Figure 94 shows an additional application where S-Bond® can attach silicon dies to lead frames or as an extension of this could be used to connect leads in leadframes to dies. Although this research project did not target dies or interconnects, the work completed in this task can lead to the conclusion that such applications of S-Bond® technology are possible.

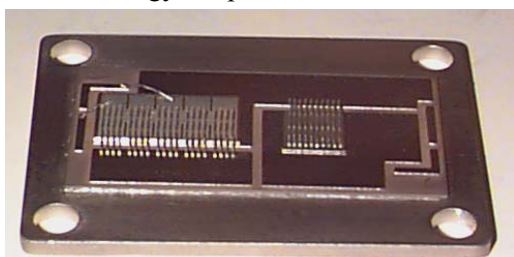


Figure 93. Power electronic device bonded to AL-MMC heat spreader.

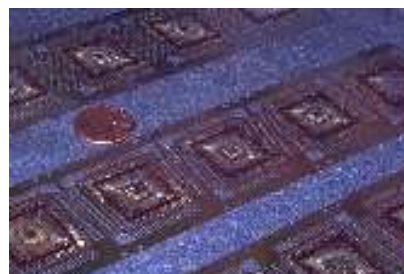


Figure 94. Die attachment on leadframe.

In the investigation, as part of Task 3.0, S-Bond® was evaluated for joining Al-MMCs in electronic packages for managing thermal expansion and heat transfer. Table 4 indicates some of the material joint combinations tested for possible applications. Electronic packages include ceramic substrates (aluminum oxide / aluminum nitride), which serve as an electrical insulator from the package and are bonded to heat spreaders (aluminum, copper, Al:SiC or Al:Gr). These assemblies are then bonded to and packaged in low-expansion metals such as Kovar®. In this task, MRi procured Al-MMC samples (Al:SiC and Al-Graphite) to assess two types of Al-MMC materials for packaging application, as well as AlN, Al₂O₃, and Kovar for use in electronic packages.

Table 4. Candidate Materials for Electronic Components

| Base / Substrate | Lid | Comments |
|--------------------------------|---------------|---------------------------------|
| Al:SiC(60v/o) | Kovar, Al:SiC | Hermetic package |
| Al:Gr | Kovar, Al:Gr | Hermetic package |
| AlN | none | Substrate bond to Al:SiC and Si |
| Al ₂ O ₃ | none | Substrate bond to Al:SiC and Si |
| Low CTE Alloys (Kovar®) | N/A | Lead frame interconnect |

In order to assess the utility of some of these materials and their compatibility with S-Bond alloys and joining procedures, tests were performed to measure the strengths of various S-Bond joints in these materials, and scaled samples were made for testing the hermeticity of the S-Bond joints and the base materials for use in electronic packages.

4.3.2 General Material Studies

4.3.2.1 General Materials Testing - Approach and Procedures

Single lap shear specimens were initially made and tested to evaluate the shear strengths of the joints for Al:SiC and Al-Gr composites joined to ceramic materials with S-Bond 220 and S-Bond 400. However, all SLS specimens failed in the base materials, indicating that the joints were strong but that actual joint strengths could not be measured without a change in specimen design. It was assumed that the single lap caused too severe a bending moment, which led to the fracture of the composite and/or ceramic base materials outside the joints.

MRi then conducted double notch shear (DNS) tests of S-Bond joints between AlN, Al₂O₃, or Kovar and AlSiC or Al:Gr. Figure 95 shows a schematic illustration of the double notch shear test samples. This design eliminated bending during the tension tests and loaded the joints in 100% shear, leading to more consistent fracture in the S-Bond joints, and proving itself an effective shear test design for these combinations of materials.

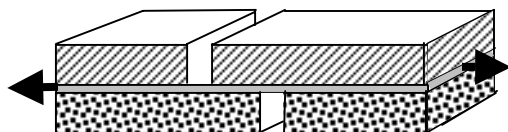


Figure 95. Illustration of double notch shear specimen designed and used to test the shear strengths of varying ceramic/composite joint combinations.

Metallographic tests were also conducted on these material joint combinations, in some cases on the actual tensile specimens themselves, which saved some time and money while allowing MRi to evaluate the actual tested shear sample joints. Results are summarized herein.

4.3.2.2 General Materials Testing - Results

Metallurgically sound dissimilar materials joints were produced between Al:Gr or Al:SiC and Kovar® using both S-Bond 220 and 400. This particular material combination is important, as most hermetic packages reportedly require bonding Al-MMCs to Kovar. Such joints made with S-Bond ultrasonic ‘wipe’ methods exhibited better quality than those made by placing S-Bond foil without any pre-wetting. S-Bond 400 (Zn-based) joined these materials at temperatures between 410 and 425°C, which led to significantly more metallurgical interaction and thicker joints due to the Al-Zn eutectic at 381°C. There was also a significant two-phase structure seen in the joint interface, including α -Al surrounded by a gray Zn phase. S-Bond 400 also enveloped the secondary phases (graphite or SiC) into the joint, as S-Bond 220 had done. Therefore S-Bond 400 demonstrated that joints could be produced for applications requiring higher temperature capability. Representative photomicrographs of these joints are shown in Figures 96-103.

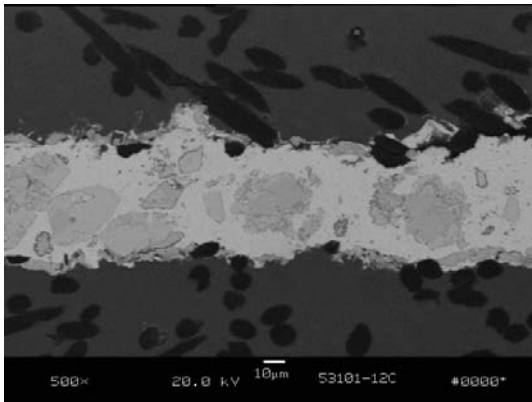


Figure 96. Al:Gr jointed to Al:Gr with S-Bond 220 using brush / U-S press method.

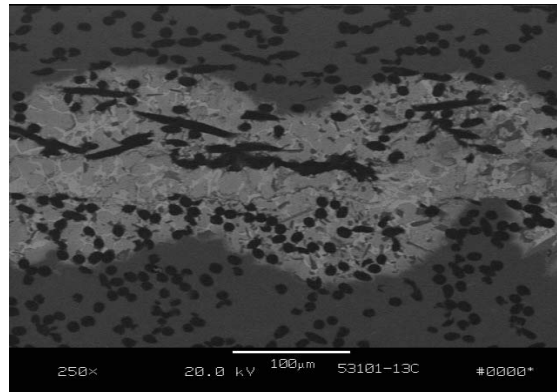


Figure 97. Al:Gr jointed to Al:Gr with S-Bond 400 using brush / U-S press method.

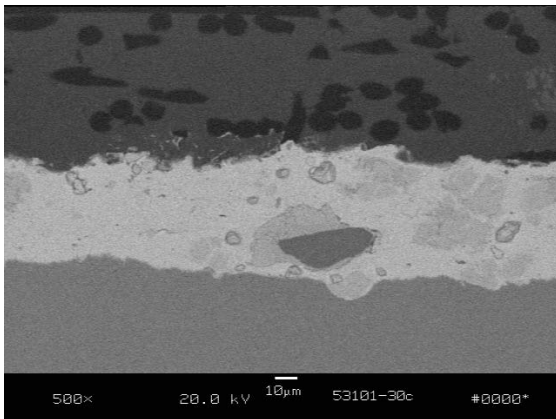


Figure 98. Al:Gr jointed to Kovar with S-Bond 220.

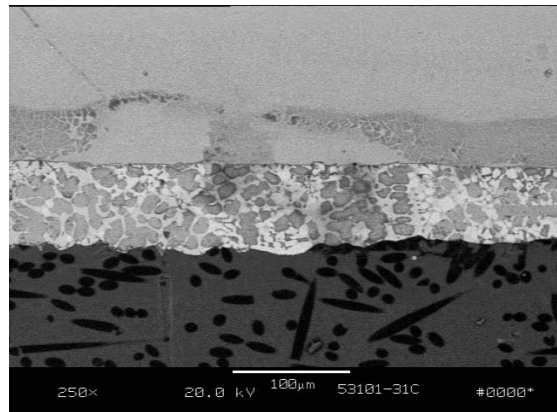


Figure 99. Al:Gr jointed to Kovar with S-Bond 400.

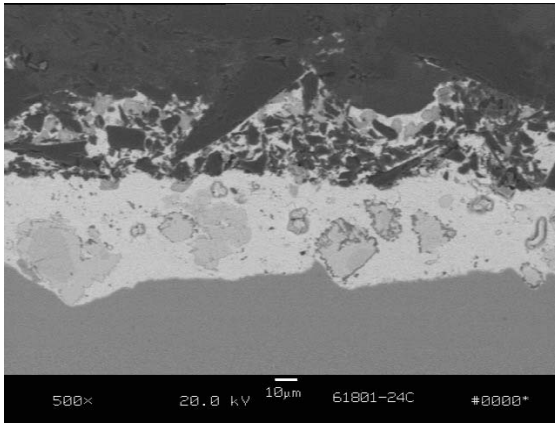


Figure 100. Al:SiC joined to Kovar with S-Bond 220 foil.

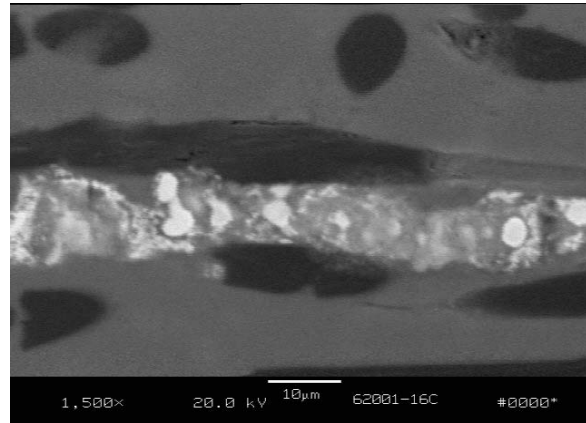


Figure 101. Al:SiC joined to Kovar with S-Bond 400 foil.

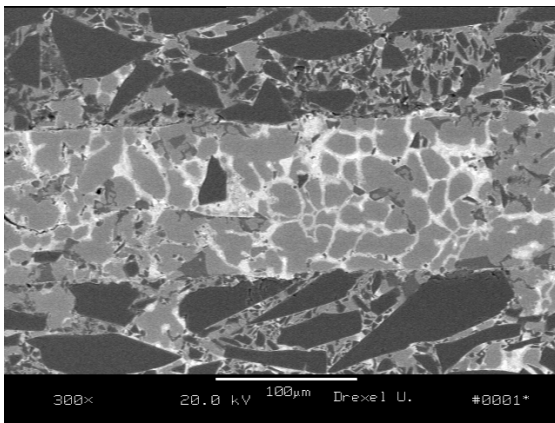


Figure 102. AlSiC bonded to Al:SiC with S-Bond 400 using manual wipe prewetting.

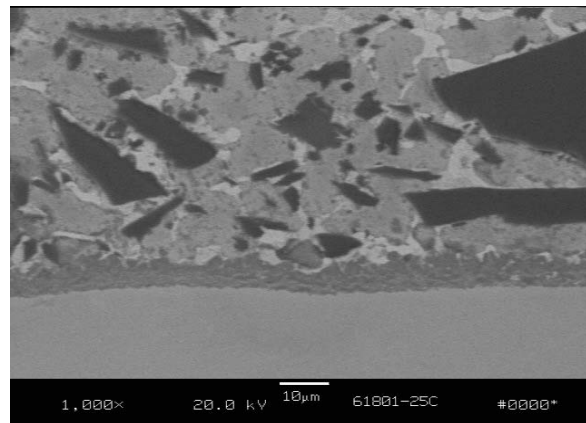


Figure 103. Al:SiC joined to Kovar with S-Bond 400.

Metallography tests revealed excellent Al-Gr and Al:SiC joints using S-Bond 220 with all joining methods. Excellent wetting and envelopment of the graphite fibers or the SiC particles could be seen. Al:SiC and Al:Gr were successfully joined to Kovar® and to ceramics such as Al_2O_3 and AlN . Such joints were sound and faying surfaces were well wetted, including the SiC particles and graphite fibers in the composites. Aluminum nitride was also bonded very well with S-Bond 220, which integrated itself into the AlN surface irregularities and enveloped AlN particles within the S-Bond joint.

Double Notch Shear testing was completed on a wide range of combinations of materials, including combinations of Al:SiC to Al:SiC, Al:SiC to Kovar, Al:SiC to Al_2O_3 , Al:Gr to Al:Gr, Al:Gr to Kovar, Al:Gr to Al_2O_3 and Al_2O_3 to Al_2O_3 . Tables 5 and 6 summarize the completed results of this room temperature testing. Two DNS specimens were prepared for each set of base materials, using S-Bond 220 and S-Bond 400 with one of two preparation methods. One method, denoted as “wipe”, involved ultrasonically brushing S-Bond onto the joining surfaces. The other method, denoted as “foil” used no pre-wetting, only placement of S-Bond foil into the joint and heating to the joining temperature. In all cases, the joining was accomplished using an ultrasonic press, with about 15 psi of pressure, and a superimposed 20 kHz ultrasonic burst for one second, followed by air cooling. Table 6 summarizes these results. Since the composite (Al:SiC or Al:Gr) or the ceramic (Al_2O_3) seemed to control the joint failures in shear, Table 5

only shows the averages of the shear strengths in the major materials categories, combining the similar and dissimilar material joints such as Al:SiC to Kovar.

Tables 5 and 6. Summary of DNS Testing on Electronic Materials

| Joint Mat'l Joining Alloy | Alloy Application Method | |
|--------------------------------|--------------------------|------------|
| | Wipe(MPa) | Foil (MPa) |
| AlGr | | |
| 220 | 46.9 | 41.3 |
| 400 | 44.9 | 32.4 |
| AlSiC | | |
| 220 | 49.7 | N/A |
| 400 | 44.4 | 45.6 |
| Al ₂ O ₃ | | |
| 220 | 38.4 | 36.5 |
| 400 | 44.2 | 43.5 |

| Joint Materials | S-Bond™ Joint Alloy | DNS Strength MPa |
|--|------------------------|---------------------|
| Al-Gr to Al-Gr | 220 | 31.0 |
| Al:SiC to Al:SiC | 220 | 35.8 |
| Al:SiC to Al:SiC | 400 | 37.3 |
| Al:SiC to Kovar | 220 | 38.7 |
| Al:SiC to Al ₂ O ₃ | 400 / Foil | 36.6 |
| Al:SiC to Al ₂ O ₃ | 400 | 35.6 |
| Al:SiC to AlN | 220 | 29.6 |
| Al:Gr to AlN | 400 | 28.5 |
| Al:Gr to AlN | 220 | 28.1 |
| Al:SiC to AlN | 400 | 36.3 |

4.3.2.3 General Materials Testing – Conclusions

Metallographic tests revealed that the tested materials could all be wetted thoroughly by the S-Bond alloys, making S-Bond a viable option for joining most aspects of the proposed power electronic packaging.

Double Notch Shear testing revealed that S-Bond 220 and 400 shear strengths were similar to each other, and did not change significantly with the changing joint material combinations. The joint shear strengths vary from 28 – 50 MPa, which should provide sufficient strength for the hermetic packages, substrates and heat spreaders being considered. Such components typically only need to withstand the mechanical stresses associated with thermal cycling.

S-Bond technology proved itself to be a viable joining process for a range of materials used in electronic packaging, including materials for thermal management, hermetic packages and interconnects. Evaluations showed that similar processing conditions to the “Structural Materials” joining procedures apply, especially the need to use ‘wiping’ methods to prewet the active solders. Joints then are made by employing ultrasonic vibration of the interfaces with an ultrasonic press. S-Bond 220 and 400 were both found effective in joining Al:SiC, Al:Gr, AlN and Al₂O₃ in combinations with low CTE metals such as Kovar.

4.3.3 Hermetic Electronic Packaging

4.3.3.1 Hermetic Packaging Approach and Procedures

S-Bond joining methods were developed for Al:SiC from dMC² and Metal Matrix Cast Components’ (MMCC) Al-Gr composites. Particulate Al:SiC has proven to be hermetic and capable of the required thermal cycling. However, MMCC indicated that its Al-Gr materials could not yet be produced that are hermetic. This was found to be due to the graphite fiber/Al-matrix interface failing during thermal cycling that led to leaks, thus making the material unsuitable for use in a hermetic electronic package. MRi and MMCC evaluated some Al-Gr samples coated with S-Bond to see if hermeticity could be achieved via an S-Bond seal, but were not able to produce consistent results, so this material was removed from evaluations for the hermetic package.

Figure 104 illustrates the initial design of the hermetic packages made for testing. The design incorporated a Kovar or Invar alloy side wall (2.0" x 2.0" x 0.265" high with a 0.095" wall thickness) bonded to an Al:SiC lid (0.063" thick) and base (0.118" thick). This assembly was then hermetically tested both before and after thermal cycling. The hole in the lid center was used as the vacuum evacuation port for helium leak check testing.

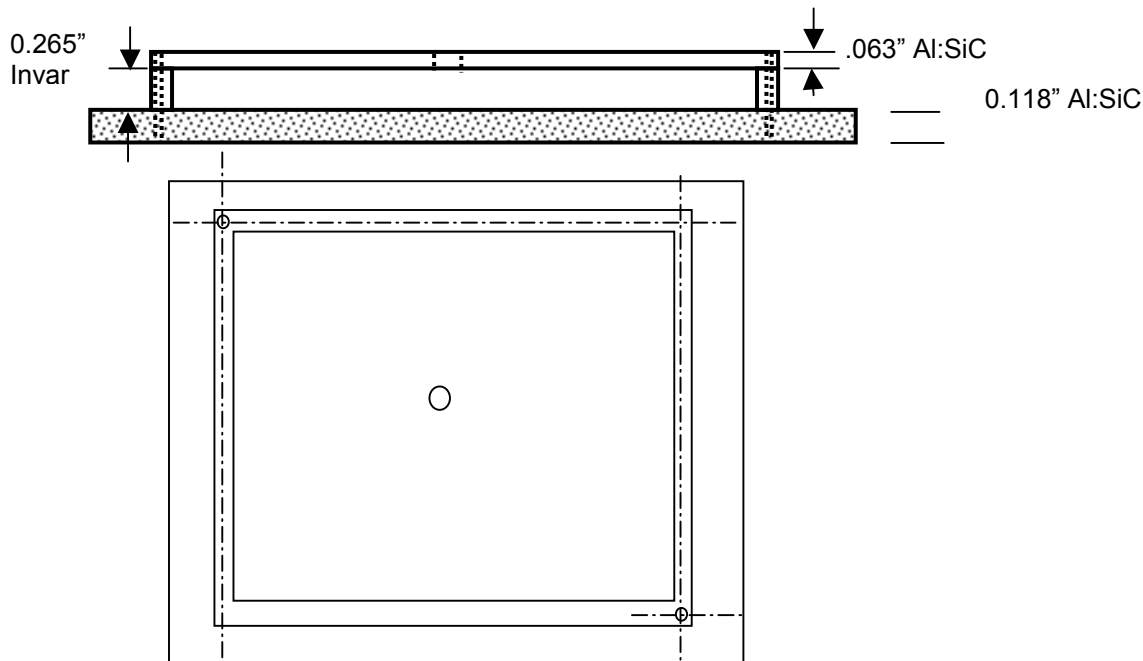


Figure 104. Illustration of the hermetic package test sample.

Figure 105 shows a photograph of a corner of one of these package enclosures. The design, consisting of two Al:SiC pieces (lid and base) and a Kovar sidewall, was used because the cost of a 100% Al:SiC box exceeded the funds available in this project. The aim of this work was to determine if such Al:SiC/Kovar packages could be fabricated and made hermetic utilizing S-Bond technology. Figure 105 shows the detail of the S-Bond™ fillet at the intersection of the Al:SiC base and the Kovar wall. The fillet on the lid side was smaller than that at the base, due to the necessary process of flipping the part over during assembly and the associated remelting of the solder from the other fillet.

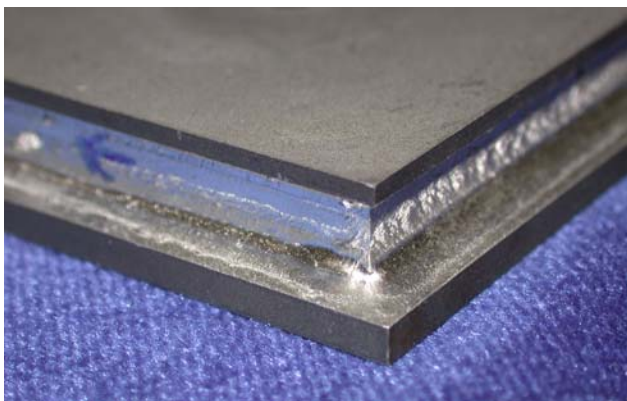


Figure 105. Al:SiC composite electronic packages assembled using S-Bond™ / showing area of leaking

These parts were helium leak checked and found to have various degrees of leaks. Many of the submitted samples could be pumped down to a leak rate between 1×10^{-7} and 1×10^{-8} cc/sec in air, but there were leaks (at least one per sample) sufficient to allow helium to pass on every part. Samples from this lot were

metallographically examined in order to characterize the S-Bond/Kovar and S-Bond/Al:SiC interfaces, and to attempt to determine the location and type of leaks detected.

The metallography results revealed evidence that the Al:SiC/S-Bond interface did not remain well-joined, though it was not clear what might have caused this. Gaps detected in the bond regions (Figure 106) could have been attributable to insufficiently wetted base material, deterioration of the composite as the molten S-Bond consumes the Al matrix (delaminating it from the ceramic particles), or metallographic sample preparation. The relatively large gaps (on the order of millimeters) observed in certain cross sections, as shown in Figure 107, likely were produced during sample preparation, as such large holes would have prevented the samples from being able to be sealed to a vacuum with a leak rate $\sim 10^{-8}$ cc/sec in air.

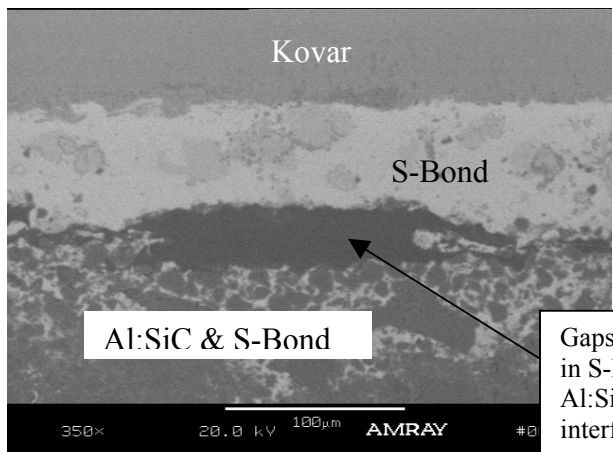


Figure 106. High magnification view of Al:SiC/Kovar® joint in an electronic package assembled using S-Bond™ 220.

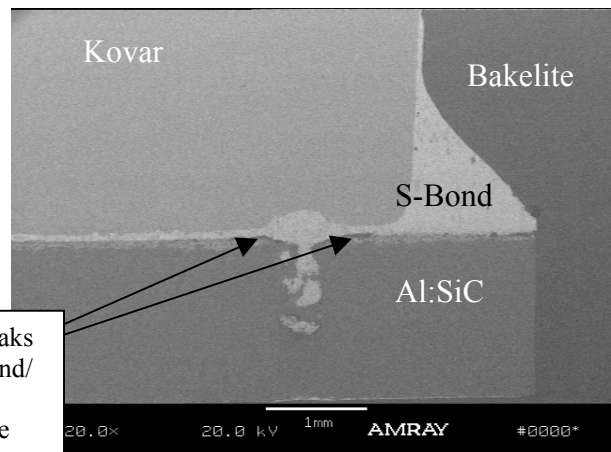


Figure 107. Al:SiC/Kovar® joint in an electronic package assembled using S-Bond™ 220.

It was suspected that the S-Bond/Al:SiC joint may have been the reason for the lack of hermeticity. Therefore, experiments were made on samples of Al:SiC that were surface prepared in different ways, in order to determine whether the as-received composite surface might not be the optimal for S-Bond wetting and joining. Al:SiC substrates were alternatively nickel shot blasted or Al_2O_3 grit blasted to prepare the joining surface for this process. The reason for these surface preparation variation was that it was possible that a thin layer of nickel might give the S-Bond something a better layer to wet and adhere to, or alternatively, that the alumina shot might remove an oxidized aluminum layer that was preventing the S-Bond from wetting to the composite surface proved. These varying surface preparation methods seemed to make little difference, since neither of these types of samples passed hermeticity tests, though the nickel blasted samples seemed the better of the two, if only because the alumina grit had not destroyed as much of the aluminum matrix wetting surface.

Hermeticity of these joints was again determined using He-leak checking, and although very good vacuum could be established on all the packages in air, most packages had very minute leaks in fillets and/or fixturing hole areas. The resulting helium leaks led to redesign of the package in two ways. One was to machine a box like base/lid made entirely of Kovar. The other was to provide a solid Al:SiC cover with only the leak checking hole present, and no fixturing holes. The elimination of one of the fillets and both of the fixturing holes helped to eliminate some sources of leaks. The newer design is shown in Figure 108.

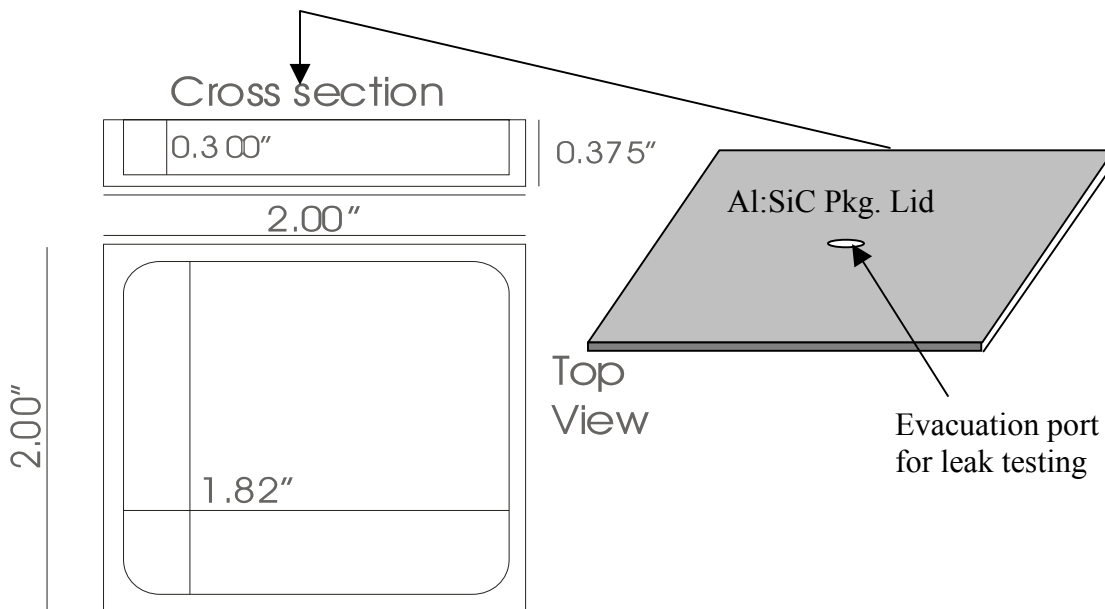


Figure 108. New composite electronic package design for S-Bond™ sealing trials.

These redesigned packages were bonded and tested hermetically, and some small leaks were detected in each of the parts, though the results were better than anything MRi had previously achieved, and were therefore encouraging. (Note: As the hermeticity requirements for these parts are not known, the ability of many of these parts to draw vacuum to a leak rate in air between 1×10^{-7} and 1×10^{-8} , some as far as 10^{-9} may be acceptable.) However, MRi maintained efforts to achieve hermetic leak rates less than 5×10^{-9} , if at all possible. Therefore, another round of test samples was assembled, this time using ultrasonics both during pretreating and during assembly, and much better results were accomplished. All of the samples achieved leak rates in air below 1×10^{-9} , and three of the four tested samples maintained this leak rate in helium. The parts were thermally cycled between approximately -20°C and $+100^{\circ}\text{C}$ 15 times and then leak-tested again. Little or no appreciable decrease in hermeticity was detected after thermal cycling and retesting, with the noted exception of the one sample that did not have a very good leak rate initially.

4.3.3.2 Hermetic Packaging Test Results

The results of the various rounds of tests for this sample configuration are summarized in Table 7. Previous sample configurations did not provide sufficiently good or consistent results to allow consistent measurements of leak rates or to make the reporting of any such measurements meaningful, so these are not shown.

Table 7. Hermeticity Testing Results for Kovar Lid/Sides and Al:SiC Base Samples

| U/S pre-wet, manual assembly, tested 9/20/2002 | | | |
|---|-------------------------|----------------------------|---------------------|
| Sample ID | Leak rate in Air | Leak rate in Helium | Comments |
| 1 | $<5 \times 10^{-9}$ | 2 @ $\sim 10^{-8}$ | Ni-Blasted Al:SiC |
| 2 | $<5 \times 10^{-9}$ | 1 @ $\sim 10^{-8}$ | Ni-Blasted Al:SiC |
| 3 | $<5 \times 10^{-9}$ | 2 @ $\sim 10^{-8}$ | Grit-Blasted Al:SiC |
| 4 | $<5 \times 10^{-9}$ | 3 @ $\sim 10^{-8}$ | Grit-Blasted Al:SiC |
| U/S pre-wet, U/S assembly, tested 1/3/2003 | | | |
| Before Thermal Cycling | | | |
| Sample ID | Air | Helium | Comments |
| 1 | $<1 \times 10^{-9}$ | $<1 \times 10^{-9}$ | Very Good |
| 2 | $<1 \times 10^{-9}$ | $<1 \times 10^{-9}$ | Very Good |
| 3 | $<1 \times 10^{-9}$ | $\sim 5 \times 10^{-8}$ | Good |
| 4 | $<1 \times 10^{-9}$ | $<1 \times 10^{-9}$ | Very Good |
| U/S pre-wet, U/S assembly, tested 1/9/2003 | | | |
| After five (5) Thermal Cycles | | | |
| Sample ID | Air | Helium | Comments |
| 1 | $<1 \times 10^{-9}$ | $<1 \times 10^{-9}$ | Still Very Good |
| 2 | $<1 \times 10^{-9}$ | $\sim 3 \times 10^{-8}$ | new, small leaks |
| 3 | $<1 \times 10^{-9}$ | $>10^{-5}$ | Severe leaks |
| 4 | $<1 \times 10^{-9}$ | $\sim 3 \times 10^{-9}$ | very small leak |
| U/S pre-wet, U/S assembly, tested 2/25/2003 | | | |
| After Ten (10) Additional Thermal Cycles | | | |
| Sample ID | Air | Helium | Comments |
| 1 | $<1 \times 10^{-9}$ | $<1 \times 10^{-9}$ | Still Very Good |
| 2 | $<1 \times 10^{-9}$ | $\sim 3 \times 10^{-8}$ | no new leaks |
| 3 | $\sim 8 \times 10^{-9}$ | $>10^{-5}$ | severe leaks |
| 4 | $<1 \times 10^{-9}$ | $\sim 3 \times 10^{-9}$ | No new leaks |

4.3.4 Hermetic Packaging Conclusions

Al-MMC composites are used in electronic packaging, as shown in Figures 91-93, to control expansion and to provide good thermal conductivity between the devices in the packages and the heat spreaders used to maintain the integrity of the packages. Such packaging is typically sealed hermetically to further the assurance of its performance in avionics and satellite enclosures. Aluminum's high thermal conductivity and low weight are required, but its inherent high CTE limited its use until Al-MMC's were developed. Now Al-MMCs increasingly used, which presents significant challenges to join the electronic substrate (either Al_2O_3 or AlN) to Al-SiC materials. S-Bond joining could facilitate and lower the cost of such a fabrication. Additionally Kovar®, a commercial low CTE iron-nickel alloy, has been used as a lid to seal the package, and sometimes as an intermediate layer to join to the heat spreader materials. S-Bond offers the opportunity to make all these joints with the same process, at the same time, thus lowering the cost of electronic enclosures. Potential future customers include Lockheed Martin, Raytheon, Loral, L³, Hughes, Honeywell and Motorola, all of whom produce electronics for satellites and/or avionics that use such Al:SiC enclosures. Figure 109 shows an electronic package that uses Al:SiC as the box to minimize CTE mismatch failures between the device

and its heat sink. The high thermal conductivity and the low CTE of the Al:SiC alloy are important. These electronic devices are then hermetically sealed with Kovar® to complete the package. S-Bond is capable both to bond the devices to the Al:SiC box and to bond the Kovar® lid to the Al:SiC base.

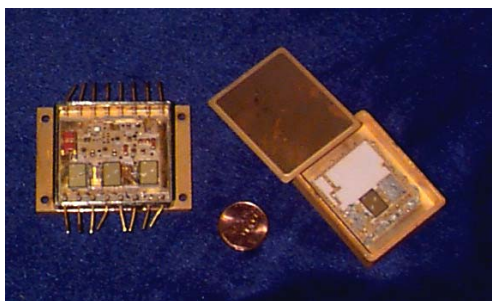


Figure 109. A power hybrid IC package used in satellite devices where an Al:SiC box and a Kovar® lid are attached. Note that these parts are gold coated, but S-Bond™ would not require such coatings to facilitate bonding.

4.3.5 S-Bond Joining of Composites in Electronic Packaging

The Phase II investigation on electronic packaging, in particular hermetic packages that are used extensively in military, aerospace and satellite applications has shown that S-Bond® has potential for joining Al-SiC and other Al-MMC materials to itself, ceramics and other metals. Thus, S-Bond® joining is a robust materials and process for joining a wide range of components. The hermetic testing showed that there is a sensitivity to the composite's side of the interface for failure which was improved by S-Bond® joining methods, such as the use of ultrasonic agitation when the S-Bond joint is made. From these Phase II results one can conclude that hermetic seals that have some thermal cycling resistance, are feasible and that S-Bond® joining has application as a means to join Al-MMC's for electronic packaging use.

5.0 CONCLUSIONS / SUMMARY

The Phase II work was focused on the joining of "lightweight composites", in particular Al-SiC and other Al-MMC's, for use in structures, armor and electronic components and packaging. This section highlights the major conclusions from each set of tasks, conducted under this Phase II SBIR.

5.1 Structures

Al-SiC has growing application in structures where high stiffness, low weight and good thermal conductivity is needed. Such applications include optical mirrors, spars for moving equipment used in space, and possibly in the ducting of fluids in various space platforms. This task evaluated geometric and material variations of the joints, joining flat bars, spars, and tubes. Materials in the various joints included

- Al-SiC - St. Steel
- St. Steel - Stainless Steel
- Al-SiC - Titanium
- Titanium - Titanium
- Al-SiC - Al:SiC
- Al - Al
- Al- St. Steel
- Al- Titanium

In all cases, S-Bond® has been demonstrated to be able to make joints and have tensile/shear strengths from 30 – 120 MPa, which for a solder filler metal is quite acceptable in many applications. The joint overlaps can be designed to fit with in the strength capabilities, provided the service temperatures for the components are below $\sim 0.85T_s$ of the filler metals, which is within 85% of the beginning of the melt temperature for the filler metals. Varying processing conditions, such as ultrasonic agitation, prewetting & sliding, and vacuum thermal treatment (a premetallization methods for difficult to wet metals such as titanium and stainless steel as well as ceramics) have all been developed and testing has shown the influence of such S-Bond joining methods on bond strength and performance. S-Bond Alloys 220 (Sn-based) and Alloy 400 (Zn-based) have been tested and results show that the S-Bond 220 alloys can be used up to $\sim 190^\circ\text{C}$ while Alloy 400 can be used up to $\sim 350^\circ\text{C}$. Joints of the various materials using either alloy system was presented and their results show that both alloys have good strength's and use/selection would be subject to their physical property differences.

There have been no long term environmental testing nor has there been studies to the effect of dynamic loading or fatigue. If one is to consider using S-Bond joining for structures, especially critical structures, the additional testing would have to be completed.

In conclusions for structures, S-Bond joining technology has use and application and its properties and materials joining versatility, especially with its ability to join Al-MMC's are unique. If MDA or other DoD programs need Al-MMC joining capability, they should be considering S-Bond joining technologies.

5.2 Armor

The consideration of S-Bond® for use in lightweight armors stemmed from the possibility that lightweight armor may find application for protecting space platforms from impacts. The concept was to bond ceramic strike plates, know to fragment incoming projectiles, and bonds them to a tougher backing plate that could subsequently absorb the impact energy of the fragmented projectiles. The Phase II evaluations of S-Bond® joining for ceramic strike plate to various base armor led to mixed results. S-Bond Alloy 220 joining technology showed it versatility to bond various ceramics, SiC and Si:SiC composites to Al-SiC composites, aluminum foams and to titanium, all these base plate materials being considered for various DoD applications. The joining of SiC strike plated to titanium was of particular interest the US Army Research lab and we studied in parallel to this work and reported to present the case for S-Bond joining of ceramic armor systems and the possibility of utilizing Al-SiC materials as part of the armor system.

Initial problems of large CTE mismatch when joining ceramic to aluminum was overcome by various S-Bond joining techniques, including the use of graded interfaces using Al-SiC composites. Although successful in addressing the bonding issues, the final test was ballistic performance. The ballistic testing results concluded that the S-Bond joints, independent of the base materials and ceramic, had for 50 caliber size projectiles, V_{50} (velocity of penetrator) penetration values near that of epoxy joints. This result showed the S-Bond joining did not achieve an improvement in performance, however, if strike plates need to be removed for any reasons, S-Bond joining offers a significant process advantage since all that has to be done is to reheat the interfaces to remove the ceramic. This may at a later date play as an advantage, without having to lose any ballistic penetration performance.

S-Bond technology for joining large ($> 4'' \times 4''$) ceramic plates has been shown to be feasible and is ready for any MDA or DoD insertion program where this capability is needed, provided ballistic penetration over epoxy joints is not required.

5.3 Electronics

MRi has demonstrated the utility and capability of its S-Bond® technology to join Al-MMC's to a myriad of materials and components that have application in electronic packing, including:

- Silicon / semiconductor dies
- Heat spreaders
- Thermal control devices
- Enclosures
- Interconnects
- Assembly equipment for electronics

This capability has been assisted by developments under this SBIR. Basic properties of joints have been reported for joints between many of the materials that are used or being considered for electronic applications. Materials that have been investigated under this SBIR include:

| | | | |
|----------|----------------------------------|-----------|----------|
| - AlN | - Al ₂ O ₃ | - Silicon | - Gold |
| - Al-SiC | - Kovar® | - Copper | - Nickel |

Results showed that depending on the material an S-Bond method was able to join such materials in different configurations, whether for thermal management as in heat sinks or in hermetic package seals.

MRi considers S-Bond joining as a very successful, versatile and capable technology for a wide range of electronic component manufacturing. As seen in the commercialization plan, S-Bond technology will have a definite focus on joining in electronic packing. There are already some major electronic and opto-electronic manufactures evaluating S-Bond technology for their use. In MDA and DoD applications, the greatest potential is in thermal management components for avionics, radar electronics, and power electronics. MRi has recently been successful in winning an MDA Phase II SBIR for joining graphite foams for thermal management. This success was an outgrowth of the success in this part of the Phase II investigation for “lightweight structures and electronics”.

6.0 COMMERCIALIZATION

MRi co-developed S-Bond joining technology with its partner, Euromat, GmbH over 8 years ago and has been developing understanding and applications over that time. MRi’s commercialization has been demonstration based and it has now evolved into a more mature stage, as presented below. The intent is now to get the technology out to as many users, to manage its adaptation by industry and to develop a manufacturing base that can support the growth of S-Bond technology, to do this MRi has spun off a new company to focus on S-Bond commercialization as the next sections present.

6.1 S-Bond Technologies, LLC

S-Bond Technologies, LLC, an engineered materials company and spin-off from Materials Resources International, plans a major expansion of S-Bond® active solder technology business. The plan calls for SBT to increase S-Bond™ technology net revenues from ~\$200,000 in 2003 to ~\$7.5M by 2007 with net income going from (~ - \$ 70,000) in 2003 to ~\$ 2M in 2007. This revenue growth will be driven by a focus on increasing application and sales with key original equipment manufacturers and the establishment of a network of S-Bond™ Service providers located in strategic locations and or industries. SBT plans to fund this growth with a combination of debt and equity over the period from 2003 – 2004 to cover negative cash flow due to investments on personnel and facilities. After 2004 SBT’s cash flow will be positive and able to pay off its initial debt in 2006 followed by EBTIDA growth to~ \$ 3M by 2007.

SBT’s active solder technology is based on adding patented combinations of elements (e.g., titanium, zirconium, hafnium, gallium, cerium) to conventional solders, and, combined with specific processing procedures, joining metal, ceramic, glass and composites at soldering temperatures without the use of chemical fluxes and in open air. Active solder joining offers advantages over active brazes, including lower joining temperatures (<850°C) and avoiding pre-metallization of the substrates, both of which simplify joining dissimilar materials. A joint formed with S-Bond is typically stronger than those obtained with conventional soldering, but equally thermally and electrically conductive.

SBT recognizes S-Bond technology will be a technical “value” sale that fits important niches in thermal management, electronics packaging, glass to metal seals and a wide range of dissimilar materials joining applications. As such, SBT aims to organize its marketing and sales plan to the technical staff of “early adaptors” in OEM organizations where SBT believes there is a technical fit for the S-Bond® product. As a technical product and process, S-Bond™ will be application driven and will need to be sold with technical know-how included. As such, SBT has adopted the OEM licensee and a licensed S-Bond™ Service Provider as key revenue drivers in a diverse market. OEM’s are significant direct users of S-Bond technology whom would use S-Bond technology in the direct or subcontracted manufacture of their products. An example OEM would be Intel that might use S-Bond® to bond integrated circuit chips to lead frames. SSP’s are joining service providers whom have their own shops and customer base where S-Bond joining technology would be applied. An example SSP would be a brazing shop such as Solar Atmospheres. These two channels would be customers for S-Bond™ technology and lead the technology application into

appropriate niches, while being well supported by SBT staff. The business plan calls for the development of these channels and the development of four revenue streams based on material sales, engineering fees, development services and royalties. A five-year plan for business growth, based on this plan, is shown in Table 9. SBT seeks to initiate this approach starting in 2003 and already has one OEM and its “beta site” for its S-Bond® Service Provider (SSP) Network.

Table 9. Summary 5-Year SBT Financial Projections

| | 2003 | 2004 | 2005* | 2006* | 2007 |
|---------------------|-------------|-------------|--------------|--------------|--------------|
| Net Revenue | \$ 186,650 | \$ 773,650 | \$ 2,238,775 | \$ 4,089,700 | \$ 7,581,700 |
| Gross Profit | \$ 132,650 | \$ 485,650 | \$ 1,419,775 | \$ 2,577,700 | \$ 4,701,700 |
| EBTIDA | \$ (56,750) | \$ 7,250 | \$ 473,975 | \$ 1,334,340 | \$ 3,184,180 |
| Net Income | \$ (68,734) | \$ (42,468) | \$ 311,5611 | \$ 817,559 | \$ 1,978,335 |

* NOTE: the growth from 2004 to 2005 is driven by the building of a materials demand from a growing number of OEM and Service Provider licensees (explained further in the text) and the assumption it takes from 18 – 24 months to grow from test and prototype into production levels where production quantities of S-Bond materials would be consumed.

Projected business growth requires SBT to form its own dedicated market and application development group that focuses on targeted “key” OEM customers whom are significant and represent a major niche in a specific market. SBT will also create a network of SSPs that will provide development services to a diverse set of smaller or less strategic markets. In combination, the additional education and development outlets will increase the number of applications in the development process, increase market awareness for the technology, and reduce barriers to acceptance. SBT’s expectation is this strategy will allow the company to sign 25 OEM licenses and 7 SSP partners by the end of 2007. These will feed three of the four revenue streams: material sales, license maintenance fees, and royalties.

The primary business objective for SBT over the next year is to identify and hire a Market Development Manager to drive growth in applications in development, identify and work with OEM accounts, and expand the SSP network. This manager will start with the current OEM and SSP already in development, a group of on-going application development programs, and a database of past contacts and projects. By providing additional focus and management, SBT expects the growth in licensed technology users to be as shown in Table 10.

Table 10. Projected Licensed Technology Users

| | 2003 | 2004 | 2005 | 2006 | 2007 |
|--------------|-------------|-------------|-------------|-------------|-------------|
| OEM’s | 1 | 3 | 8 | 15 | 25 |
| SSP’s | 1 | 3 | 5 | 6 | 7 |

SBT/MRi operations has used cash flow from current customers and from US Government Small Business Innovative Research Grants. However, the plan presented here will require approximately \$465,000 over the next three years to hire staff dedicated to generating customer applications with significant OEM customers, and to create a network of S-Bond® Service Providers (SSP’s) that will overcome the key barriers to adopting the technology: lack of market knowledge of how to apply S-Bond joining technology and the need for customers to invest in new manufacturing capability. No significant investment in capital facilities is anticipated as SBT intends to focus on research, development, and supporting its OEM and SSP licensees.

As will be shown, the key driver of SBT revenue and earnings growth after 2003 is the acquisition of OEM licensors and their average annual purchases of S-Bond materials. SBT is in the final stages of a licensing agreement with one OEM, and the structure of this license was used in creating the financial plan. Based on the proposed plan, the breakeven point for SBT, after the addition of a CEO / market development manager and application development assistance, is 3-5,000 annual pounds sold. We expect to achieve this in the 2004-2005 timeframe. The hiring of additional resources and installation of expanded facilities can be delayed until that point, and then further growth in expenses kept in line with revenue and earnings growth.

6.2 S-Bond Technologies, LLC, Business Mission

SBT is an engineered materials company, providing materials and expertise to an OEM and SSP network, while conducting the necessary product and application research and development. The mission of S-Bond Technologies LLC is to develop and market its patented active solder materials and technologies that enable the low temperature bonding of similar and dissimilar materials in situations where conventional soldering, brazing, and adhesive systems do not function well. SBT will compete against soldering, brazing, and adhesive products by offering a technically superior alternative for specific situations where processing temperature, thermal conductivity, electrical conductivity, or dissimilar materials make conventional processes impractical. This will be done by licensing S-Bond® technology and selling S-Bond® materials to both large OEM accounts that have significant product development and manufacturing capability, as well as licensed service providers that offer S-Bond® joining capability to other companies and act as regional and industry specific application development centers.

6.3 S-Bond Market

Although the S-Bond technology is positioned as part of the broad category of material joining processes, it primarily competes against soldering, brazing, and conductive adhesive techniques. These techniques are used in the production of a wide variety of products among a diverse manufacturer base across GNP level growth industries, with the exception of electronic packaging. The materials used in brazing and soldering are a small part of the overall market valuations. For example, the thermal management market in 2004 is estimated to be \$6.1 B worldwide, while the market for joining materials is estimated to be below \$100M. Therefore, market size is difficult to assess. However, specific applications where these techniques are used are growing, and SBT's development work has identified several promising areas. These include thermal management for semiconductors and electronic products, aerospace and defense systems, and other thermal management products such as glass:metal seals. The growth in the use of engineered materials and multi-material systems in sophisticated equipment is the key driving force for adopting S-Bond joining technology.

A secondary market trend is the move away from lead-based solder materials. Current replacement products do not perform as well in all applications causing companies to identify other joining techniques. While SBT will benefit from this trend by an increase in the number of potential applications, adoption of lead-free systems should not substantially alter the overall market demand for joining materials.

S-Bond technology includes the patented material in combination with S-Bond joining techniques. Therefore, SBT does not compete directly against solder and braze material manufacturers, but against other joining, such as epoxy joining, metallizing followed by conventional soldering or brazing. This requires that SBT marketing efforts focus on winning individual applications for the technology.

The S-Bond materials (active solders) are a specific subset of filler metals used in solder and braze joining. There are many manufacturers such as Cookson, Kester Solder, AIM, Lucas Milhaupt, Wolverine, etc. whom produce filler metals in large quantities. Such filler metal producers could be competitors, if were not for SBT's patents. SBT is looking at these "potential competitors" as possible contract suppliers for S-Bond® filler metals, since SBT has no large capital investment plans for the melting and forming of solder

filler. SBT's plan is to qualify one or two of these manufacturers as suppliers and at the appropriate time look to such suppliers as strategic partners that might invest in SBT.

Conventional joining methods that compete with S-Bond technology fall into three broad categories:

1. *Efficient, well-known solder and brazing methods.* The processes are well understood and the industry is tooled and trained to use them.
2. *Inefficient, multi-step, expensive solder and brazing methods (pre-metallizations and/or active brazing).* These currently available methods enable the joining of two dissimilar materials and/or ceramic metal joining materials, but cannot be joined by the usual methods.
3. *Alternative bonding methods for which a solder based method would be preferred if available.* such as adhesives or other types of mechanical fastening.

S-Bond offers a substitute method for situations 2 and 3 where there are issues with dissimilar materials, significant differences in coefficient of thermal expansion (CTE), or performance issues with adhesives. Examples of applications for the second category are found in integrated circuit assembly; radiator and refrigeration condenser manufacturing; heat sink and cold plate attachment for electronics and telecommunications packages; sputter targets; glass: metal joints such as optoelectronic interconnects; windows and feedthroughs; and miscellaneous structures and containers that rely on dissimilar materials combinations. Representative of the third category are brake pad assemblies and high voltage electric isolators, applications where parts are currently glued together. Additional potential markets are sporting goods, such as golf clubs and tennis rackets.

The following specific applications were identified through SBT's product development programs and customer contacts.

1. *Joining components requiring thermal management capabilities* (e.g., computer chip packages, satellite-space electronics). This includes power semiconductor packaging where heat dissipation is needed and the bonding of metallic heat sinks to their ceramic bodies. Such markets include electronics applications, automotive and industrial sectors, and are growing at more than 10 percent per year. *Semiconductor manufacturing equipment is currently a US\$140 billion market.*
2. *Joining aluminum, aluminum composites and dissimilar metal combinations* such as aluminum to copper, aluminum to titanium, aluminum to steel, Kovar® or Kovar to other metals and composites, etc. *Estimated to be a market of more than \$5 million annually.*
3. *Electronic packaging* (e.g., packaging fragile silicon wafers into a robust, useable module such as integrated circuits, switches, transmitters). An estimated worldwide market of \$250 billion.
4. *Joining glass to metal* (e.g., electrical insulation, sensors, opto-electronics, light bulbs, fluorescent tubing). This is a diverse market and difficult to measure, however it is believed to be a market of over \$500M annually. This type of joining is found in electrical feedthroughs and contacts, sensors, process windows and sight glass and in power electronics.
5. *Bonding ceramics (oxides and nitrides), carbides, graphite and metal ceramic composites, including joining ceramic, to metal.* The key feature being sought by this market is a stronger, thermally conductive bond that can survive higher temperatures as compared to currently used adhesives and cements. *Similar to the glass metal seal, ceramic:metal bonds can be found in a*

diverse set of industries from electronics and aerospace to petrochemical and mining. The value of the services and materials joining market also exceeds \$500M annually.

6. *Joining light metal alloys* such as aluminum, magnesium, titanium, and beryllium. An example of this application is to bond copper to aluminum pipe fittings for the refrigeration, automotive radiator, and other auto-parts applications. Fabricated heat exchangers and condensers had an estimated total market value of \$3.6 billion dollars in the US alone. Other applications of light metals include aerospace, biomedical implants, pharmaceutical and chemical processing and increasingly in sports and other consumer equipment. These markets could add another \$3-4 billion annually in component sales but it is difficult to ascertain the value of the “joining” product market from this total market value.

A summary of market potential is shown in the Table 11 below

Table 11. Market Areas for S-Bond Joining Technology

| Application | Industry | Component Market Size | S-Bond Opportunity |
|--------------------------------|---|-----------------------|--------------------|
| Cold plates | Electronics, telecom, avionics, satellites, radar, automotive, power electronics | \$500 M | \$10 – 20 M |
| Heat Sinks | | \$ 1B | \$20 – 100M |
| Radiators | ↓ | \$ 250M | \$5-10M |
| Electronic Packaging | Servers, high end computers telecommunications/broadband Satellites / avionics / military | \$5B | \$10 – 50M |
| Microelectronics/interconnects | All electronics | \$30B | \$100 – 200M |
| Optical Packages | Networks, telecommunications | \$10B | |
| Electrical Connectors | Power electronics, | Unknown | \$5-20M |
| Glass/Metal Seals | | Unknown | \$20-50M |
| Aluminum / Light Metals | general | Unknown | \$20 – 100M |
| Composite Metals | High speed assembly equipment, optical equipment, military | \$1-2B | \$10-50M |

6.4 Commercialization / Summary

6.4.1 Commercial Highlights

The commercial success of active solder joining (S-Bond™) will be dictated by the capability of the process to be done in production settings. Although many of the techniques practiced in this Phase II work were manual, the S-Bond process can be automated to varying degrees. The most production sensitive application cited in this Phase II SBIR work is electronics. If these methods are to be commercialized, then automation of the S-Bond process is needed. Table 12 lists commercial prospects for S-Bond joining in electronics, the subject of the joining technology, the level of interaction and comments on their joining the SBIR S-Bond R&D efforts.

Table 12. Commercial Prospects for S-Bond™ Joining/Lightweight Structures & Electronics

| Organization | Application / Topic | Current Interaction | Future Interaction |
|------------------------------|--|--|---|
| MMCC, Inc. | Al:Gr Composites | Evaluating the suitability of S-Bond™ for joining Al:Gr composites. | Providing Al-Gr for heat spreader testing |
| US Army Research Lab | SiC / Ti Armor | P.O. for development services joining SiC to Ti6-4 plate. Continues in test. | Expect joining Phase II work and possible Phase III purchases of test plates. |
| Simula / MCubed | Composite Armor Si:SiC strike plates | Phase I SBIR proposal submitted to Army 01.2 topic / rejected. | Design and test of composite, S-Bond™ joined armor tiles, and supply of ceramic strike plates. |
| Matec Instruments | NDE / Acoustic testing of Armor tiles | Testing of initial Al-foam / ceramic face plate bonds. | Development and procurement of system to non-destructively evaluate bond interfaces. |
| Ceramic Processors | Joining Al:SiC in electronic cooling modules | Evaluations underway for the electronic vehicle systems. | After testing and qualifications, MRi will collaborate with CP and their customers, including the US Navy for Power Electronic Building Blocks for the all electric ship and in radar and other high power electronic applications. |
| NASA Marshall | Ti-joining | R&D Kit for evaluating joining coolant loops. | Future purchases of S-Bond™ alloys. |
| Cookson Electronic Materials | S-Bond™ alloy production | Development of production methods for S-Bond materials | Possible partner with MRi to produce quantities of S-Bond™ alloys |
| Kulicke & Soffa | Electronic package assembly equipment | “Thermo sonic” micro-joining studies | Agreement to develop electronic package joining equipment. |
| Kulicke & Soffa | Electronic assembly equipment | Joining hardened tool inserts onto Al-SiC | A license to manufacture components in is under development. |

In parallel to this Phase II work, MRi / SBT has and continues invested its own funds as well as loan funds from the Ben Franklin Partnership Program to help develop S-Bond automation processes for high production S-Bond joining. Such procedures would be suitable to the fabrication of electronic packages, and therefore these studies support the commercialization. The figures below show the results of the work to date. Working with an automation supplier, DEMCO, MRi assembled and tested a unit designed as a carousel (turn table) device for bonding aluminum fins to flat copper base plates. The unit preheats an assembly of the fin/plate that has an S-Bond 220 foil insert. Then the fixture is placed on the turn-table and rotated to stations that have infrared (IR) heating lamps and air heaters. Once the parts reach the joining temperature (~250°C), controlled by a PC, the tool with part is placed under an ultrasonic horn where the mechanical activation needed for S-Bond joining is applied. The cycle time of this unit is currently about 30 seconds per unit bond, though faster cycle times could be achieved with some engineering studies, as the cycle time appears to only be limited by the preheat time.

Figure 110 illustrates the overall unit. Figure 102 shows details of the turn-table with IR heat lamps and ultrasonic press station. Figure 52 shows the details of the ultrasonic press station, activated after the parts have been brought to the joining temperature, melting the S-Bond 220 foils that had been placed with the pick and place unit seen in a station in Figure 111. In Figure 112, a graphite tool locates and positions the parts to be joined as the ultrasonic horn mechanically agitates the joint.

MRi proceeded with several commercial customers in the thermal management-electronics market to further advance such production units.



Figure 110. Automated S-Bonder™ Carousel System

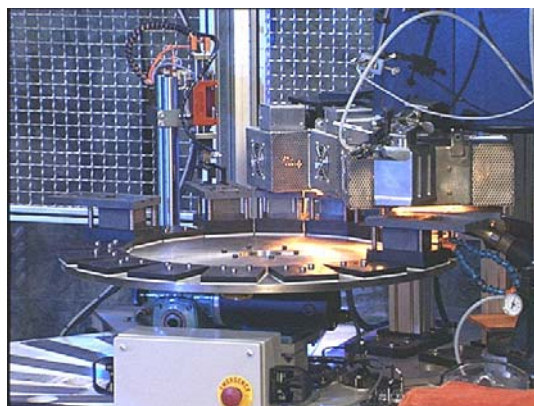


Figure 111. View of Carousel System with Infrared Heater Lamp Stations

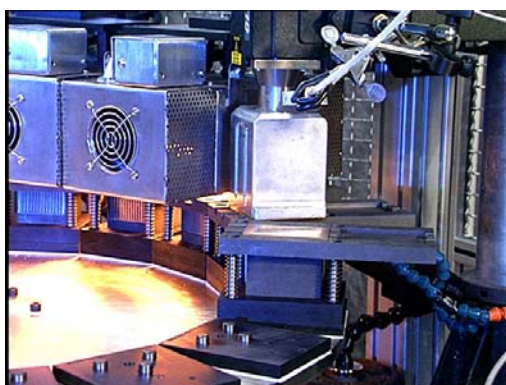


Figure 112. View of Ultrasonic S-Bonder™ Press Station

6.4.2 Commercial Integration into MDA / DoD Programs

S-Bond Technologies, LLC is now the commercialization company for MRi's S-Bond developments stemming from this work and from its own developments. As presented above, S-Bond® technology has been shown to be able to join Al-MMC's and many other metals, ceramics and composites. Such versatility presents MDA and other DoD programs with an opportunity to have a bonding technology that can be used in the fabrication of structures and electronic packaging, with some possibility or bonded armor strike plates.

MRi, now through its S-Bond Technologies, LLC, affiliate, is prepared to offer and license DoD contractors for use of S-Bond technologies. SBT is already working with companies, such as Lockheed Martin and Raytheon in electronics cooling and thermal management of spacecraft. SBT is seeking commercial avenues with such contractors and has not yet teamed with DoD contractors for specific MDA programs. One of the next focuses of SBT will be to develop relationships with several major MDA / DoD contractors to evaluate the potential of S-Bond joining in order to exploit certain opportunities, with an emphasis on electronic packages and thermal management, but also SBT will look at the opportunities in structures.

SBT is now offer commercial quantities of S-Bond alloys, R&D Kits, and is pursuing commercial licenses for several users. SBT has a presence on the web and offers these materials and technology for sale. To date, as presented about, for 2003 S-Bond revenues will be exceeding \$200,000 annually.